

University of Memphis

## University of Memphis Digital Commons

---

Electronic Theses and Dissertations

---

4-16-2012

### Design and Biophysicochemical Properties of Chitosan-Collagen-Calcium Phosphate Microparticles and Scaffolds for Bone Tissue Regeneration

Monica Viorica Zugravu

Follow this and additional works at: <https://digitalcommons.memphis.edu/etd>

---

#### Recommended Citation

Zugravu, Monica Viorica, "Design and Biophysicochemical Properties of Chitosan-Collagen-Calcium Phosphate Microparticles and Scaffolds for Bone Tissue Regeneration" (2012). *Electronic Theses and Dissertations*. 426.

<https://digitalcommons.memphis.edu/etd/426>

This Thesis is brought to you for free and open access by University of Memphis Digital Commons. It has been accepted for inclusion in Electronic Theses and Dissertations by an authorized administrator of University of Memphis Digital Commons. For more information, please contact [khggerty@memphis.edu](mailto:khggerty@memphis.edu).

DESIGN AND BIOPHYSICOCHEMICAL PROPERTIES OF CHITOSAN-COLLAGEN-  
CALCIUM PHOSPHATE MICROPARTICLES AND SCAFFOLDS FOR BONE TISSUE  
REGENERATION

by

Monica Viorica Zugravu

A Thesis

Submitted in Partial Fulfillment of the

Requirements for the Degree of Master

of Science

Major: Biomedical Engineering

The University of Memphis

May 2012

## **DEDICATION**

This thesis is dedicated to God, who gifted me with an inquisitive mind, good health, the best family in the world and best friends, excellent colleagues, whom I can call advisors and intelligent professors.

## ACKNOWLEDGEMENTS

First of all, this work would not have been accomplished without the will of God, so I thank God from the bottom of my heart for giving me the opportunity to obtain positive results in my research.

I would like to acknowledge and extend my sincere gratitude to a number of individuals for their guidance and support. I would like to thank my advisor, Dr. Joel Bumgardner, for improving my analytical thinking and correcting my thesis. Special thanks also go to my committee members for their insight, to Dr. Richard D. Smith for helping incorporate collagen in the microparticles and to Dr. Haggard for providing a reason not to use the present microparticles in cartilage engineering.

I would like to thank many other individuals for their contributions to this research, without whom this research would not have been a success: Benjamin Taylor Reves and Jared O. Cooper, the former for suggestions for effective bead washing, selection of cell seeding concentrations, reporting the correct Young's modulus and the latter for suggestions with the hydroxyproline assay, LIVE/DEAD assay and both for being there when I needed guidance and humor. I couldn't ask for better advisors for my experiments! Next, Dr. Sanjay Mishra and his graduate student, Binod Raj, were very helpful in recording the XRD data. Warm thanks go to Dr. Amber Jennings who provided assistance with my statistical analysis of the results. I would also like to thank Marvin Mecwan for helping report # cells/well for the CellTiter-Glo® Luminescent Cell Viability Assay, for other research planning discussions and for his funny remarks. I am grateful to Dr. John Williams for suggesting reporting Young's modulus at values of strain where bone would not fracture, providing examples of applications for the

scaffolds and for helping with mechanical testing setup. I would like to extend my gratitude to Dr. Ernő Lindner for suggesting using regression analysis for degradation. Finally, I am especially grateful to my graduate school lab mates and colleagues Jonathan McCanless (for suggestions for the hydroxyproline assay), Keaton Smith, Heather Doty, Drew Norowski, John Matthew Goodhart (great humor and good ideas), Andrew Noblett, Duong Nguyen, Hengjie Su, Vinay Bhal, Lauren Eichaker, Alayne White, Ashley Cox Parker, Felynnica Rainey, Gregg Kisiel, Tina Fortune, James Sheppard, Alexander Maclin, Israel Quintal Xix for welcoming me to Memphis. I would like to also thank Rick Voyles and Robert Jordan from the Machine shop for making several molds for me and for teaching me how to make molds and cut blunt needles. I would like to thank Nate Webb and William Clem from Wright Medical for getting the samples  $\gamma$ -sterilized.

I am also thankful to the creators of aliluia.ro, who supported me with heavenly Byzantine chant through long nights of experiments and thesis writing. I couldn't have done it without you!

One person I am endowed to thank is Dr. Preza, who supported me financially in my last semester at University of Memphis and allowed me to write my thesis, while getting image acquisition and processing experience.

Lastly, but not least, I would like to recognize my *family*: *family* members and my best *friends*: Jie Wang, Chris Banasiak, Helen Wheeler and Kathy Nash for their mental support and love through one of the toughest periods in my life.

## **ABSTRACT**

Zugravu, Monica Viorica. MS. The University of Memphis. May 2012.  
Design and Biophysicochemical Properties of Chitosan-Collagen-Calcium Phosphate  
Microparticles and Scaffolds for Bone Tissue Regeneration. Major Professor: Joel D.  
Bumgardner, Ph.D.

Due to limitations of bone autografts and allografts there is much research directed at designing synthetic bone grafts. In this work, collagen-chitosan-calcium phosphate microparticles and microparticle-based scaffolds were compared to their counterparts without collagen in terms of degradation, cytocompatibility (porosity and stiffness only for scaffolds). Microparticles exhibited 20% decrease in mass over 6 weeks and provided an optimal environment for 3-5 fold cell proliferation over 7 days-culture period. Although there was no effect of collagen addition to microparticles, all the formulations may be suitable as bone tissue fillers. Further, there was no difference between control and collagen scaffolds. In general, scaffolds exhibited 23% porosity, 0.6-1.2 MPa Young's modulus, 10-25% degradation over 4 weeks, and supported a 4-7-fold increase in osteoblast cell number over 7 days in culture. While there is room to improve Young's modulus of the scaffolds, they are satisfactory bone graft substitutes.

## TABLE OF CONTENTS

	Page
List of Tables	viii
List of Figures	ix
Appendices	x
Chapter	
1 Introduction	
1.1 Clinical Problem Statement	1
1.2 Hypothesis and Objectives	6
1.2.1 Objectives	7
1.2.2 Significance	9
2 Background and Literature Review	
2.1 Brief description of skeleton and bones	10
2.1.1 Bone classification	10
2.1.2 Bone anatomy	10
2.2 Bone injury and repair	12
2.3 Bone grafts	16
2.3.1 Autografts	16
2.3.2 Allografts	16
2.3.3 Synthetic bone grafts	16
2.3.3.1 Ceramics	18
2.3.3.2 Polymers	20
2.3.3.3 Composites	22
2.4 Chitosan	30
2.5 Calcium Phosphate	31
2.6 Collagen	32
2.7 Composite chitosan-collagen biomaterials	33
2.8 Conclusions	37
3 Materials and Methods	39
4 Results	50
5 Discussion	70
6 Conclusions	84
7 Future work	86
References	88

## Appendices

A. Degradation, cell attachment & growth on microparticles	100
B. Young's modulus, degradation and viability of osteoblasts on scaffolds	105



## LIST OF TABLES

Table		Page
1	Characteristics of bone grafts	28
2	Physical and compositional properties of the chitosan-collagen-calcium phosphate composite microparticles	52
3	The change in mass of beads in PBS only vs. degradation solution respectively, after six weeks	54
4	The change in mass of scaffolds fused with either acetic or glycolic acid for PBS + enzymes and PBS degradation solution only, respectively, after four weeks	64
5	Young's modulus of various bone scaffolds	78
6	Proliferation of osteoblasts or osteoblast-like cells on bone scaffolds	81
7	Ranking of the scaffolds based on top three factors	82

## LIST OF FIGURES

Figure	Page
1 Digital images of composite chitosan-collagen-calcium phosphate microparticles	50
2 Representative XRD spectra of composite chitosan-collagen-calcium phosphate microparticles compared with chitosan	53
3 Degradation of microparticles in PBS + enzymes	54
4 Degradation of microparticles in PBS	55
5 % fibroblasts' attachment on beads	56
6 % osteoblasts' attachment on beads	56
7 Fibroblasts' proliferation on beads	57
8 Osteoblasts' proliferation on beads	57
9 Fibroblasts' viability on 25% collagen-chitosan-calcium phosphate microparticles after one week	58
10 Digital images of composite chitosan-collagen-calcium phosphate scaffolds: full view and close up to show pore structure	59
11 Porosity of scaffolds made of chitosan, 10% collagen or 25% collagen and fused with either acetic acid or glycolic acid	61
12 Representative stress-strain curve for scaffolds	62
13 Young's modulus in compression of composite scaffolds	63
14 Degradation of scaffolds in PBS + enzymes	65
15 Degradation of scaffolds in PBS	66
16 Osteoblasts' attachment on scaffolds	67
17 Osteoblasts' growth on scaffolds	69

## Appendices

A. Degradation, cell attachment & growth on microparticles	Page
Table	
1 Regression lines of the degradation of microparticles in PBS + enzymes	100
2 Regression lines of the degradation of microparticles in PBS	101
3 Cell attachment on microparticles	101
4 Cell proliferation on microparticles on the last day of proliferation	102
5 Regression lines of fibroblasts' proliferation on microparticles	102
Figure	
1 Degradation of microparticles in PBS + enzymes	100
2 Degradation of microparticles in PBS (control)	101
3 Regression for fibroblasts' proliferation on microparticles	103
4 Fibroblasts' viability on microparticles.	103
5 Osteoblasts' viability on microparticles	104
B. Young's modulus, degradation and viability of osteoblasts on scaffolds	
Table	
6 Regression lines of the degradation of scaffolds in PBS +enzymes	105
7 Regression lines of the degradation of scaffolds in PBS	106
8 Regression lines of the osteoblasts' proliferation on scaffolds	107

Figure		Page
6	Young's modulus in compression of composite scaffolds for $\epsilon=0.1$	105
7	Degradation of scaffolds fused with acetic vs. glycolic acid in PBS + enzymes	106
8	Degradation of scaffolds fused with acetic vs. glycolic acid in PBS	107
9	Regression analysis of osteoblasts' proliferation on scaffolds	108
10	Osteoblasts' viability on scaffolds fused with acetic acid	109
11	Osteoblasts' viability on scaffolds fused with glycolic acid	110

## CHAPTER 1: INTRODUCTION

### 1.1 Clinical problem statement

Over 1,500,000 bone graft operations are performed every year in the United States for the treatment of musculoskeletal injuries/diseases including bone fractures, painful vertebrae, missing teeth, trauma (e.g., craniofacial trauma), osteosarcoma and birth defects.<sup>1-3</sup> The gold standard for bone graft therapies is the patient's own bone, which is called an autograft. Autografts are considered the "gold standard" by many surgeons because they exhibit osteoconductive, osteogenic and osteoinductive properties due to resident growth factors.<sup>1,4-6</sup> However, an autograft involves a secondary surgery with donor site morbidity or pain and increased surgical time.<sup>7</sup> Allografts are bone grafts which come from cadavers and, while they have osteoconductive properties, they have limited osteoinductive properties and availability.<sup>1</sup> There is a need to develop synthetic bone graft materials for bone regeneration.

Some of the synthetic bone graft substitutes are calcium-phosphate ceramic-based. The advantages of these ceramics are: similarity to the mineral phase of bone—making them osteoconductive—their ability to form direct bonds with the surrounding bone and minimal immunological and foreign body reactions.<sup>8</sup> The disadvantages of ceramics are: lack of osteoinductivity,<sup>8</sup> brittleness and the difficulty to machine into complex shapes and porous constructs.<sup>9</sup> While there has been much research and development with these materials, their clinical efficacy has been questioned based on the small sample size, lack of control or comparison groups in most studies and the absence of a formal assessment of clinical outcomes.<sup>9</sup>

Other synthetic bone graft substitutes are polymer-based: natural or synthetic. On one hand, naturally derived polymers, such as alginate, chitin, chitosan, hyaluronic acid, collagen etc. are known to support cell attachment, but have poor mechanical strength.<sup>10</sup> On the other hand, synthetic polymers, such as poly(lactic acid), poly(glycolic acid), poly(lactide-co-glycolic acid), poly-hydroxyl-butarate, poly( $\epsilon$ -caprolactone) have relatively good mechanical strength (however, in the porous form required for a bone graft, their Young's modulus is below the 10 MPa inferior limit of cancellous bone, e.g. PCL scaffolds<sup>11</sup>), tunable degradation rates and can be manipulated into desired shapes, but may have undesirable acidic degradation products, which may stimulate an inflammatory reaction.<sup>12,13</sup>

Synthetic bone grafts can incorporate bone morphogenetic proteins (BMPs), which are growth factors belonging to the transforming growth factor beta superfamily.<sup>14</sup> BMPs (e.g., BMP-2 and BMP-7) can be added to osteoconductive graft materials like calcium phosphates and polymers to make them osteoinductive. BMP-2 was used in various therapeutic interventions such as bone defects, non-union fractures, osteoporosis, spinal fusion and root canal surgery.<sup>14</sup> Recombinant bone morphogenetic osteoinductive substitutes<sup>15</sup> include composite scaffolds like the Infuse<sup>®</sup> Bone Graft/LT-Cage<sup>®</sup> Lumbar Tapered Fusion for the treatment of degenerative disc disease (DDD) in skeletally mature patients. The Infuse<sup>®</sup> Bone Graft was approved as an alternative to autogenous bone grafts for sinus augmentations, and for localized alveolar ridge augmentations for defects associated with extraction sockets.<sup>16</sup> The Infuse<sup>®</sup> Bone Graft consists of a solution of recombinant human bone morphogenetic protein-2 (rhBMP-2) and an absorbable type I collagen sponge, which acts as a degradable scaffold for the formation of new bone. The Ti alloy LT-Cage<sup>®</sup> Lumbar Tapered Fusion is intended to restore the degenerated disc

space to its original height. Not all components of the Infuse® system are biodegradable, as is the case of the LT-Cage® or of the intramedullary nail used together with the Infuse™ Bone Graft to help heal the fractures of the tibia.<sup>9</sup> Some of the contraindications of Infuse® include: known hypersensitivity to rhBMP-2, bovine Type I collagen or Ti alloy; placement in the vicinity of a resected or extant tumor in patients who are skeletally immature, or in patients with an active infection at the operative site.<sup>17</sup> Along the same lines, the safety and effectiveness of this device during pregnancy or nursing has not been established.<sup>17</sup>

In 2008 the FDA issued a Public Health Notification regarding life-threatening complications associated with rhBMP when used in the cervical spine.<sup>18</sup> There have been several reports of complications, occurring between 2 and 14 days post-op, such as swelling of neck and throat tissue, resulting in compression of the airway and/or neurological structures in the neck; difficulty swallowing, breathing or speaking; and severe dysphagia following cervical spine fusion with rhBMP due to the anatomical proximity of the cervical spine to airway structures in the body. Safety and effectiveness of rhBMP in the cervical spine have not been demonstrated and rhBMP is not approved by FDA for this use.<sup>19</sup>

Additionally, osteoinductive growth factors like BMP-2 are expensive (50 µg BMP-2 are \$955, while 10 µg BMP-7 are \$400<sup>20</sup>), are subject to a limited shelf life,<sup>21</sup> may have adverse effects like antibody formation and immunological reactions, especially in cervical spine surgery when the margin for error is minimal.<sup>22</sup> Incorrect placement of the BMP-carrier can induce undesired ectopic bone formation in surrounding tissues (muscles, nerves, blood vessels).<sup>23</sup>

Another strategy to make bone graft materials osteoinductive is to add mesenchymal stem cells. Cell-based bone graft substitutes include Osteocel Plus, marketed by ACE Surgical Supply, Inc. It has been investigated for various procedures, such as spinal fusion and for intervertebral disc regeneration.<sup>15</sup> The product contains living bone cells, including mesenchymal stem cells. It also contains a polymer scaffold, which helps to enhance and encourage bone growth.<sup>15</sup> Currently, clinical studies for Osteocel Plus are ongoing.<sup>24</sup> Safety and efficacy have not been established for cell-based bone graft substitutes.<sup>9</sup>

While there are several bone graft substitutes available clinically, they are not optimal for healing and/or regenerating bone because of the high cost of using growth factors, high dosing of growth factors, low mechanical properties which require an external fixation device and unestablished safety and efficacy.<sup>3</sup> While some of the characteristics of ideal bone grafts have been met: cytocompatibility, osteoinductivity, moldability, peripheric vascularization, handling in the operating room, degradability, there is still room for improvement. A good vascular supply is imperative for the successful integration of a bone graft. Histological analysis of bone grafts demonstrates only 2-3 mm of vascular invasion into the material.<sup>25</sup> To increase and maintain the vascular supply and to avoid necrosis at the core<sup>26</sup>, a blood vessel may be implanted or vascular channels and necessary growth factors may be incorporated into the scaffold.<sup>25</sup>

Two characteristics to consider when evaluating bone grafts are stiffness and degradation. Although both are desired, stiffness is inversely proportional to degradation or polymer chain scission<sup>27</sup> below the glass transition temperature of chitosan<sup>28</sup>, so the right balance has to be achieved. Some bone grafts have the Young's modulus of cortical bone, but show low degradation *in vitro* after six weeks (12%) and *in vivo* after one



month.<sup>29</sup> Other bone grafts may have compressive strength close to that of bone, but biocompatibility has not been assessed.<sup>30</sup> Further, other bone grafts may even replace cancellous bone due to Young's modulus at lower limit for cancellous bone, but are brittle,<sup>31</sup> while other bone grafts have Young's modulus too high even for cortical bone replacement and are brittle.<sup>32</sup>

Chitosan, a polysaccharide from the exoskeleton of crustaceans, is one of the promising bone graft biomaterials due to its attractive properties: osteoconductivity, biocompatibility, non-toxic and non-acidic degradation products.<sup>33-39</sup> Chitosan also promotes wound healing, is mucoadhesive, antibacterial and moldable into three-dimensional (3D) scaffolds, can deliver antibiotics and bone morphogenetic proteins (in case the latter become cheaper in the future for treatment of a larger population).<sup>33-39</sup>

To address the limits of autografts and allografts, our research group had previously developed composite co-precipitated chitosan/nanohydroxyapatite microsphere-based scaffolds as bone graft substitutes, which may also be used to deliver drugs locally.<sup>40-42</sup> The 3-D scaffolds mimic the porous architecture of cancellous bone and have good biocompatibility with osteoblasts, supporting new bone ingrowth *in vitro* and *in vivo*.<sup>40,41</sup> Young's modulus ( $9.3 \pm 0.8$  MPa) approached the values for cancellous bone (10-2000 MPa).<sup>43</sup> The microspheres/microparticles or scaffolds can be loaded with antibiotics and/or growth factors to enhance osteoconductivity and biocompatibility at complex fracture sites, such as comminuted fractures and segmental bone defects.<sup>42</sup> One drawback of these scaffolds is a slow degradation profile,<sup>40-42</sup> that can be attributed in part to the high degree of deacetylation (DDA). The high DDA may limit the bone ingrowth and reduce the overall bone regeneration.<sup>44</sup>

We would like not only to maintain the desirable mechanical, cytocompatible or osteoconductive characteristics of chitosan-calcium phosphate microsphere-based scaffolds, but also to increase degradation and tissue ingrowth characteristics of the scaffold. This was achieved by adding a more degradable polymer to the composite composition. Collagen is a biocompatible and degradable natural polymer that can be easily combined with chitosan since both are soluble in dilute acids. Additionally, the inclusion of collagen will help to mimic the native bone extracellular matrix since collagen is a major constituent of bone along with the calcium phosphate mineral. We envision/hypothesize that adding collagen to our chitosan-calcium phosphate composite will improve degradation of the scaffold material without compromising initial mechanical properties.

## **1.2 Hypothesis and objectives**

Our goal is to develop a scaffold that maintains mechanical strength during the first 4 months with increased degradation over time. The 4 months are chosen knowing that the reparative phase of bone healing takes around 18 weeks.<sup>45</sup> Further, we would like the scaffold to degrade completely within 13 months because the remodeling phase and maturation of bone takes up to 54 weeks.<sup>46</sup> This proposal would allow the native bone to regenerate and fill the void.

Our research approach is to incorporate collagen in a chitosan-based composite to make a more biomimetic construct, composed of collagen, chitosan (a natural polymer) and a mineral, calcium phosphate. Chitosan, which contains glucosamine, mimics the glycosaminoglycan-components of the extracellular matrix, can actively direct the behavior of cells to facilitate regeneration of bone, is osteoconductive, biocompatible, mucoadhesive, antibacterial, moldable into three-dimensional (3D) scaffolds and has non-

toxic and non-acidic degradation products.<sup>33-39</sup> Calcium phosphate mimics the chemical structure of native bone mineral and provides mechanical strength due to its ceramic structure. Collagen type I will provide an additional biomimetic component to the composite because it is the most prevalent protein in the extracellular matrix of bone and is also biodegradable.<sup>47</sup> Collagen concentration was chosen as 25% because this value is almost constant with age in tibial trabecular bone.<sup>48</sup> 10% collagen was chosen arbitrarily as an intermediate concentration between 0 and 25%.

**We hypothesize that the incorporation of collagen type I into chitosan-calcium phosphate composite microspheres increases the degradation rate of the chitosan-calcium phosphate microspheres and microsphere-based scaffolds. Furthermore, we hypothesize that incorporating collagen type I into chitosan-calcium phosphate microspheres will increase the compatibility of microspheres with osteoblasts and fibroblasts and of scaffolds with osteoblasts.**

### **1.2.1 Objectives**

To test these hypotheses, the following specific objectives were undertaken:

#### ***Objective I***

Prepare and characterize composite collagen-chitosan-calcium phosphate microparticles.

- a) Incorporate collagen into chitosan-calcium phosphate microparticles (10 mass% and 25 mass%) via a drip co-precipitation method.
- b) Determine the amount of type I collagen within the composite collagen-chitosan-calcium phosphate microparticles.
- c) Determine the amount of calcium phosphate within the microparticles.
- d) Characterize the composite collagen-chitosan-calcium phosphate

microparticles for shape using digital microscopy; for crystallinity via x-ray diffraction spectrometry.

### ***Objective II***

Characterize the *in vitro* degradation profile and cytocompatibility of composite collagen-chitosan-calcium phosphate microparticles.

- a) Determine the percent change in mass of the composite microparticles over a six week-period in a lysozyme-collagenase solution as compared to plain chitosan microparticles.
- b) Determine the percent cell attachment on the surface of the composite microparticles as compared to chitosan-calcium phosphate microspheres.
- c) Determine the proliferation of cells on the surface of the composite microspheres quantitatively as well as qualitatively as compared to chitosan-calcium phosphate microspheres.

### ***Objective III***

Characterize the porosity, and mechanical compressive properties of composite scaffolds based on fusion of collagen-chitosan-calcium phosphate microparticles using acetic acid and glycolic acid.

- a) Determine the porosity of the scaffolds via Archimedes' principle.
- b) Determine Young's compressive modulus of the scaffolds via compression testing of hydrated constructs.

### ***Objective IV***

Characterize the *in vitro* degradation profile and cytocompatibility of composite collagen-chitosan-calcium phosphate scaffolds.

- a) Determine the percent change in mass of the composite scaffolds over a month-period in a lysozyme-collagenase solution as compared to chitosan-calcium phosphate scaffolds.
- b) Determine the percent cell attachment on the surface of the composite scaffolds as compared to chitosan-calcium phosphate scaffolds.
- c) Determine the proliferation of cells on the surface of the composite scaffolds quantitatively, as well as qualitatively, as compared to chitosan-calcium phosphate scaffolds.

### **1.2.2 Significance**

We propose that the fabrication of composite chitosan-collagen-calcium phosphate microspheres using a co-precipitation method will result in a bone graft substitute material that will be effective at healing the bone defect. The incorporation of collagen would make the composites more compatible (since bone is composed of collagen) and help increase the degradation rate of chitosan scaffolds without losing initial mechanical strength or the overall osteoconductivity of the polymer-ceramic composite. This preliminary research is significant as the results would provide data to support the potential use of a composite collagen-chitosan-calcium phosphate micro-particle system as a tissue filler or part of bone graft material (mimicking cancellous bone) for bone tissue engineering applications *in vivo* before starting clinical trials.

## **CHAPTER 2: BACKGROUND AND LITERATURE REVIEW**

### **2.1 Brief description of skeleton and bones**

Bones are organs of the skeletal system.<sup>49</sup> Bone tissue, one of the specialized connective tissues, is characterized by a mineralized extracellular matrix.<sup>50</sup> The mineralization of the matrix is the reason why bone is an extremely hard tissue that is capable of providing support and protection to the body.<sup>50</sup>

#### **2.1.1 Bone classification**

Bone can be divided in two major types: cortical and cancellous. Cortical bone forms the outside of the bone and is a compact and dense layer, while cancellous bone forms the interior of the bone and consists of trabeculae (thin, anastomosing spicules of bone tissue), weaved in a sponge-like meshwork.<sup>49</sup> The spaces within the meshwork are continuous and are occupied by marrow and blood vessels in living bone.<sup>49</sup> Cancellous bone is typically found at the core of cuboid bones, such as vertebral bones in the spine, and at the ends of the long bones, such as the femur or tibia.<sup>51</sup>

#### **2.1.2 Bone anatomy**

The mineral in the extracellular matrix of bone is calcium phosphate, mainly in the form of hydroxyapatite crystals,  $\text{Ca}_{10}(\text{PO}_4)_6(\text{OH})_2$ .<sup>50</sup> Thus, bone provides a storage site for  $\text{Ca}^{2+}$  and  $\text{PO}_4^{3-}$ .<sup>50</sup> Both can be mobilized from the bone matrix and taken up by the blood as needed to maintain normal levels.<sup>50</sup> At the molecular level, the mineralized collagen fibrils of bone are made up of strings of alternating collagen molecules and hydroxyapatite, HA crystals, which appear in stair-step configuration.<sup>52</sup> When pressure is applied to the fibrils, some of the weak bonds between the collagen molecules and HA crystals break, creating small gaps in the fibrils.<sup>52</sup> The gaps spread the pressure over a broader area and protect other, stronger bonds within the collagen molecule itself, which

might break if all the pressure were focused on it.<sup>52</sup> The stretching between fibrils lets the tiny HA crystals shift position in response to the force, rather than shatter, which would be the likely response of a larger crystal.<sup>52</sup> Hydroxyapatite crystals are chalk-like<sup>52</sup> and have 30 nm in length and about 2 nm in thickness.<sup>53</sup> Hydroxyapatite significantly enhances the tensile modulus and strength of bone compared with a tropocollagen molecule alone.<sup>54</sup> The stiffening effect depends on the thickness of the mineral crystal until a plateau is reached at 2 nm.<sup>54</sup>

As previously mentioned, bone matrix contains type I collagen (90%) and, in small amounts, a number of other types of collagen (i.e., types V, III, XI and XIII).<sup>50,55</sup> Other proteins that constitute the ground substance of bone are present, such as proteoglycan molecules (which contain a core protein with various numbers of covalently attached side chains of glycosaminoglycans), multi-adhesive glycoproteins, bone-specific vitamin K-dependent proteins, growth factors and cytokines.<sup>50</sup> The inorganic part of bone consists of calcium carbonate, magnesium, sodium, sulfate, potassium, chloride, nitrogen, fluoride and 20% water.<sup>55,56</sup>

There are five types of cells. Firstly, osteocytes are cells found within spaces (lacunae) in the matrix.<sup>49</sup> Each osteocyte extends processes to communicate with cell processes of neighboring osteocytes through gap junctions.<sup>49</sup> Bone depends on osteocytes to maintain viability.<sup>49</sup> Secondly, osteoprogenitor cells are cells derived from mesenchymal stem cells, which give rise to osteoblasts.<sup>49</sup> Thirdly, osteoblasts are cells that secrete the extracellular matrix of bone.<sup>49</sup> Once the cell is surrounded by its secreted matrix, it is called osteocyte. Fourthly, bone-lining cells are cells that remain on the bone surface when no active growth occurs.<sup>49</sup> They are derived from those osteoblasts that

remain after the bone deposition ceases.<sup>49</sup> Fifthly, osteoclasts are phagocytic cells, which remove bone or are present where the bone has been damaged or is being remodeled.<sup>49</sup>

Bones are covered by periosteum, a sheath of dense fibrous connective tissue containing osteoprogenitor cells.<sup>49</sup> Bones that articulate with neighboring bones possess synovial joints covered by hyaline cartilage.<sup>49</sup> Bone cavities are lined by the endosteum, a layer of connective tissue containing osteoprogenitor cells.<sup>49</sup> The medullary cavity and the spaces in spongy bone contain bone marrow.<sup>49</sup> Mature compact bone is composed of cylindrical units called osteons or Haversian canals.<sup>49</sup> The osteons are composed of concentric lamellae of bone matrix surrounding the central, Haversian canal, which contains the vascular and the nerve supply of the osteon.<sup>49</sup> Interstitial lamellae are remnants of previous concentric lamellae between osteons.<sup>49</sup> Because of this organization, mature bone is also called lamellar bone.<sup>49</sup> Circumferential lamellae follow the entire inner and outer surfaces of the shaft of a long bone, appearing much like the growth rings of a tree.<sup>49</sup> Perforating canals (Volkmann's canals) are channels in lamellar bone through which blood vessels and nerves travel from the periosteum and endosteum to reach the Haversian canal, as well as connecting one Haversian canal to another.<sup>49</sup> The blood that nourishes bone moves from the marrow cavity into and through the bone tissue and out via periosteal veins.<sup>49</sup> Thus, the flow to bone tissue is essentially centrifugal.<sup>49</sup>

## **2.2 Bone injury and repair**

In the US approximately six million bone fractures occur each year.<sup>45</sup> Five to ten percent of all fractures will have insufficient repair.<sup>45,57</sup> Worldwide, in 2000 it was estimated that 9 million new osteoporotic fractures occurred, of which 1.6 million were at the hip, 1.7 million were at the forearm and 1.4 million were clinical vertebral fractures.<sup>58</sup> The Americas and Europe accounted for 51% of all these fractures, while



most of the remainder occurred in the Western Pacific region and Southeast Asia.<sup>58</sup>

Osteoporosis and consequently, bone fractures take a huge toll: in Europe, the disability due to osteoporosis is greater than that caused by cancer (with the exception of lung cancer) and is comparable or greater than that lost to a variety of chronic diseases, such as rheumatoid arthritis, asthma and high blood pressure related heart disease.<sup>58</sup>

Regarding military injuries, the musculoskeletal combat casualty rate for a US Army Brigade Combat Team during operation Iraqi freedom was 34.2 per 1,000 soldier combat-years.<sup>59</sup> Spine, pelvis, and long bone fractures comprised 55.9% of the total fractures sustained in combat.<sup>59</sup> Open fractures comprised 5.0 per 1,000 combat-years.<sup>59</sup>

Natural disasters also have a high incidence of orthopaedic trauma. For example, other than wound debridement, the most commonly performed procedure during the first three weeks after the 2010 earthquake in Haiti was fixation of long bone fractures, which constituted approximately one third of all surgical procedures.<sup>60</sup>

For car accidents orthopaedic trauma, in a defined area of central Sydney from mid-1991 to mid-1994, 21.5% of all adult car occupants and 49% of pedestrians sustaining major injury suffered lower extremity long bone fractures.<sup>61</sup>

For malignancies of the bone reported by the Surveillance, Epidemiology and End Results (SEER) program areas from 1975 to 1995, the average annual incidence rate was 8.7 per million children younger than 20 years of age, comprising about 6% of childhood cancer.<sup>62</sup> Bone cancer non-unions arise from this population with bone malignancies.

A retrospective study of 120 consecutive patients treated by a single surgeon for delayed or failed bone healing with a direct current bone stimulator, showed 86.8% fracture non-unions, 3.3% arthrodesis non-unions, 2.5% osteotomy non-unions, 4.1%

malunion osteotomy, and 3.3% primary fixation of open fractures with large segmental bony defects.<sup>63</sup>

The cases of orthopaedic fractures listed above shows the potential market for bone grafts. In 2010, it was estimated that 600,000 bone graft procedures are performed in the United States annually, and roughly 2.2 million procedures are performed worldwide, which cost approximately \$2.5 billion per year.<sup>64</sup>

A fracture is a break in bone, which, in some cases, results in bleeding at the fracture site.<sup>65</sup> The initial strength of the bone, the magnitude, direction and rate at which force is applied determine the extent of the fracture.<sup>66</sup> Fractures can be caused by sudden, high impact forces or by low-level cyclic forces.<sup>66</sup> Sudden, high energy forces produce some of the most severe fractures: comminuted and segmental bone fractures.<sup>67-70</sup>

Comminuted fractures have more than two fragments, while segmented fractures are the ones in which the bone fragment is completely separated from non-fractured bone by fracture lines.<sup>70</sup> In closed (simple) fractures in which the skin is not breached, normal bone healing takes place. Bone healing occurs in three different stages: the early inflammatory stage (hematoma formation), the repair stage (the fibrocartilaginous and bony callus formation) and the remodeling stage.<sup>55,57,69,70</sup> When a fracture occurs, not only is there a discontinuity in the bone, but also in the surrounding vascular system.<sup>66</sup> A hematoma forms at the fracture site and inflammatory cells and fibroblasts migrate to the fracture site due to prostaglandin and growth factor release.<sup>66</sup> Next, granulation tissue is formed, vascular ingrowth is initiated and mesenchymal cells begin to migrate to the fracture site.<sup>55,57,70</sup> In the repair stage, as the blood supply to the fracture area improves, osteoblasts secrete osteoid and a collagen matrix is formed.<sup>66</sup> Four to six weeks after the initial fracture the periosteum undergoes intramembraneous ossification and a

fibrocartilaginous, soft external callus is formed. The internal osteoid mineralizes and the internal callus develops into woven bone. In the last stage of bone healing, the woven bone is replaced by cortical bone and the bone is restored to its original shape and strength.<sup>55,57</sup> Bone remodeling can last for months to years and occurs where forces require it, as stated by Wolff's law.<sup>55</sup>

In large comminuted or open compound fractures, the vascular supply to the bone tissue may be completely destroyed. Segmental and comminuted fractures are at increased risk for the development of non-unions (no development between bone fragments) and for becoming infected and developing osteomyelitis.<sup>67-71</sup> These two types of fractures are so discomfoting because the blood supply to the fracture area is destroyed and necrosis of the bone can occur. These fractures can be caused by war injuries, motor vehicle accidents, gunshot wounds and crush injuries.<sup>67,68</sup> Normal bone healing does not occur in large fractures/injuries where the vasculature is destroyed. To treat these situations, bone grafts are used to fill in the gap and to help heal the bone in order to maintain normal geometry and size of the bone.

The ability of bone to repair itself is lost in a critical size defect. Factors that cause critical size defects include non-unions, bone cancer and birth defects. The critical size bone defect in humans is not clearly defined, but usually a defect > 1cm is considered to be a critical-sized defect.<sup>72</sup> The length of segmental bone defects ranges from 0.4 to 7.6 cm and depends on the anatomical location of the defect.<sup>73</sup> Usually, the treatment of critical size bone defects involves bone graft implantation in conjunction with internal fixation in addition to long-lasting therapies to restore bone continuity and stability.<sup>74,75</sup>

## **2.3 Bone grafts**

Current treatment options for non-unions and bone defects include: autografts, allografts and synthetic bone grafts.

**2.3.1 Autografts** are bone grafts which come from the patient's body. Considered the "gold standard" by many surgeons, it has very good osteoconductivity and also great osteoinductivity due to its high content of resident growth factors.<sup>6</sup> The disadvantages are: the higher morbidity of the donor site, the secondary surgical access in a remote location of the body in order to harvest the bone (hip, for larger quantities, chin or the back of the jaw).<sup>6</sup> Autogenous bone grafts have shown to be some of the most predictable grafts in surgery<sup>6</sup> and are highly dependent on the quality of the patient's bone.

**2.3.2 Allografts** are a close relative of the autograft, in that they are of human origin, usually from cadavers from a bone bank.<sup>6</sup> Despite the lack of a secondary surgery for harvest and the osteoconductive properties, allografts have very little if any osteoinductive properties because they lack bone cells and exposed osteoinductive proteins.<sup>6</sup> Thus, graft assimilation and maturation takes longer than with the autografts.<sup>6</sup>

### **2.3.3 Synthetic bone grafts**

Due to the disadvantages of autografts and allografts, scientists have looked for alternatives with quicker recovery times, lower costs and reduced risks, such as synthetic bone grafts. In these, scientists have tried to tailor biophysical properties so that an ideal scaffold can result.

In case bone fails to unite over a defect, a bone graft offers a framework on which cells can attach and proliferate.<sup>76</sup> The sine qua non for success of bone grafts includes:

1. Interconnective pores to promote osseointegration and vascularization<sup>77</sup>

2. Controlled biodegradability so that the tissue will eventually replace the scaffold
3. Adequate surface chemistry to favor cell attachment, proliferation and differentiation
4. Appropriate mechanical properties to match the intended site of implantation and handling
5. No serious adverse effects
6. Easy manufacture and sterilization
7. Easy handling in the operating room<sup>45,76</sup>

Porosity, as a physical parameter, should provide adequate space for cell migration and expansion and maintain the transport of nutrients and waste products.<sup>78</sup>

Various percentages exist for 3D scaffold fabrication, with porosities ranging from 10 to 97%.<sup>79</sup> However, increasing the porosity decreases mechanical strength, so a balance has to be achieved between porosity and mechanical stability.<sup>80</sup> Scaffold pores ought to be at least 50  $\mu\text{m}$  to promote osteogenesis.<sup>66</sup>

A scaffold ought to maintain mechanical strength during the first 4 months with increased degradation over time because the reparative phase of bone healing takes around 18 weeks.<sup>45</sup> Further, the scaffold ought to degrade completely within 13 months because the remodeling phase and maturation of bone takes up to 54 weeks.<sup>46</sup> This would allow the native bone to regenerate and fill the void.

Cells respond to the chemistry, topography and surface energy of the substrates with which they interact.<sup>45</sup> The material substrates should have molecules of the extracellular matrix and initiate the attachment of proteins of the right type, amount and conformation, which modulate cell functions.<sup>81</sup> It was shown that hydrophobic

biomaterials promote the adsorption and retention of proteins like fibronectin and fibrinogen.<sup>82</sup> Moreover, calcium-based ceramics dissolve and precipitate on their surface, forming a carbonate-containing hydroxyapatite layer, which is osteoconductive.<sup>83</sup>

Scaffolds should have no adverse side effects like immunogenicity, cytotoxicity and tumorigenicity.<sup>45</sup> Scaffolds should be easy to manufacture and sterilize (without compromising properties) for mass production. Bone grafts should be easy to handle in the operating room, without preparatory procedures so that infections would be minimized.

### **2.3.3.1 Ceramics**

Ceramic-based bone grafts include calcium phosphate, calcium sulfate, and bioglass, which can be used alone or in combination with other materials.

Most of the ceramic-based bone graft substitutes currently available are calcium phosphates.<sup>15</sup> Several types of calcium phosphates exist: tricalcium phosphate, synthetic hydroxyapatite, and coralline hydroxyapatite, and are available in pastes, putties, solid matrices, and granules.<sup>15</sup> Such calcium phosphate products include Bio-Oss (Osteohealth, Inc, Shirley, New York) and OsteoGraf.<sup>15</sup> Bio-Oss uses hydroxyapatite as a particulate while OsteoGraf uses HA as blocks and particulates.<sup>15</sup> Vitoss (Orthovita, Inc) is a tricalcium phosphate available in the form of a solid piece, putties or pastes.<sup>15</sup> ProOsteon is a unique product based on sea coral, which contains HA and is similar in structure to trabecular bone. Nevertheless, like many of the solid calcium phosphates, ProOsteon is brittle and not suitable for use in load-bearing sites.<sup>15</sup>

Vitoss<sup>®</sup> Scaffold Synthetic Cancellous is a non-load bearing calcium phosphate-based Bone Void Filler (Orthovita Inc.) indicated for use in the treatment of surgically created osseous defects or osseous defects resulting from traumatic injury to the bone

(i.e., the extremities, spine, and pelvis).<sup>9</sup> It can be administrated using a prefilled syringe.<sup>9</sup> The surgeon can use either a secondary syringe or the vacuum line to aspirate blood or marrow into the Vitoss-Filled Cartridge.<sup>9</sup> Bone void fillers similar to Vitoss include Biosorb<sup>®</sup> Resorbable Bone Filler (Science for Biomaterials) and chronOS<sup>™</sup> (Synthes-Stratec Inc.), although they are less porous.<sup>9</sup> Similar to other  $\beta$ -TCP, Cross Bone is a resorbable, biphasic ceramic implant composed of 60% hydroxyapatite and 40%  $\beta$ -TCP in the form of granules used for bone reconstruction.<sup>9</sup> Examples of calcium phosphate-based bone grafts include: Actifuse (a silicate-substituted calcium phosphate), BoneSource, BoneSave, HydroSet (Stryker, Kalamazoo, Missouri), and OsSatura TCP from Integra Orthobiologics, Plainsboro, New Jersey (pure  $\beta$ -TCP; it forms a well-defined interconnected porosity that provides a high level of osteoconductivity).<sup>15</sup>

Calcium phosphates are easily handled as putties or pastes, but do not have appropriate mechanical properties for load-bearing sites because they are brittle at high Young's modulus (in the case of hydroxyapatite). One more important issue with calcium phosphates is that they can possess a slow degradation rate, which may vary from months to years or it might even be incomplete.<sup>84</sup>

Calcium sulfate, also known as plaster of Paris, is biocompatible, bioactive, and resorbable after 30-60 days.<sup>15</sup> Because of its rapid degradation it also rapidly loses its mechanical properties.<sup>15</sup> Hence, it is a questionable choice for load-bearing applications.<sup>15</sup> Calcium-sulfate bone grafts include: Osteoset, a tablet for use for defect packing which is degraded in approximately 60 days (Wright Medical technology, Inc.) and AlloMatrix, which is Osteoset combined with demineralized bone matrix, DBM. The latter is sold as a putty or an injectable paste.<sup>15</sup> However, a 13.8%-19.0% incidence of self-limited and benign adverse reaction was reported to OsteoSet bone graft substitute, a

surgical grade calcium sulfate in a pure, uniform, crystalline form (Wright Medical)<sup>85</sup>, which spurs the quest for new materials or material combinations for bone grafts. As there is no known cell-mediated regulatory connection between the degradation of calcium sulfate cements and the new bone formation, there is a risk that degradation might be too rapid, causing a new space if bone formation is not fast enough.<sup>86</sup>

Bioactive glass (in particular, bioglass) is a biologically active silicate-based glass.<sup>15</sup> Its applications are limited by high modulus and brittle, but it has been used in combination with polymethylmethacrylate to form bioactive bone cement. It has also been used as a coating on metal implants in the form a calcium-deficient carbonated calcium phosphate layer, which facilitates the chemical bonding of the implant to surrounding bone. Products from bioglass include Biogran (developed by Orthovita and licensed to Biomet 3i, Implant Innovations, Inc, Palm Beach Gardens, Florida) and Novabone (NovaBone Products, LLC, Alachua, Florida).

In conclusion, the advantages of ceramics for bone grafts are: similarity to the mineral phase of bone—making them osteoconductive—their ability to form direct bonds with the surrounding bone, biocompatibility and minimal immunological and foreign body reactions due to the lack of proteins associated with them.<sup>8</sup> The disadvantages of ceramics are: lack of osteoinductivity,<sup>8</sup> brittleness, the difficulty to machine into complex shapes and porous constructs, and low degradation for the ceramics with Young's modulus close to that of cancellous<sup>29</sup> or cortical bone.<sup>87</sup>

### **2.3.3.2 Polymers**

Polymers used as bone graft substitutes for bone tissue engineering applications can be either derived from natural sources: polysaccharides such as alginate, chitin, chitosan and hyaluronic acid, or proteins such as soy, collagen, fibrin



and silk--or from synthetic sources: poly(lactic acid), poly(glycolic acid), poly(lactide-co-glycolide), poly( $\epsilon$ -caprolactone) and polyhydroxybutyrate.<sup>10,88,89</sup> On one hand, naturally derived polymers are known to support cell attachment but have poor mechanical strength.<sup>10</sup> On the other hand, synthetic polymers have relatively good mechanical strength (however, in the porous form required for a bone graft, their Young's modulus is below the 10 MPa inferior limit of cancellous bone, e.g. PCL scaffolds<sup>11</sup>), tunable degradation rates and can be manipulated into desired shapes, but may have undesirable acidic degradation products, which may stimulate an inflammatory reaction.<sup>12,13</sup> Examples include: Cortoss (Orthovita, Inc, Malvern, PA), made of bis-glycidyl methacrylate; Open Porosity Poly(lactic Acid) polymer, OPLA, (TMH Biomedical, Inc., Duluth, MN), made of a PLA/PGA copolymer; Immix (Osteobiologics, Smith and Nephew, Memphis, Tennessee), made of a PLA/PGA copolymer as the base material and PGA fibers, Bioglass (a 45S5-type glass), and calcium sulfate as additives to vary stiffness; and Healos (Depuy Orthopaedics Inc, Warsaw, Indiana), an osteoconductive matrix made of cross-linked collagen fibers that are fully coated with HA through a proprietary 360 accretion process).<sup>15</sup> Lastly, Ahn et al. produced highly porous and surface-roughened/layer-by-layer 3D poly( $\epsilon$ -caprolactone) scaffolds with thickness of more than 2 mm with high osteoblast-like MG63 cell viability, increased ALP activity and calcium mineral.<sup>90</sup> One of their limitations is the stable size control of micro/nanosized electrohydrodynamic direct-printed struts.<sup>90</sup>

### **2.3.3.3 Composites**

Composite systems maximize the advantages of two or more materials, while minimizing their individual disadvantages. Three examples of bone void fillers available on the market are provided:

1. Healos (DePuy Orthopaedics, Inc, Warsaw, Ind) is a polymer-ceramic composite consisting of collagen fibers coated with hydroxyapatite and indicated for spinal fusions,<sup>15</sup> which is osteoconductive and stronger than collagen alone due to addition of hydroxyapatite, a crystalline form of calcium phosphate. However, neither does it bear loads, nor does it have a dual structure to mimic the cortical and cancellous lamellar composition of bone. All available bone graft materials are limited in the latter regard: they do not mimic the 3D bone architecture of bone. Using solely a cancellous bone replacement consists in the use of external fixation devices, which have to be removed surgically, while cortical bone replacements used as a stand-alone may cause stress-shielding.
2. The Vitoss<sup>®</sup> Scaffold Foam<sup>™</sup> (Orthovita Inc., Malvern, PA), a bone void filler, consists of a mixture of  $\beta$ -tricalcium phosphate,  $\beta$ -TCP, and Type I bovine collagen in a hydroxyapatite carrier.<sup>9</sup> Used alone, this product does not have osteoinductive properties, and, since most if it is made of  $\beta$ -TCP, it is brittle.<sup>91</sup>
3. Integra MOZAIK<sup>™</sup> Osteoconductive Scaffold (Integra LifeSciences Plainsboro Township, NJ ) is made of 80% tricalcium phosphate and 20% type I collagen; it resorbs at a rate consistent with the formation of new

bone<sup>15</sup>. Similarly, this product does not have osteoinductive properties, and, since most of it is made of  $\beta$ -TCP, it is brittle.

Several research labs are investigating alternative bone grafts: Chen et al. developed a PLLA scaffold with apatite/collagen composite coating.<sup>92</sup> PLLA scaffolds with apatite/collagen coating exhibited better Saos-2 cell viability than uncoated PLLA scaffolds or PLLA scaffolds with hydroxyapatite coating<sup>92</sup>. Similarly, Kim et al. produced porous poly(D,L-lactic-co-glycolic acid)/nanohydroxyapatite (PLGA/ HA) composite scaffolds, coated with HA in simulated body fluid, SBF. The PLGA/HA scaffolds exhibited higher osteoblast cell growth, alkaline phosphatase activity and mineralization than PLGA scaffolds<sup>93</sup>. Ciapetti et al. found that the HA-added poly( $\epsilon$ -caprolactone)-based polymers obtained the best colonization by Saos-2 cells after 3-4 weeks and that more mineral was formed on HA-added poly(caprolactone)-based polymers coated in simulated body fluid, SBF than on PCL-based polymers.<sup>94</sup> Lickorish et al. found that a porous, collagenous scaffold, biomimetically coated with hydroxyapatite using SBF, supported L-929 fibroblasts and rabbit periosteal cellular attachment and proliferation (it is assumed that the scaffold is weak because the majority of the scaffold is comprised of collagen).<sup>95</sup> MG63 osteoblasts attached to collagen-derived gelatin/hydroxyapatite (HA) nanocomposites to a significantly higher degree and subsequently proliferated more than those conventionally mixed gelatin-HA composites.<sup>96</sup> The nanocomposite scaffolds retained less-crystallized and smaller-sized apatite crystals (~40 nm) and a more developed pore configuration than the conventional ones.<sup>96</sup> Collagen beads can be formed by extruding collagen solution into chondroitin sulfate A solution.<sup>97</sup> Subsequently, the collagen beads thus formed are soaked in SBF solution to form nanohydroxyapatite on the surface and mimic the

formation process of natural bone matrix, providing a substrate for cell growth and enhancing the osteoblast-like cell differentiation of MG63 cells.<sup>97</sup> Further, MC3T3-E1 cells proliferated on poly-L-lactic acid (PLLA), chitosan and hydroxyapatite (HA) microsphere-based scaffolds (macroporosity >50%) and formed an extracellular matrix network, while differentiating into mature osteoblasts, as indicated by alkaline phosphatase activity.<sup>98</sup> While no degradation was assessed, Young's modulus of 0.42 MPa indicated their use in non-load bearing applications.<sup>98</sup> In spite of the promising cell growth (osteoblasts, in particular) and even increased ALP activity and mineralization in some cases, the mechanical properties constitute an issue that needs to be addressed so that the scaffolds may become load-bearing.

Recently, a calcium phosphate/polyurethane with both HA and  $\beta$ -TCP composites was developed for weight-bearing implants.<sup>29</sup> Although it reached high compressive modulus values which ranged from 2.5 to 3.6 GPa, this potential bone graft cannot be used to replace cancellous bone and may cause stress shielding. Although the clonal osteoblastic cell line, 2T3, isolated from murine calvaria shows the biocompatibility of the implants, both the *in vitro* (12% degradation after 6 weeks) and *in vivo* degradation in a rat model are low.<sup>29</sup> The problem with the low degradation rate is that the bone defect is not completely healed, since the partly degraded scaffold-new bone combination may not be as stiff and cohesive as native bone itself.

Chitosan, a natural-based nontoxic, biocompatible, and biodegradable polymer with anti-microbial activity, is also reported to promote osteogenic progenitor cell recruitment and attachment, facilitating bone formation.<sup>38,99</sup> Chitosan and its derivatives are believed to accelerate wound healing by enhancing the functions of inflammatory

cells and repairing cells.<sup>38</sup> Recent studies further indicated that chitosan and its derivatives also are novel scaffold materials for tissue engineering and gene delivery.<sup>38</sup>

One property of chitosan that must be taken into account when designing chitosan biomaterials is the degree of deacetylation (DDA). Chitin has no DDA or 0% DDA, while pure chitosan has 100% DDA.<sup>66</sup> Chitosan materials with DDA close to 50% are the most degradable *in vitro* and *in vivo*.<sup>33,38,100</sup> Below or above 50% DDA, chitosan loses degradability due to the fact that its chains pack more closely together, giving it a more crystalline character.<sup>66</sup> Chitosan with DDA>95% has been known to last for months.<sup>33,38,100</sup>

Chitosan has been modified or combined with other materials in bone regeneration. For example, lyophilized N,N-dicarboxymethyl chitosan-calcium phosphate sponges quicken bone wound healing in femurs of sheep and in humans undergoing apicectomies and dental avulsions.<sup>101</sup> However, the surgical defect in sheep was filled with a tissue without the histoarchitectural characteristic of bone tissue and the dental defect was weakly load-bearing, so the bone graft is non-load-bearing.<sup>101</sup> Hydroxyapatite-chitin lyophilized gels were loaded with MSC-induced osteoblasts were reported to be osteoinductive and exhibited neovascularization and rapid degradation after 3 months *in vivo* compared to the chitin control.<sup>102</sup> The imidazole-linked chitosan material promoted mineralization, induced bone formation and filled critical size bone defects with the apposition of trabecular bone in the femoral condyle of sheep.<sup>103</sup> Chitosan/tricalcium phosphate sponges incorporating platelet-derived growth factor (PDGF) induced new bone formation in a rat calvarial defect.<sup>104</sup> Chitosan-alginate gel/mesenchymal stem cells/bone morphogenetic protein-2 composites were found to stimulate new bone formation when injected into a mouse.<sup>105</sup> Even though most of these

chitosan gels and sponges stimulate bone formation, they still lack stiffness needed for load-bearing applications or the quality of the bone produced is poor (i.e. cancellous bone on the outside with a central mineralization nodule in association with a fibrous component).<sup>103</sup>

Other groups are also struggling with degradation of chitosan scaffolds: 3D-bioplotting, cell-seeded tricalciumphosphate/chitosan/collagen and tricalciumphosphate/collagen scaffolds increased the amount of newly formed bone within ovine critical-size calvarial defects, but stiffness and biodegradation of materials are not appropriate for the application in cranio-facial surgery and have to be improved.<sup>106</sup>

When compared to plain chitosan scaffolds, composite chitosan-hydroxapatite scaffolds exhibited rougher surface and greater surface area for cell attachment, about 3x higher Young's modulus and increased pre-osteoblast proliferation.<sup>107</sup> The chitosan-crystalline calcium phosphate scaffolds were tougher and more flexible than what has been reported for pure calcium phosphate scaffolds.<sup>107</sup>

Several researchers have investigated chitosan,<sup>108-111</sup> and chitosan composites with calcium phosphate,<sup>40,112-114</sup> beta-tricalcium phosphate ( $\beta$ -TCP) and gelatin crosslinked with glutaraldehyde,<sup>115</sup> collagen,<sup>116</sup> hydroxyapatite,<sup>117-119</sup> but the shortcoming of the materials is that their Young's modulus was below that of cancellous bone. For collagen-based implants reinforced by chitin fibers values for mechanical strength were not reported, which may be low due to the collagen base material.<sup>120</sup> Macroporous HA/ $\beta$ -TCP nesting chitosan sponges exhibited higher Young's modulus of 15 MPa, but they are brittle due to high percentage of ceramics.<sup>31</sup> Further, it was reported that Young's modulus of nanocomposites of chitosan-hydroxyapatite-polygalacturonan was 23.63 GPa, which is too high even for cortical bone replacement;

moreover, the composites can be brittle in nature due to HA.<sup>32</sup> In another study by Li et al. 30/70 chitosan/n-HA composite had compressive strength of 119.86 MPa close to that of bone, but no cell studies were pursued.<sup>30</sup> Lastly, cellulose derivatives-based scaffolds showed Young's modulus and strength in the mid-range of human trabecular bone, but had low degradation: mass loss of 10-15% after 6 months.<sup>121</sup> All in all, these studies show the lack of scaffolds with a Young's modulus close to that of bone, that are also not brittle, slowly degrading and showing cell viability.

Broadly, composite bone grafts (with or without chitosan) have been shown to be osteoconductive,<sup>15</sup> and osteoinductive when loaded with MSC-induced osteoblasts.<sup>102</sup> Composite grafts show high osteoblast,<sup>29,90,92,94,96,97</sup> periosteal and associated cells viability,<sup>95</sup> increased ALP activity<sup>77, 78, 80</sup> and mineralization,<sup>77, 78, 103</sup> exhibit neovascularization,<sup>102</sup> rapid degradation<sup>102</sup> and new bone formation *in vivo*.<sup>102,103,105</sup> Their main limitation is that they are non-load-bearing or no mechanical properties are observed. Some bone grafts have Young's modulus of cortical bone, but show low degradation *in vitro* after six weeks (12%) and *in vivo* after one month.<sup>29</sup> Some bone grafts may have compressive strength close to that of bone, but no biocompatibility was assessed.<sup>30</sup> Further, some bone grafts have Young's modulus at the lower limit for cancellous bone, but are brittle,<sup>31</sup> while other bone grafts have Young's modulus too high even for cortical bone replacement and are also brittle.<sup>32</sup> A summary of bone graft types together with their advantages and disadvantages is presented in Table 1.

**Table 1.** Characteristics of the classes of bone grafts.

Bone graft type	Pros	Cons
Ceramics: CaP, CaSO <sub>4</sub> , bioglass	<ul style="list-style-type: none"> <li>• osteoconductive</li> <li>• direct bonds with the surrounding bone</li> <li>• biocompatibility</li> <li>• minimal immunological and foreign body reactions<sup>8</sup></li> </ul>	<ul style="list-style-type: none"> <li>• lack of osteoinductivity<sup>8</sup></li> <li>• brittleness</li> <li>• the difficulty to machine into complex shapes and porous constructs</li> <li>• low degradation for the ceramics with Young's modulus of cancellous<sup>29</sup>/cortical bone.<sup>87</sup></li> </ul>
Polymers: <ul style="list-style-type: none"> <li>• Natural:               <ul style="list-style-type: none"> <li>• Polysaccharides: alginate, chitin, chitosan and hyaluronic acid</li> <li>• Proteins: soy, collagen, fibrin and silk</li> </ul> </li> </ul>	<ul style="list-style-type: none"> <li>• support cell attachment</li> </ul>	<ul style="list-style-type: none"> <li>• poor mechanical strength.<sup>10</sup></li> </ul>
<ul style="list-style-type: none"> <li>• Synthetic: PLA, PGA, PLGA, PCL and PHB<sup>10,88,89</sup></li> </ul>	<ul style="list-style-type: none"> <li>• relatively good mechanical strength</li> <li>• good degradation rates</li> <li>• anatomical fit</li> </ul>	<ul style="list-style-type: none"> <li>• undesirable acidic degradation products, which may stimulate an inflammatory reaction.<sup>12,13</sup></li> </ul>
Composites <ul style="list-style-type: none"> <li>• calcium phosphate/polyurethane with both HA and <math>\beta</math>-TCP</li> <li>• collagen fibers coated with HA</li> <li>• PLGA/HA scaffolds</li> <li>• Gelatin/HA</li> <li>• Collagen beads coated w/ HA</li> <li>• PLLA/chitosan/HA scaffolds</li> <li>• Chitosan/TCP sponges</li> </ul>	<ul style="list-style-type: none"> <li>• osteoconductive<sup>15</sup></li> <li>• osteoinductive when loaded with MSC-induced osteoblasts<sup>102</sup></li> <li>• high osteoblast,<sup>29,90,93,95-98</sup> fibroblast and periosteal cell viability<sup>96</sup></li> <li>• ALP activity<sup>80,82,104</sup> and mineralization<sup>80, 82, 106</sup></li> <li>• neovascularization<sup>102</sup></li> <li>• rapid degradation<sup>102</sup></li> <li>• new bone formation <i>in vivo</i><sup>40,102,106</sup></li> </ul>	<ul style="list-style-type: none"> <li>• are non-load-bearing</li> <li>• non-optimized growth factor loading</li> <li>• no mechanical properties are observed</li> </ul>



One strategy to improve tissue engineering scaffolds for bone grafts is through the use of microspheres. The microspheres when packed together like balls in a box, provide for complete interconnected porosity for cell/tissue ingrowth. The microspheres provide a stronger 3D network to improve mechanical loading, and serve as a negative template for bone formation and organization.<sup>122</sup>

The ease of packing into various shapes also makes microsphere-based bone grafts attractive for filling irregular bone defects. Using this approach, Chesnutt et al. developed a co-precipitation method to form chitosan – calcium phosphate composite microspheres and then formed scaffolds by fusing the beads.<sup>40</sup> The scaffolds were made with a chitosan with a high degree of deacetylation: 92.3%. The addition of hydroxyapatite to chitosan increased the surface roughness, the compressive modulus (by almost 3x), when compared to other chitosan-calcium phosphate composites or calcium phosphate scaffolds alone. Not only were the scaffolds stronger, but also they showed better osteoblast proliferation as compared to chitosan scaffolds.<sup>40</sup> The Young's modulus of these scaffolds,  $9.3 \pm 0.8$  MPa, was at the lower limit for cancellous bone. In the *in vivo* rat calvarial defect study, the scaffolds showed good osteoconductivity, but the *in vivo* degradation of scaffolds was low, which may have also limited bone tissue ingrowth.<sup>41</sup> Chesnutt showed the potential of chitosan-calcium phosphate microsphere-based scaffolds to serve as bone grafts through osteoblast proliferation, Young's modulus at the lower range of cancellous bone, good osteoconductivity, but the material had a limitation: low degradation, attributed in part to the high DDA.<sup>41</sup>

Consequently, the main focus of this study was to improve the degradation of these chitosan-calcium phosphate scaffolds, which may be used as cancellous bone replacement. One way to improve their degradation is to add collagen to the chitosan-

calcium phosphate composite material. Degradation would increase, in part because collagen is highly degradable. The biomimetic nature of the composite would also be increased since collagen is the major ECM protein of bone which may further enhance its potential to serve as a bone graft substitute material.

Since native bone is composed of mineral, collagen and glycosaminoglycans, the biomimetic composite scaffold was designed with calcium phosphate mineral, collagen and chitosan instead of glycosaminoglycans to mimic bone composition. The three building materials of the microspheres and the rationale for combining all these biomaterials into bone grafts will be further discussed.

## **2.4 Chitosan**

Chitosan, a partially N-deacetylated derivative of chitin, is a natural linear polysaccharide derived from the exoskeleton of crustaceans. Chitosan holds promise in biomedical research due to its attractive properties of osteoconductivity, biocompatibility, non-toxic and non-acidic degradation products, promotion of healing, mucoadhesiveness, wound healing properties, moldability into three-dimensional (3D) scaffolds, making it an ideal candidate for tissue engineering and drug delivery applications.<sup>33-39</sup> Chitosan exists in various forms: microspheres, films, scaffolds, gels, bioactive coatings for orthopaedic and craniofacial implants, which support bone cell in-growth and is able to deliver antibiotics and bone morphogenetic proteins.<sup>113</sup> Chitosan sponges fabricated by freeze-drying,<sup>123</sup> chitosan microspheres<sup>39</sup> and cross-linked chitosan microspheres<sup>124</sup> were used in bone regeneration, albeit for non-load-bearing purposes.

In spite of its nontoxic degradation byproducts: saccharides and glucosamines which are incorporated into glycoproteins or excreted as CO<sub>2</sub>,<sup>33</sup> chitosan's slow degradation profile due to the high degree of deacetylation, DDA, can limit the bone

growth within the scaffold and bone defect volume<sup>44</sup>, consequently restraining the use of chitosan as a bone graft for tissue engineering and drug delivery.

The DDA and the molecular weight are two important properties of chitosan and are known to affect how chitosan will perform clinically. It has been reported that biodegradation of chitosan increases with the decrease in degree of deacetylation<sup>110</sup> (up to 50% DDA<sup>33,38,100</sup>) as well as with the decrease in molecular weight of the polymer.<sup>125,126</sup> The decrease in DDA reflects lower crystallinity. Therefore, a lower DDA and molecular weight chitosan is a way to increase degradation.

It has also been reported that the mechanical strength of chitosan decreases with the decrease in the degree of deacetylation<sup>127,128</sup> and molecular weight of chitosan.<sup>129</sup> Since the scaffolds are aimed at a load-bearing application, the lowest DDA and molecular weight should not be chosen, which brings up the issue of finding a suitable low DDA and molecular weight, which will provide some mechanical strength and increase degradation.

On the one hand, chitosan has immense potential as an orthopaedic biomaterial<sup>41,42,130-134</sup>. On the other, the low degradation rate of chitosan microsphere-based 3D scaffolds limits its use in tissue engineering and drug delivery applications. To increase degradation, collagen was added to the microparticles because it undergoes rapid degradation upon implantation.<sup>44</sup> Calcium phosphate, which is osteoconductive, was added as well to mimic the major component of the inorganic phase of bone.<sup>42</sup>

## **2.5 Calcium phosphate**

Calcium phosphate is added to the microparticles because it is osteoconductive, has good strength and hardness.<sup>66</sup> Calcium phosphates have been used in implant coatings, drug delivery systems, bone grafts and other biomedical applications.<sup>113,135-139</sup>

The reason for combining bioactive ceramics with degradable polymers, such as chitosan, is to create scaffolds that maintain the bioactivity and strength of calcium phosphate.

## **2.6 Collagen**

Collagen is the most widely found protein in mammals (25% of our total protein mass) and is the major provider of strength to tissue.<sup>140</sup> A typical collagen molecule consists of three intertwined protein chains that form a helical structure.<sup>140</sup> These molecules polymerize together to form collagen fibers of varying length, thickness, and interweaving pattern (ropelike structures, meshes or networks).<sup>140</sup> The predominant form used in biomaterial applications is type I collagen, which is a "rope-forming" collagen and can be found almost everywhere in the body, including tendons, the endomysium of myofibrils and the organic part of bone.<sup>141</sup> The basic unit of the extracellular matrix consists of mineralized type I collagen fibrils, with collagen comprising about 90% of the protein.<sup>142</sup>

Collagen is resorbable, non-toxic and excellent for attachment and biological interaction with cells.<sup>143</sup> Moreover, collagen may be processed into a variety of formats, including porous sponges, gels, and sheets, and can be cross-linked with chemicals to make it stronger or to alter its degradation rate.<sup>143</sup> Collagen has been used in many types of surgery (e.g., plastic surgery), cosmetics, drug delivery, as well as in bioprosthetic implants and tissue-engineering of multiple organs.<sup>143</sup> Collagen has its own disadvantages though: depending on how it is processed, it can potentially cause alteration of cell behavior (*e.g.*, changes in growth or movement), have inappropriate mechanical properties, or undergo contraction (shrinkage).<sup>143,144</sup> Because cells interact so easily with collagen, cells can actually pull and reorganize collagen fibers, causing scaffolds to lose their shape if they are not properly stabilized by crosslinking or mixing

with another less "vulnerable" material (chitosan, in our case). Exciting research is being performed to bind various proteins or growth factors to collagen as signaling molecules in order to tailor cell behavior to specific applications of interest.<sup>143</sup> One may attach molecules that encourage cells to grow (e.g. bone morphogenetic proteins), to move, to make new blood vessels, to make a certain protein, or to perform many other actions. The biocompatibility and high degradation rate of collagen are exploited in this work by combining collagen with the chitosan.

## **2.7 Composite chitosan-collagen biomaterials**

Initially, chitosan and collagen have been studied as extracellular matrix components. Tan et al. observed that overall matrix integrity increased with the proportion of chitosan to collagen.<sup>145</sup> The addition of chitosan greatly influences ultrastructure and changes collagen fiber cross-linking, reinforcing the structure and increasing pore size.<sup>145</sup> Although the proliferation of K562 lymphoblasts was inhibited with an increasing proportion of chitosan, cell function-based on cytokine-release was greatly augmented.<sup>145</sup> The cell line was inappropriate for bone tissue engineering and the gels are non-load bearing. Similarly, Wang et al. demonstrated that human bone marrow stem cells, hBMSC can attach and proliferate in three-dimensional matrices composed of glyoxal-crosslinked 50/50 chitosan/collagen, and that these hydrogels supported osteogenic differentiation in response to stimulation.<sup>146</sup> Likewise, Wang et al. used beta-glycerophosphate (beta-GP), an osteogenic medium supplement and a weak base, to simultaneously initiate gelation of chitosan-collagen composite materials at physiological pH and temperature.<sup>147</sup> DNA content for adult human bone marrow-derived stem cells (hBMSC) encapsulated in such hydrogels increased twofold in materials containing collagen.<sup>147</sup> Collagen-containing materials compacted more strongly and were

significantly stiffer than pure chitosan gels.<sup>147</sup> The presence of chitosan in materials resulted in higher expression of osterix and bone sialoprotein genes in medium with and without osteogenic supplements, higher phosphatase activity and calcium deposition in osteogenic medium.<sup>147</sup> Chitosan-collagen composite materials have potential as matrices for cell encapsulation and delivery, or as in situ gel-forming materials for non-load bearing bone repair.<sup>147</sup>

Nitzsche et al. used a suspension-quick-freezing and lyophilization method to incorporate nanohydroxyapatite into a polymeric matrix consisting of collagen and chitosan.<sup>148</sup> *In vitro* and *in vivo* studies need to be carried out.

In order to remineralize dentine affected by caries, Xu et al. modified the surface of partially demineralized dentine sections, mainly composed of type I collagen, by covalent immobilization of phosphorylated chitosan, P-chi on the collagen surface.<sup>149</sup> The results indicated that the covalent immobilization of P-chi can significantly induce biomimetic deposition of calcium phosphate.<sup>149</sup> No mechanical testing was carried out.

Several chitosan cement formulations were prepared, none of which were load-bearing: Zhao et al. developed a novel human umbilical cord mesenchymal stem cell (hUCMSC)-encapsulating, fiber-reinforced injectable calcium phosphate cement (CPCF) scaffold, which incorporated calcium phosphate powders, chitosan, and absorbable fibers.<sup>150</sup> The results indicated that the osteogenic media method with hUCMSCs in CPCF was promising for bone regeneration, and that hUCMSCs represent a desired alternative to the gold-standard bone marrow MSCs because the former do not require an invasive procedure to harvest.<sup>150</sup> Next, the following researchers used tricomponent systems with similar composition, but different fabrication method to ours: Lian et al. reinforced self-hardened calcium phosphate cement, CPC with collagen-coated chitosan

fibres to reach a fiber volume content of 5%.<sup>151</sup> They achieved compressive strength of the CPC-fibre implant fourfold higher than that of the CPC control (33 MPa when the strain was 2.4 per cent ).<sup>151</sup> This value is about 6 x less than that for human bone.<sup>152</sup> Nine cylindrical implants including six CPC-fiber implants were implanted into bone defects of nine dogs and were then post-operatively observed.<sup>151</sup> After 20 weeks *in vivo*, new callus from the healthy tissue of the defect entirely integrated with the CPC-fiber implant and new bone was formed as the implant degraded, thus facilitating bone process repair *in vivo*.<sup>151</sup> Further, Li et al. created a novel salmon calcitonin-loaded bioactive injectable calcium phosphate cement for treating an osteoporosis-induced bone defect.<sup>153</sup> The injectable time for the cement is 12 minutes, the compressive strength is low for a load-bearing application (12 MPa), the final setting time is 40 minutes and the release of the containing salmon calcitonin was controlled easily through adjusting the ratio of chitosan oligosaccharide and collagen polypeptide.<sup>153</sup>

Although chitosan and collagen were used in scaffolds with or without growth factor delivery, no mechanical testing was performed. For example, chitosan/collagen scaffolds were fabricated by a freeze-drying method and were loaded with VEGF protein and adenovirus expressing BMP-2.<sup>146</sup> The *in vitro* study revealed a burst and rapid release of VEGF with a sustained high-level expression of BMP-2, while the *in vivo* study showed the scaffolds enhanced bone formation, bone-to-implant contact and mean peak removal torque when compared to other groups.<sup>146</sup>

Ravindran et al. developed a novel collagen/chitosan template that is embedded within the native extracellular matrix, ECM of differentiating human marrow stromal cells (HMSCs) to facilitate osteoblast differentiation.<sup>154</sup> Gene expression analysis showed that the ECM scaffold supported osteogenic differentiation of undifferentiated

HMSCs and the nucleation of calcium phosphate polymorphs to form a mineralized matrix, which is promising for bone tissue engineering.<sup>154</sup>

Recently, Pallela et al. created a scaffold containing chitosan, hydroxyapatite and marine sponge collagen using the lyophilization method.<sup>155</sup> The interconnected porosity was 50-170  $\mu\text{m}$  and the human osteosarcoma, MG-63 cell proliferation was higher than on pure chitosan, which makes these composite scaffolds promising for matrix-based bone repair and bone augmentation.

Moreover, a new delivery system for multiple bioactive factors and an inductive implant scaffold for bone regeneration was invented by Niu et al.<sup>156</sup> Compared with the rapid release from chitosan microspheres (CMs), the bone morphogenetic protein-2-derived synthetic peptide was delivered from CMs incorporated into nanohydroxyapatite/collagen (nHAC), and poly(L-lactide), CMs/nHAC/PLLA microsphere-scaffold composite in a temporally controlled manner, depending on the degradation of both incorporated CMs and PLLA matrix.<sup>156</sup> The results indicated that, with the appearance of CMs in microsphere-scaffold composite, the MC3T3-E1 osteoblasts exhibit better morphology and proliferation ability. Moreover, it was demonstrated that the CMs/nHAC/PLLA scaffolds possess better biocompatibility in a 6 mm rabbit femoral condyle defect, which should be attributed to both the incorporated chitosan component and the encapsulated bioactive synthetic peptide.<sup>156</sup>

Zhang, Wang and coworkers used chitosan (CS) as a dispersant in a bone matrix constructed with collagen (Col) and hydroxyapatite (HA).<sup>157,158</sup> Solid-liquid phase separation was used to shape a three-dimensional porous structure to support cell growth.<sup>157,158</sup> Mesenchymal stem cells proliferated more with spreading and ECM



secretion along collagen fibers and the scaffolds repaired a 1.0x.6 cm<sup>2</sup> bone defect in the mandibles of rabbits in 3 months.<sup>157,158</sup>

All in all, none of the above scaffolds possess load bearing abilities and most of them don't present the degradation needed to see if the scaffolds are suitable for bone regeneration.

## **2.8 Conclusions**

The above articles summarize the benefits of using chitosan and collagen or chitosan, collagen and a crystalline form of calcium phosphate for bone tissue repair: osteogenic differentiation of undifferentiated human mesenchymal stem cells, the nucleation of calcium phosphate polymorphs to form a mineralized matrix, induction of biomimetic deposition of calcium phosphate, better morphology and proliferation ability of osteoblasts, enhanced bone formation, bone-to-implant contact and mean peak removal torque, higher expression of osterix and bone sialoprotein genes in medium with and without osteogenic supplements, higher phosphatase activity and calcium deposition in osteogenic medium and finally, healing a bone defect completely. We hope to adopt a similar strategy by preparing composite chitosan-collagen-calcium phosphate microspheres using a unique method of incorporating collagen within chitosan microspheres via a precipitation method. The addition of collagen to chitosan and calcium phosphate will help increase the degradation rate of chitosan scaffolds without compromising the overall mechanical strength. Although chitosan and the denatured form of collagen, gelatin, have been used for cartilage tissue engineering, the addition of calcium phosphate can improve the mechanical strength and make the present tricomponent scaffolds suitable for bone tissue engineering. Thus, this study would provide data on the potential of using a composite chitosan-collagen-calcium phosphate

system as a bone graft substitute for bone tissue plerosis for the treatment of non-unions and bone defects.

## CHAPTER 3: MATERIALS AND METHODS

### **Part 1. Microspheres' Fabrication, Characterization, Degradation and Cell Culture.**

#### ***Preparation of Composite Chitosan-Collagen-Calcium Phosphate Microspheres***

Chitosan-calcium phosphate and chitosan-collagen-calcium phosphate composite microspheres were made based on the co-precipitation technique, as previously described.<sup>33</sup> To make chitosan-calcium phosphate microspheres, a 2.67 % solution of chitosan powder (61% DDA, MW=220 kDa, Primex, Siglufjordur, Iceland) was prepared in 2 v/v% acetic acid solution and allowed to dissolve for 24 h.  $\text{CaCl}_2$  and  $\text{NaH}_2\text{PO}_4$  were added to achieve a 0.06 M  $\text{Ca}^{2+}$  and 0.03 M  $\text{PO}_4^{3-}$  with a Ca:P=2. The solution was filtered through a nylon mesh with a pore diameter of 180  $\mu\text{m}$  (Gilson Company, Inc., Ohio, USA). For the chitosan-collagen-calcium phosphate composites, an appropriate volume of 0.03% collagen in 2%  $\text{CH}_3\text{COOH}$  was mixed manually with the filtered chitosan solution to achieve 10 or 25 wt% collagen. Note: a 3.16 wt% chitosan solution was used for making microspheres with 25 wt% collagen.

Using a KDS 200 two-syringe infusion pump (KD Scientific, Holliston, MA), the chitosan solutions were dripped at 4°C through a 21G needle (BD Medical, Franklin Lakes, NJ) into a base solution of 20 mass% NaOH, 30%  $\text{CH}_3\text{OH}$  and 50%  $\text{H}_2\text{O}$  at flow rates between 0.15-0.29 mL/min to precipitate the chitosan-based composites into beads with a spherical shape. The microspheres were stirred in the base solution for 10-20 min. before being washed with copious volumes of distilled water,  $\text{dH}_2\text{O}$ , until a pH=7.4-7.8 was obtained. The last wash was in deionized water, DI  $\text{H}_2\text{O}$ . The chitosan-composite microspheres were air dried in a fume hood overnight.

### ***Ash Content for the Determination of Calcium Phosphate in Microspheres***

The amount of calcium phosphate salts/mineral present in the microspheres was determined using a combustion method.<sup>159</sup> Approximately 0.5 g beads were weighed and heated for about 2 h at 60<sup>0</sup>C under vacuum until the mass change was less than 0.1% to remove excess moisture. Clean ceramic crucibles were weighed and placed into a high temperature oven at 550±20<sup>0</sup>C for 30 min. The crucibles were allowed to cool in a desiccator for 30 min. The crucibles were re-weighed and the heating process was repeated until a constant mass for the crucible was reached (<0.1% mass change). The microspheres were transferred to a crucible and combusted by placing the crucible over a Bunsen burner. The crucibles were then transferred to a high temperature oven at 550±20<sup>0</sup>C for 3 hours (h). The crucibles were cooled down in a desiccator and the heating process was repeated until constant mass was reached (<0.1% mass change). The percentage of ash was calculated using the formula:

$$\text{Ash content (\%)} = \frac{m_2 - m_0}{m_1} \times 100$$

Where  $m_0$  is the constant mass of the crucible (g),  $m_1$  is the mass of the sample (g) and  $m_2$  is the constant mass of the ash and crucible (g). Three samples were used to determine the ash content of each of the three chitosan composite groups plus a control, which consisted of chitosan beads with no calcium phosphate to account for salts or other impurities in the initial chitosan powder.

### ***Hydroxyproline Assay for the Determination of the Amount of Collagen Incorporated***

The hydroxyproline assay<sup>160</sup> was used to estimate the amount of collagen incorporated into the microspheres due to the high levels of the amino acid found in the collagen polymer. Approximately 0.1 g of each type of composite beads were weighed

and heated for about 2 h at 60°C under vacuum until the mass change was less than 0.1%. This was done to remove excess moisture in the beads. Teflon tape was applied to the threads of 2-mL screw cap microcentrifuge tubes (PCR-PT from SARSTEDT, Germany) which contained O-rings inside the caps to withstand positive pressure. The beads were transferred to the microcentrifuge tubes and approximately 1.9 mL of 6M HCl was added to each tube. The tubes were placed in a high heat resistant glass bottle to equalize pressure during incubation at 110°C for at least 16 h. This was done to hydrolyze the proteins into amino acids. After cooling to room temperature, the samples were centrifuged for 10 min. at 14,000 RPM to separate particulates from the aqueous solution containing hydrolyzed amino acids. 1 mL of the aqueous solution was transferred to a 15 mL centrifuge tube and 4 mL DI H<sub>2</sub>O was added. The solution was placed in a -80°C freezer for at least 1h and lyophilized in a 2.5 L Labconco freeze dryer. The lyophilization procedure was repeated in order to remove the residual acid. The resulting hydrolyzed amino acid powder was solubilized in 1 mL of DI H<sub>2</sub>O, vortexed and then a 25 µL aliquot was added to a well of a 96-well plate. A 112.5µL volume of chloramine-T reagent was added to each test sample and incubated for 20 min at room temperature to oxidize the hydroxyproline to a pyrrole derivative. Then 125 µL of Ehrlich's reagent was added to each sample, heated in an oven at 65°C for 20 min. to generate a colored chromagen product. The absorbance was read at 550 nm. Absorbance was converted to µg/mL hydroxyproline using hydroxyproline (Sigma-Aldrich) standards. The collagen concentration was calculated taking into account that the measured hydroxyproline is 10.8% in collagen.<sup>161</sup> The concentration of collagen in the microspheres was determined based on the mass of collagen from the assay and the initial mass of microspheres without calcium phosphate

given by the ash content assay. Triplicate samples were measured for each composite group.

### ***Shape Characterization***

Images of the microspheres were obtained with a KEYENCE VHX 1000 digital microscope. 40 samples from each group were placed on a weigh boat and viewed with a 100x objective eyepiece (200x objective for close-up). Since the microspheres exhibited elliptical shapes, the length of the major and minor axis of the microparticles were measured and used to calculate a sphericity index based on the following equation:

$$\text{Sphericity index} = \frac{\text{major axis}}{\text{minor axis}}.$$

### **X-ray Diffraction Analysis**

To check for the presence of chitosan and calcium phosphate crystalline structures composite microspheres were examined by x-ray diffraction using a Bruker D8 Advance Diffractometer (Bruker AXS Inc., Madison, WI) using Cu-K $\alpha$  radiation at 40 kV and 40 mA. Prior to XRD analysis, approximately 5 mg of each type of microsphere (n=2) were placed in a micro centrifuge tube and then immersed for 5 min. in liquid N $_2$ . The frozen microspheres were then ground into fine powder using a pestle and mortar. The diffraction patterns of the powders were obtained in the scan range  $2\theta=5-40^\circ$  with a step size of  $0.04^\circ$  and a time/step of 0.302 s.

### ***In Vitro Degradation of Composite Chitosan-Collagen-Calcium Phosphate***

#### ***Microspheres***

The *in vitro* degradation of composite chitosan-collagen-calcium phosphate microspheres was based on change in mass over a 6-week period. All the samples were gamma sterilized prior to starting the study by irradiating at 32 kGy for 2h. The

degradation solution used consisted of 50 µg/mL collagenase type IA (Clostridium hystoliticum, Sigma Aldrich) and 100 µg/mL lysozyme in 1x PBS supplemented with Penicillin-10,000 IU/mL, Streptomycin-10 mg/mL, Amphotericin B-25 µg/mL. As control, microspheres of each type were also incubated in PBS with antibiotics/antimycotic (AB/AM) but without enzymes.

Approximately 30 mg samples (n=4) for each of the composite chitosan-collagen-calcium phosphate treatment group were weighed and exact mass recorded, and then placed in 1.5 mL microcentrifuges. To each sample of microspheres, 1.5 mL of degradation solution were added and the samples were placed in an incubator at 37°C with constant shaking using a plate rocker. The degradation solution was changed every 2-3 days in order to avoid the complete loss of enzymes' activity. At 1, 3, 5, 7, 14, 21, 28 and 42 days, the samples were washed with DI H<sub>2</sub>O five times to remove any precipitated salts and proteins before drying in an oven at 40°C for at least 24 h. The samples were then weighed and the percent change in mass was calculated from the initial mass. The data was reported as percent mass loss  $\pm$  standard deviation.

### ***In Vitro Cytocompatibility of Composite Chitosan-Collagen-Calcium Phosphate Microparticles and Scaffolds***

The cytocompatibility of the gamma-sterilized composite chitosan-collagen-calcium phosphate microspheres was evaluated using a murine fibroblast cell line (NIH/3T3, ATCC® Number: CRL-1568™) and a human osteosarcoma cell line (Saos-2, ATCC® Number: HTB-85™). The cell attachment and growth study was conducted in complete growth medium composed of Dulbecco's Modified Eagle's Medium with 10% FBS and 1x antibiotic/antimycotic for NIH/3T3, and McCoy's 5A Medium with 15% FBS and 1x antibiotic/antimycotic for Saos-2.

Briefly, 60 microspheres of each sample group were placed in glass culture tubes, 13 x 100mm with screw cap (PYREX® Laboratory Glassware, CORNING, MA USA). The microspheres were soaked in 200 µL complete growth medium for 3-4 h. Then, the medium was removed and 2 mL of medium with cells ( $3.9 \times 10^5$  NIH/3T3 cells/mL or  $1.5 \times 10^5$  Saos-2 cells/mL) were added. The tubes were placed in an incubator (Model 3158, Forma Scientific, Marietta OH) at 37°C and 5%CO<sub>2</sub>. After 4 h incubation, cell attachment to microspheres was measured using the CellTiter-Glo® Luminescent Cell Viability Assay (Promega, WI, USA). The assay estimates number of cells based on the presence of ATP via the luciferase-luciferin reaction. The growth medium was replaced every 2 days for NIH/3T3 and every 3 days for Saos-2. After 1, 3 or 7 days cell proliferation was measured using the CellTiter-Glo® Luminescent Cell Viability Assay. The seeding concentration for proliferation for fibroblasts was  $1.8 \times 10^5$  cells/mL and for osteoblasts,  $1.2 \times 10^5$  cells/mL. The data for attachment was reported as % cell attached  $\pm$  standard deviation, while for proliferation the data was reported as # cells /microparticle  $\pm$  standard deviation.

In addition, at each time point, samples of each chitosan composite microsphere were evaluated using a LIVE/DEAD® Viability/Cytotoxicity Kit for mammalian cells (Invitrogen Corporation, CA, USA) to determine the viability of cells based on plasma membrane integrity and esterase activity of the cells.

### ***Statistical Analysis***

Regression analysis was used for the degradation of microparticles, one-way ANOVA & post-hoc tests were used in SigmaStat 3.5 to evaluate the % cell attachment on beads for both cell types. For cell proliferation studies on microparticles a two-way



ANOVA with Tukey's post-hoc test was used. A  $p$  value  $< 0.05$  was considered significant.

## **Part 2. Scaffolds' Fabrication, Characterization, Physical and Mechanical Properties, Degradation and Cell Culture.**

### ***Scaffold Fabrication***

Microspheres for each type of composite were made as described in the section "Preparation of Composite Chitosan-Collagen-Calcium Phosphate Microspheres". To make scaffolds, 40 mg beads were fused with 1 drop of either 1 v/v% acetic acid,  $\text{CH}_3\text{COOH}$  or 2 v/v% glycolic acid,  $\text{HOCH}_2\text{CO}_2\text{H}$  and packed into a cylindrical mold with an inner diameter of 6 mm and height of about 15 mm. Scaffolds were gamma-sterilized at 32 kGy for 2h and kept sealed at room temperature for one week before degradation. The scaffolds for cell attachment and proliferation were kept at room temperature for one month before the experiments and the scaffolds for mechanical testing were kept at room temperature for six weeks before mechanical testing. The scaffolds had a height twice the diameter (approximately 14 mm tall by 6 mm diameter) to follow ASTM D695 - 10 Standard Test Method for Compressive Properties of Rigid Plastics.

### ***Morphological Characterization***

Images of the scaffolds were obtained with a KEYENCE VHX 1000 digital microscope. The samples ( $n=5$ ) were placed on a weigh boat and viewed with a 100x objective eyepiece (200x objective for close-up). A rough estimate of the size of the pores was obtained from the small sequence of images taken ( $n=5$ ). The longest distance in the pore was measured.

### ***Porosity Determination***

The porosity was determined by liquid volume displacement method using a density determination kit (Mettler Toledo, Switzerland), with a Mettler Toledo balance. The diameter and height of the cylindrical scaffolds were recorded and methanol was poured in the beaker where the gem holder was immersed, to cover the wire basket of the gem holder by at least 1 cm. The temperature of the room was recorded in order to have the correct value for the density of methanol. The gem holder was attached and the balance was tared to read 0. The dry scaffold was placed in the upper cup of the gem holder and the mass recorded as mass A in mg. The balance was tared again, the scaffold was placed in the beaker and the beaker with methanol and a scaffold were placed under vacuum and kept for 4 min. to remove bubbles entrapped in the porous scaffold. The scaffold was placed in the wire basket in methanol and the mass, P or buoyancy was recorded. The density was calculated by the formula:

$$\rho = \frac{A \times \rho_{CH_3OH}}{P},$$

Where A and P are the masses recorded as indicated above,  $\rho_{CH_3OH}$  is the density of methanol, which at 21°C is 0.7918 g/cm<sup>3</sup>. The total volume of the cylindrical scaffold was calculated using the following equation:

$$V_{tot} = \frac{\pi \times D^2 \times H}{4},$$

Where D=diameter of the scaffold and H=height of the scaffold.

The volume without pores was calculated using the formula:

$$V_{\text{without pores}} = \frac{A}{\rho},$$

Where the mass A and the density  $\rho$  are previously defined.

The porosity was calculated using the formula:

$$\text{Porosity} = \frac{V_{\text{tot}} - V_{\text{withoutpores}}}{V_{\text{tot}}} \times 100$$

This measurement was done for n=10 scaffolds from each group.

### ***Mechanical Testing***

The compressive modulus of scaffolds was determined using an Instron load frame (Model #33R 4465). The scaffolds had a height twice the diameter (approximately 14 mm tall by 6 mm diameter) to follow ASTM D695 - 10 Standard Test Method for Compressive Properties of Rigid Plastics. A 500 N load cell of the Instron was operated at a rate of 1 mm/min. The scaffolds were hydrated for 25 h in dH<sub>2</sub>O prior to testing. The scaffolds were conditioned by first compressing samples by 5% of the height, and then unloaded. Test specimens were then compressed up to 50% of the height with Teflon tape above and below the scaffold to allow for equal load distribution. The compressive stress and strain were recorded and Young's modulus was calculated for n=10 replicates for each type of scaffold.

### ***In Vitro Degradation of Composite Chitosan-Collagen-Calcium Phosphate scaffolds***

The degradation of the scaffolds was evaluated over a 4 week-period by measuring the change in mass at 1 week-intervals. All the samples were gamma sterilized at 32 kGy for 2h prior to starting the study. The degradation solution used consisted of 50 µg/mL collagenase type IA (Clostridium hystolicum, Sigma Aldrich) and 100 µg/mL lysozyme in 1x PBS supplemented with Penicillin-10,000 IU/mL, Streptomycin-10 mg/mL, Amphotericin B-25 µg/mL. As control, scaffolds of each type were also incubated in PBS with antibiotics-antimycotic, but without enzymes.

Samples (n=4) for each of the composite chitosan-collagen-calcium phosphate

treatment group were weighed (~ 40 mg) and placed in glass scintillation vials. To each scaffold, 3 mL of degradation solution were added and the samples were placed in an incubator at 37°C with constant shaking using a plate rocker. The degradation solution was changed every 2-3 days in order to avoid the complete loss of enzymes' activity. At each time point, the samples were washed with 15 mL DI H<sub>2</sub>O before drying in an oven at 40°C for at least 24 h, weighed and the percent change in mass was calculated. The data was reported as percent mass loss  $\pm$  standard deviation.

### ***In Vitro Cytocompatibility of Composite Chitosan-Collagen-Calcium Phosphate Scaffolds***

The cytocompatibility of the gamma-sterilized composite chitosan-collagen-calcium phosphate scaffolds was evaluated using a human osteosarcoma cell line (Saos-2, ATCC® Number: HTB-85™). The cell attachment and growth study was conducted in McCoy's 5A Medium with 15% FBS and 1x antibiotic/antimycotic.

Each scaffold (~40 mg) was soaked for 17 h in 2 mL medium in a well of a 24 well plate so that proteins would attach to scaffolds and the cells wouldn't fall off during the swelling of the scaffolds. The medium was removed, 1.5 mL sterile PBS was added so that residual acetic or glycolic acid in the scaffolds will diffuse into the PBS. The scaffolds were left in the incubator at 37°C and 5% CO<sub>2</sub> for 1 h. They were shaken by hand for a few seconds and the PBS was removed and the scaffolds were seeded with 100  $\mu$ L with 10<sup>5</sup> osteoblasts/mL. After 1.5 h, 1 mL medium was added to cover the samples in the wells. The medium was replaced every 3 days. Samples were evaluated at 4 h for cell attachment and at days 1, 3 and 7 for cell proliferation using the CellTiter-Glo® Luminescent Cell Viability Assay (Promega, WI, USA). For cell attachment, the data was reported as mean % cell attachment  $\pm$  standard deviation, while for cell

proliferation, the data was reported as mean # cells/scaffold  $\pm$  standard deviation. At each time point, the samples were examined for viability using a LIVE/DEAD® Viability/Cytotoxicity Kit for mammalian cells (Invitrogen Corporation, CA, USA).

### ***Statistical Analysis***

A one-way ANOVA & Tukey's post-hoc tests were used in SigmaStat 3.5 to evaluate the porosity, Young's modulus and cell attachment. Regression analysis was used for the degradation of scaffolds. For Saos-2 proliferation on scaffolds, a two-way ANOVA with Tukey's post-hoc tests were used. A  $p$  value  $< 0.05$  was considered significant.

## CHAPTER 4: RESULTS

### Part 1. Microspheres' Characterization, Degradation and Cell Culture.

Representative digital images of the three types of microparticles are shown (Figure 1).

All microparticles present surface texture.

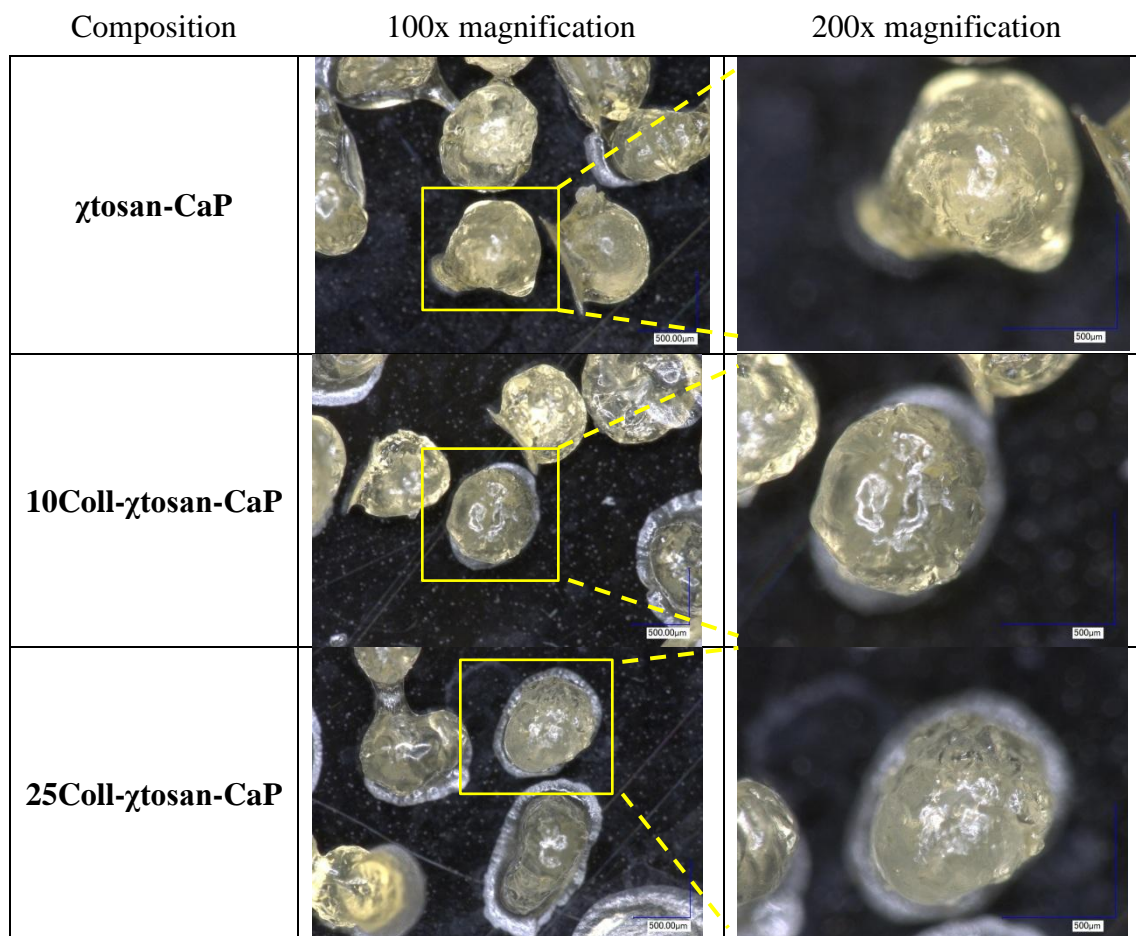


**Figure 1.** Digital images of composite chitosan-collagen-calcium phosphate microparticles.  $\chi$ tosan-CaP: chitosan-calcium phosphate; 10Coll- $\chi$ tosan-CaP: 10% collagen-chitosan-calcium phosphate; 25Coll- $\chi$ tosan-CaP: 25% collagen-chitosan-calcium phosphate. Scale shown: 500  $\mu$ m.

### *Physicochemical characterization*

The results of the determination of the shape, collagen content and ash content of the microparticles are summarized in Table 2. The diameters of the microparticles were determined with KEYENCE VHX-1000 digital microscope. Because the particles exhibited ellipsoidal shapes, both the major and minor axes were measured. The ratio of the major axis to minor axis was used to calculate a sphericity index. The closer the index value is to 1, the more spherical the particles tend to be. The sphericity index, close to 1.3 for all groups, indicates that the microparticles are ellipsoidal and one-way ANOVA indicated there was no statistically significant difference in sphericity index between the three groups.

The ash content of the composite microspheres was determined via combustion and was used as an estimate of the amount of calcium-phosphate mineral/salt in the particles. The ash content of plain chitosan beads without calcium phosphate was subtracted from the three experimental composites to account for any residual minerals/salts in the starting chitosan material.

The actual amount of collagen incorporated into the composite microparticles was determined based on the hydroxyproline assay. It was found that the microspheres with the target 10.0% and 25.0% collagen actually had approximately 2.6% collagen and 7.6% collagen, respectively. The hydroxyproline assay for the negative control, chitosan-calcium phosphate composite beads without collagen, indicated a very low protein content,  $0.024 \pm 0.004\%$ , while the positive control, the collagen stock solution, had  $89.4 \pm 4.7\%$  collagen.

**Table 2.** Physical and compositional properties of the chitosan-collagen-calcium phosphate composite microparticles

		$\chi$ tosan-CaP	10Coll- $\chi$ tosan-CaP	25Coll- $\chi$ tosan-CaP
<b>Sphericity Index</b>		<b>1.35±0.21</b>	<b>1.35±0.21</b>	<b>1.31±0.19</b>
<b>Major axis (μm)</b>		986±118	998±92	937±95
<b>Minor axis (μm)</b>		736±75	751±103	726±85
<b>Ash (%)</b>		<b>8.94±0.50</b>	<b>6.77±0.82</b>	<b>9.13±1.16</b>
<b>Coll (%)</b>	<i>theoretical</i>	0	<b>10.0</b>	<b>25.0</b>
	<i>empirical</i>	0.024±0.004	<b>2.6±0.2</b>	<b>7.6±0.8</b>

X-ray diffraction (XRD) analysis was used to identify crystalline phases present in the different microparticle composite formulations. Representative XRD spectra of the different composite materials are shown in Figure 2. The peaks at  $2\theta \sim 11^\circ$  and  $2\theta \sim 20^\circ$  are indicative of the hydrous and anhydrous peaks of chitosan respectively.<sup>40</sup> In the spectra for the chitosan-calcium phosphate composite microparticles, two additional peaks at  $2\theta \sim 32^\circ$  and at  $2\theta = 34.4^\circ$  were observed. The peak at  $2\theta \sim 32^\circ$  corresponds to the (211) plane of hydroxyapatite (HA) and the peak at  $2\theta = 34.4^\circ$  corresponds to the (220) plane of tricalcium phosphate (TCP).<sup>162</sup> The presence of these peaks indicates that calcium phosphate is present partly in crystalline form. With the addition of increasing amounts of collagen, both the chitosan and the HA peak at  $2\theta \sim 32^\circ$  and TCP peak at  $2\theta = 34.4^\circ$  reduced in intensity until they disappeared for 25% collagen.



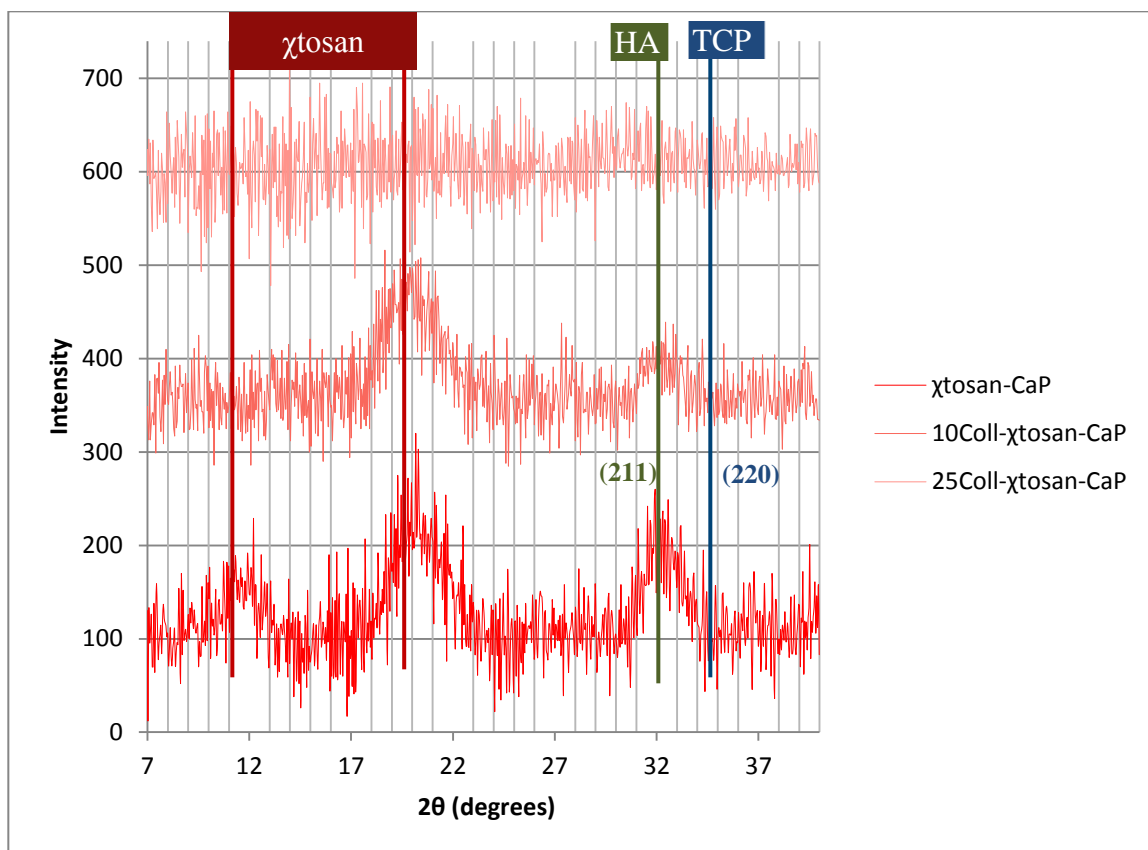


**Figure 2.** Representative XRD spectra of composite chitosan-collagen-calcium phosphate microparticles compared with chitosan. A shift in the hydrous peak of chitosan from  $2\theta=10^\circ$  to  $2\theta=11^\circ$  is observed, while the anhydrous peak is noticed at  $2\theta=20^\circ$ . The peak at  $2\theta=32^\circ$  corresponds to the (211) plane of hydroxyapatite (HA, in green) and the peak at  $2\theta=34.4^\circ$  corresponds to the (220) plane of tricalcium phosphate<sup>162</sup> (TCP, in dark blue).

### *Degradation study*

The total mass loss seen after 6 weeks in both degradation solutions is summarized in Table 2. ANOVA analysis indicated that all groups lost significantly more mass in the solution with enzymes than in the plain PBS solution. For the microparticles in PBS with enzymes (Figure 3) and in the control solution (Figure 4), regression analysis showed a significant loss in mass overtime for all composite groups ( $p<0.05$ ), but there were no statistically significant differences in degradation between

groups ( $p>0.05$ ). A two-way ANOVA with post hoc test showed there is a statistically significant increase in degradation in PBS + enzymes versus the control solution ( $p\leq 0.001$ , Table 3).

**Table 3.** The change in mass of beads in PBS only vs. degradation solution respectively, after six weeks.

$\Delta\text{mass}_{\text{microparticles}} (\%)$			
solution	$\chi\text{tosan-CaP}$	10Coll- $\chi\text{tosan-CaP}$	25Coll- $\chi\text{tosan-CaP}$
Control (PBS)	$10.0\pm 6.8^a$	$13.2\pm 2.2^a$	$8.3\pm 3.7^a$
enzymes	$20.5\pm 4.1^b$	$18.5\pm 3.2^b$	$20.0\pm 4.3^b$

a and b superscript letters indicate statistical differences between degradation solution

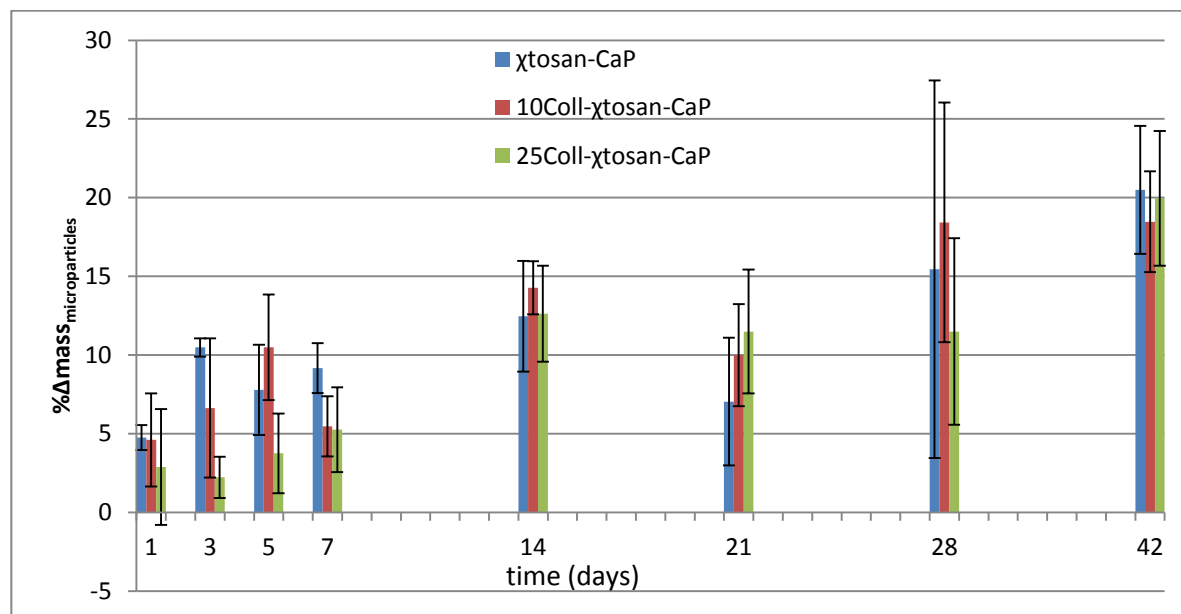


**Figure 3.** Degradation of microparticles in PBS + enzymes. Tukey's test and one-way ANOVA showed that all initial masses are statistically different ( $p<0.05$ ). Regression analysis showed that the degradation rates are similar ( $\alpha=0.05$ ).  $n=4$

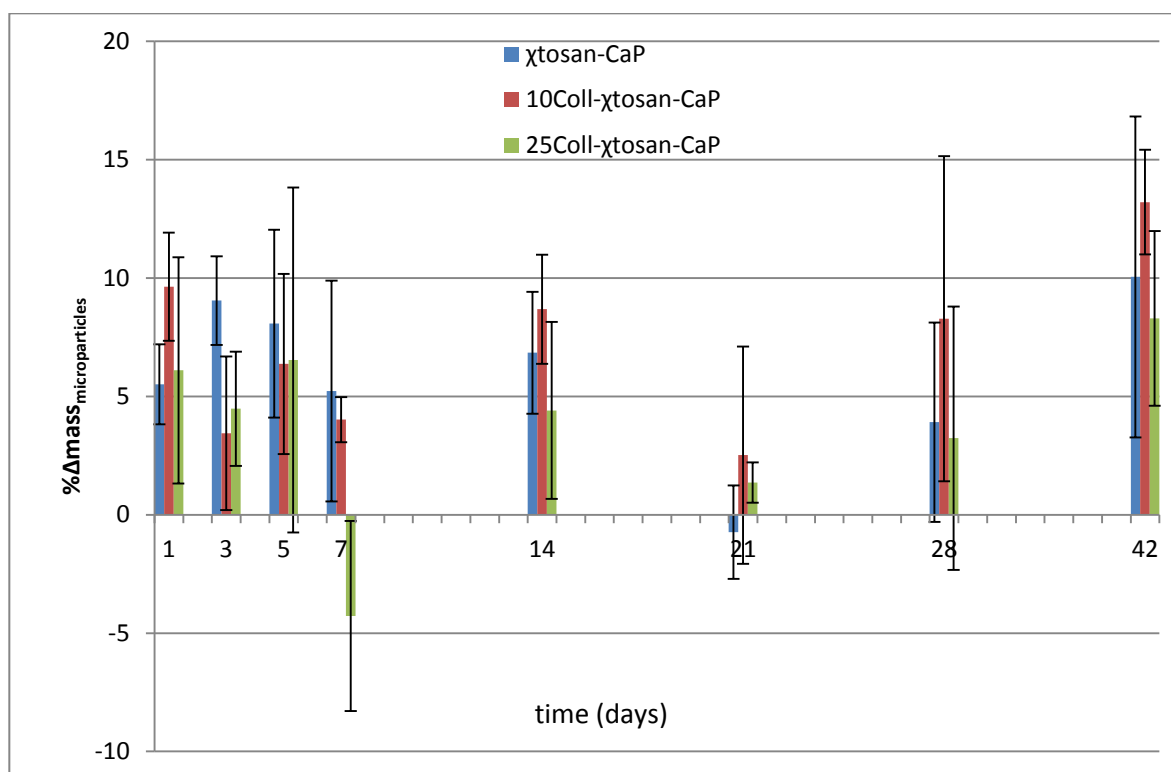


**Figure 4.** Degradation of microparticles in PBS. One-way ANOVA and Tukey's test showed that all initial masses are statistically different ( $p < 0.05$ ). The beads showed a loss of mass over time. Regression analysis<sup>163</sup> showed there were no differences in the degradation rate ( $p < 0.05$ ).  $n=4$

#### *Osteoblast and fibroblast attachment and proliferation on microparticles*

Cellular attachment and proliferation studies on microparticles were performed with two cell lines: NIH/3T3 murine fibroblasts and Saos-2 human sarcoma osteoblasts.

For the attachment of both fibroblasts and osteoblasts on microparticles, one-way ANOVA analysis, followed by Tukey's multiple comparison test showed there is no difference in percentages of cells attached on the 3 groups of microparticles (Figure 5, 6). More fibroblasts than osteoblasts seem to have attached to the microparticles (one-way ANOVA,  $p < 0.05$ ), without taking into account initial cell seeding concentration.

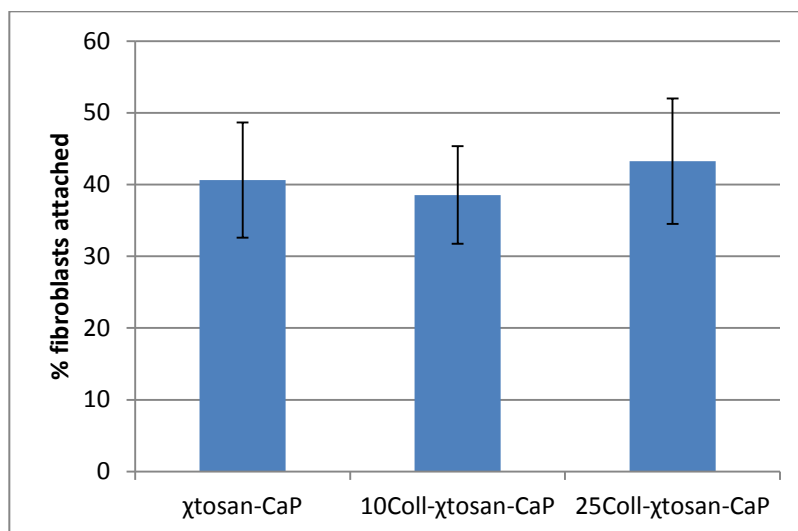


**Figure 5.** Fibroblasts' attachment (%) on beads. One-way ANOVA analysis, followed by Tukey's and then Bonferroni's t-tests showed there is no difference between groups for  $\alpha=0.05$  ( $n=5$ ).

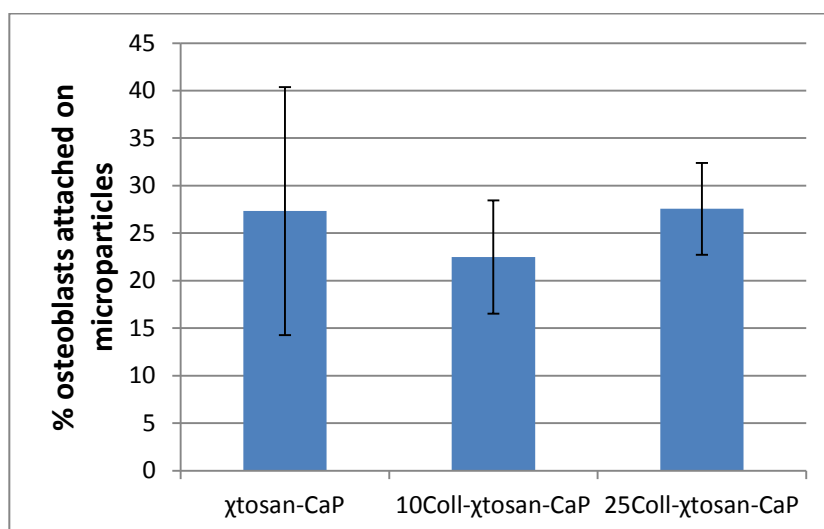


**Figure 6.** Osteoblasts' attachment (%) on beads. One-way ANOVA analysis, followed by Tukey's multiple comparison test showed there is no difference between groups for  $\alpha=0.05$  ( $n=4$ ).

Overall, cells proliferated on all treatment groups of microparticles over the 7 day-cell culture period, but there was no statistically significant difference between groups for fibroblasts (Figure 7) or osteoblasts (Figure 8). At the end of a week, fibroblasts increased 5x in number and osteoblasts multiplied 3-4x on microparticles.

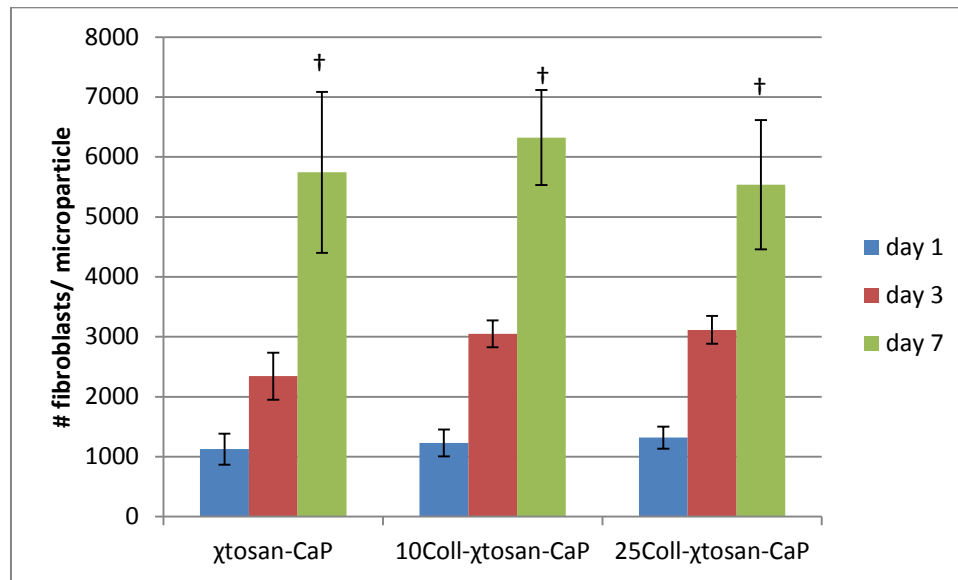


**Figure 7.** Fibroblasts' proliferation on beads. Regression analysis showed no significant difference between groups for NIH/3T3 cells ( $p < 0.05$ ), while one-way ANOVA showed an increase with time: †=difference between all previous time points ( $p < 0.0005$ ),  $n=4$  (except day 1, where  $n=3$  and 10% collagen microparticles on day 7, where  $n=2$ ).

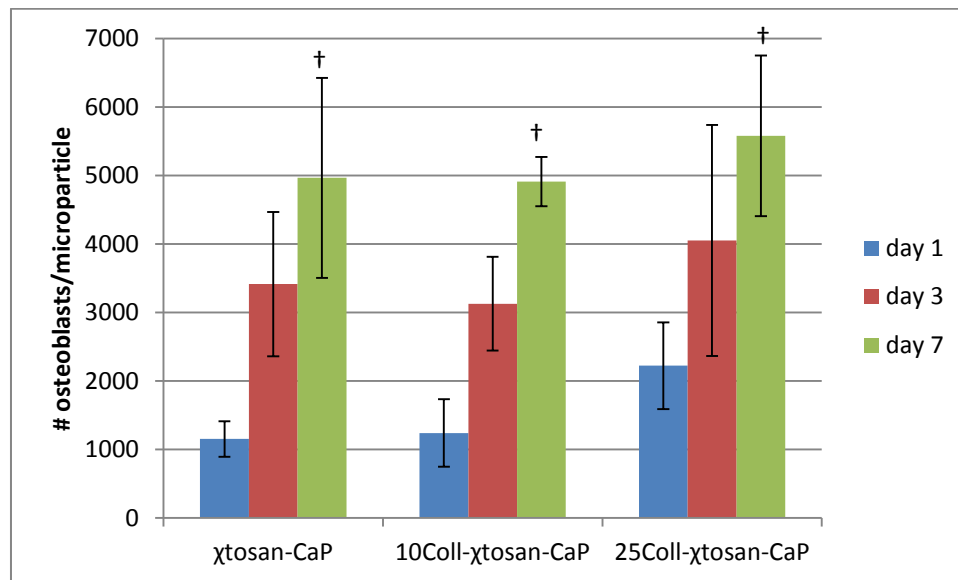


**Figure 8.** Osteoblasts' proliferation on beads. Two-way ANOVA showed that there is a statistically significant increase in osteoblast numbers per day ( $p < 0.001$ ), which means that cells proliferate, but there is no difference between the different bead types. †=difference between all previous time points ( $p < 0.001$ ),  $n=4$ .

A representative LIVE/DEAD image of cell viability on constructs, taken using a Nikon ECLIPSE TE300 microscope with BIOQUANT OSTEO II software, is shown in Figure 9.

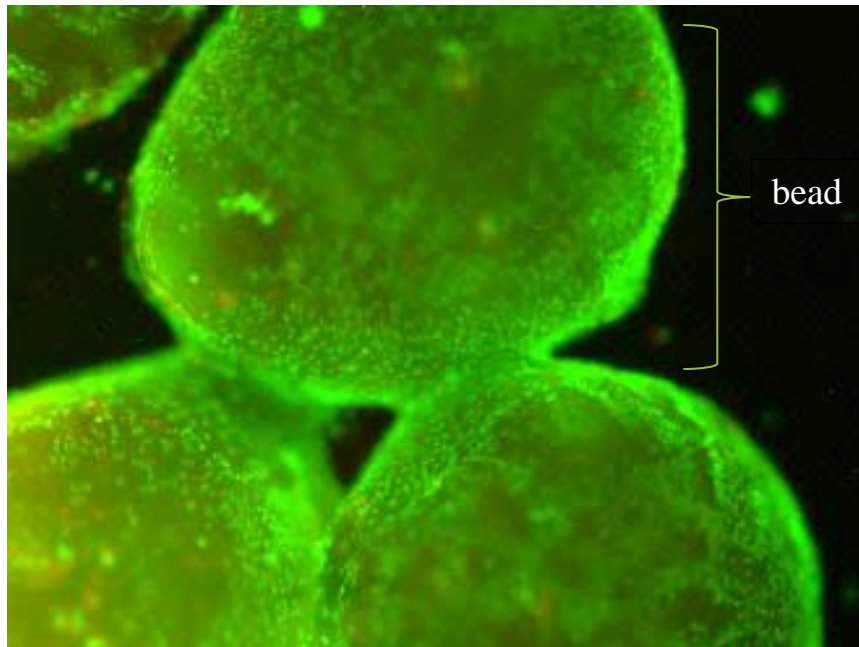


**Figure 9.** Fibroblasts' viability on 25% collagen-chitosan-calcium phosphate microparticles after one week. Light green dots represent fibroblasts.

## **Part 2. Scaffolds' Characterization, Physical and Mechanical**

### **Properties, Degradation and Cell Culture.**

Representative digital images of scaffolds made of the three different bead types fused with either acetic acid or glycolic acid are shown (Figure 10). From the small sequence of images taken ( $n=5$ /scaffold type), the pore size in the gamma-sterilized scaffolds is estimated to be between 100-400  $\mu\text{m}$ . Scaffolds fused with acetic acid appeared darker brown as compared to the scaffolds fused with glycolic acid, which had a lighter brown/yellow appearance. Some of the scaffolds are covered in a sheet of melted

chitosan right next to where the walls of the mold that held the scaffold were. The sheet may result from addition of more acid solution than needed in fusion.

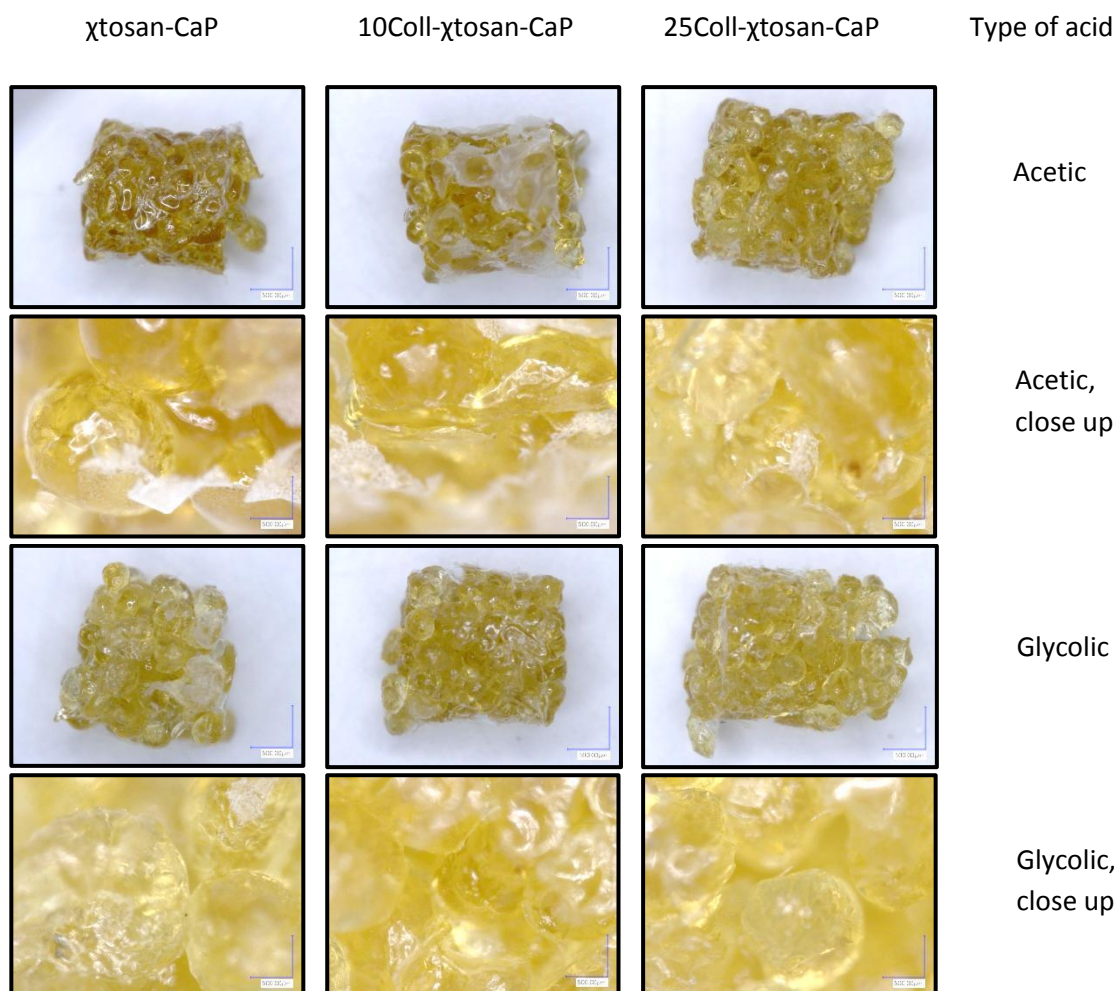


**Figure 10.** Digital images of composite chitosan-collagen-calcium phosphate scaffolds: 100x magnification and close up (200x magnification) to show pore structure. Scale shown: 500  $\mu\text{m}$ .

In order to see if the scaffolds may allow cell migration, growth and also allow for diffusion of nutrients and waste products, the porosity of the scaffolds was measured using a density determination kit. Two-factor ANOVA using the composition of microparticles as one factor and the type of acid used for fusing as another factor, indicated that there were differences in porosity of the scaffolds based on composition ( $p = 0.03$ ), no

differences based on type of acid used for fusing ( $p=0.3$ ), and there was a significant interaction between the composition and type of acid used for fusing ( $p=0.02$ ). Due to interaction, separate one-factor ANOVA's for the type of fusing acid were performed. One-factor ANOVA of acetic acid-fused scaffolds indicated that there was no significant difference in the porosity of the scaffolds due to composition ( $p=0.4$ ). However, one factor ANOVA analyses of the glycolic acid fused scaffolds indicated that there was a difference in porosity of the scaffolds ( $p=0.0002$ ). Tukey's post-hoc test indicated that 25Coll- $\chi$ tosan-CaP, gly\_ac had higher porosity than the  $\chi$ tosan-CaP, gly-ac group but no difference in porosity was observed between the 25Coll- $\chi$ tosan-CaP and the 10Coll- $\chi$ tosan-CaP or between 10Coll- $\chi$ tosan-CaP and the  $\chi$ tosan-CaP groups (Figure 11).



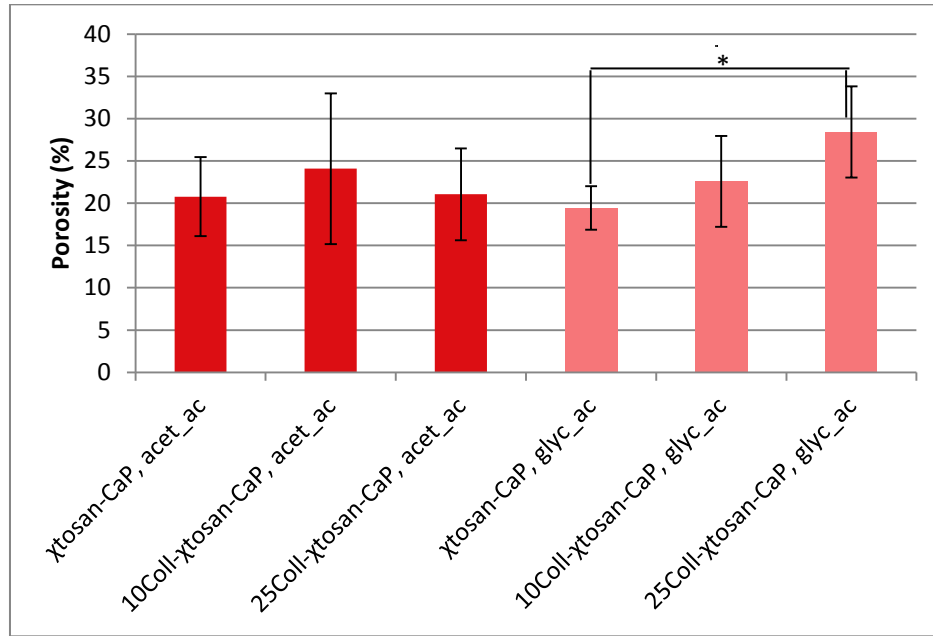


**Figure 11.** Porosity of scaffolds made of chitosan, 10% collagen or 25% collagen and fused with either acetic acid or glycolic acid. Acet\_ac: acetic acid; glyc\_ac: glycolic acid. Two-way ANOVA showed that the porosity of scaffolds among the different levels of composition was different ( $p=0.032$ ), but that based on fusion was not statistically significant. The porosity of 25% collagen-chitosan-calcium phosphate beads fused with glycolic acid (28.4% mean porosity) is higher than that of 25% collagen beads fused with acetic acid and chitosan beads fused with glycolic acid ( $p<0.05$ ). \*=difference between groups ( $p<0.005$ )

To evaluate the load-bearing capacity of the scaffolds, the mechanical properties were determined in compression. A representative stress-strain curve for the scaffolds is presented in Figure 12. Two linear regions were observed in the curves for the scaffolds.

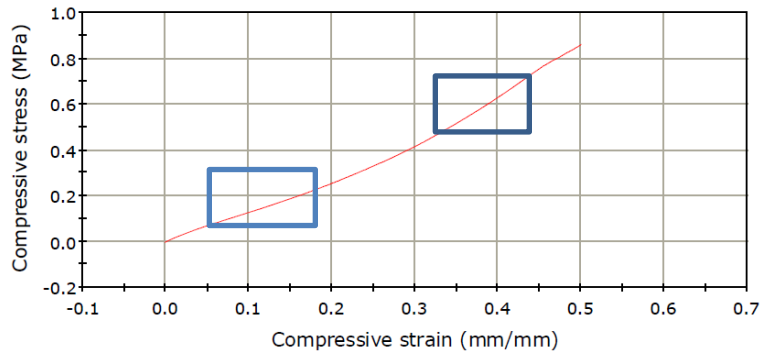


**Figure 12.** Representative stress-strain curve for scaffolds. The two rectangles surround linear portions of the curve.

The linear region at strain=0.05 was used to calculate the compressive modulus. The 5% strain, which was contained within the first linear region of the stress-strain curve of the scaffold, was higher than the maximum strain for the linear region of the stress-strain curve for bone, 0.7%.<sup>152</sup> This already shows that the stress-strain curve for the scaffold is different than that of bone. The second linear region observed in compression tests at higher strains, was associated with the collapse of the composite structure and not with the properties of the porous scaffold. Two-factor ANOVA indicated that there were significant differences in the modulus of the scaffolds based on composition, type of fusing acid, and that there was a significant interaction between the composition and type of fusing acid ( $p \leq 0.001$ ). Due to interaction, separate one-factor ANOVA's based on the type of fusing acid were performed. For scaffolds fused with acetic acid, one-way ANOVA indicated that there were no statistical differences in modulus of the scaffolds based on composition ( $p = 0.7$ ), but that glycolic acid-fused scaffolds had lower modulus than acetic acid-fused scaffolds ( $p < 0.001$ ). For scaffolds fused with glycolic acid, ANOVA indicated that there were differences in the modulus of the different scaffolds based on composition ( $p = 0.001$ ). Tukey's post hoc test indicated a significantly higher modulus for 10% collagen scaffolds vs. 25% collagen scaffolds and chitosan scaffolds

( $p < 0.001$ ). Consequently,  $\chi$ tosan-CaP, acet\_ac, 10Coll- $\chi$ tosan-CaP, glyc\_ac and 25Coll- $\chi$ tosan-CaP, acet\_ac had the significantly higher E ( $p < 0.05$ ) while there was no difference in E between 25Coll- $\chi$ tosan-CaP or the  $\chi$ tosan-CaP composite groups (Figure 13).

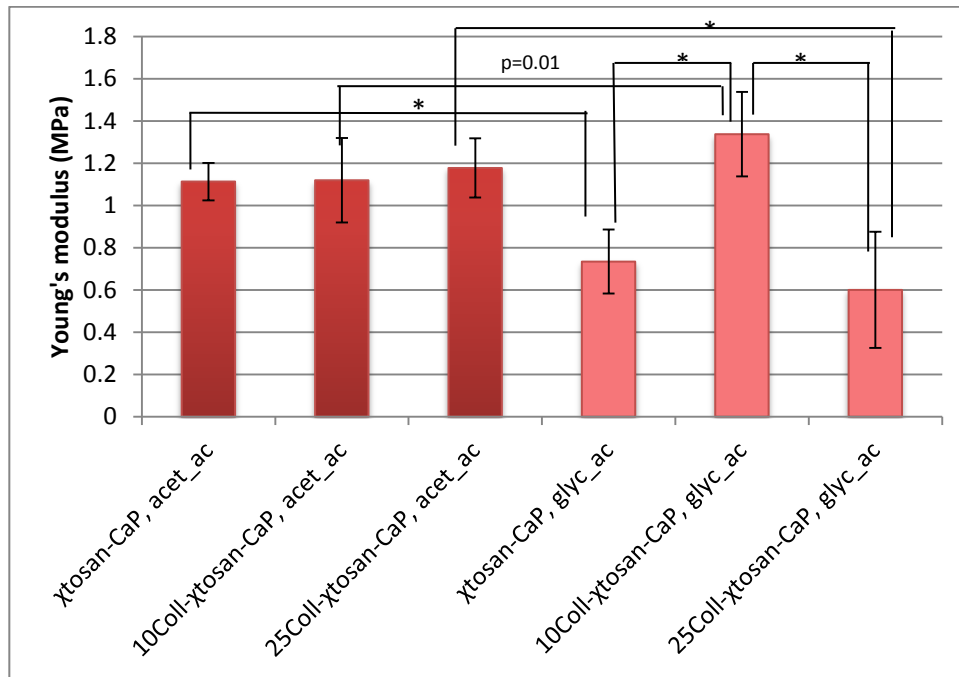


**Figure 13.** Young's modulus in compression of composite scaffolds. Acet\_ac: acetic acid; glyc\_ac: glycolic acid. Two-way ANOVA showed that Young's modulus was higher for all three types of microparticles fused acetic acid than that of microparticles fused with glycolic acid ( $n=10$ ). Error bars are standard deviations. \*=difference between groups' means ( $p < 0.001$ ).

### *Degradation study*

In order to see if fusing the different composite microparticles with acids affects the degradation rate, scaffolds of the three bead compositions fused with acetic acid versus glycolic acid were degraded in control solution or in degradation solution for 4 weeks.

The results of the scaffold degradation study after 4 weeks are summarized in Table 4. Three-way ANOVA followed by post-hoc tests showed there is no statistically significant difference between scaffolds with 10% collagen and chitosan scaffolds, but the glycolic acid-fused microparticles degraded significantly more than the acetic acid-fused

ones ( $p < 0.001$ ). There is a significant increase in the  $\% \Delta \text{mass}$  in degradation solution versus the control solution ( $p < 0.001$ ). In the degradation solution there is a significant group x fusion interaction ( $p \leq 0.001$ ) and difference among different groups within acetic acid: 25Coll- $\chi$ tosan-CaP, acet\_ac vs. 10Coll- $\chi$ tosan-CaP, acet\_ac ( $p < 0.001$ ) and vs.  $\chi$ tosan-CaP, acet\_ac ( $p = 0.002$ ) (Table 4). In degradation solution, based on the type of acid used for fusion, chitosan and 10% collagen scaffolds fused with glycolic acid degraded significantly quicker than those fused with acetic acid.

**Table 4.** The change in mass of scaffolds fused with either acetic or glycolic acid for PBS + enzymes and PBS degradation solution only, respectively, after four weeks.

$\Delta \text{mass}_{\text{scaffolds}}$ (%)						
solution	$\chi$ tosan-CaP, acet_ac	10Coll- $\chi$ tosan-CaP, acet_ac	25Coll- $\chi$ tosan-CaP, acet_ac	$\chi$ tosan-CaP, glyc_ac	10Coll- $\chi$ tosan-CaP, glyc_ac	25Coll- $\chi$ tosan-CaP, glyc_ac
control	1.8 $\pm$ 0.6	2.4 $\pm$ 2.0	1.0 $\pm$ 1.1	6.1 $\pm$ 5.0	9.4 $\pm$ 2.6	2.5 $\pm$ 2.8
enzymes	10.7 $\pm$ 2.5	11.5 $\pm$ 2.0	18.3 $\pm$ 1.2	23.0 $\pm$ 2.6	25.8 $\pm$ 3.4	21.3 $\pm$ 2.5

Regression analysis showed significant increase in the degradation profile ( $p < 0.05$ ) in the enzymes' solution based on composition: chitosan and 10% collagen fused with glycolic acid vs. acetic acid (Figure 14). The scaffolds degraded with time.  $\chi$ tosan-CaP, glyc\_ac and 10Coll- $\chi$ tosan-CaP, glyc\_ac exhibited the highest degradation rate: 6.5-6.6  $\% \Delta \text{m/day}$ .

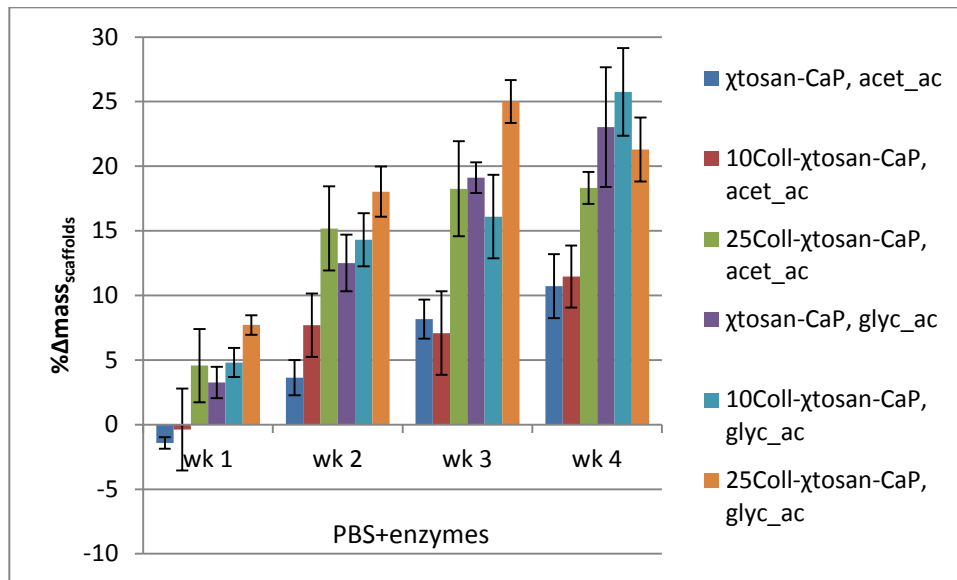


**Figure 14.** Degradation of scaffolds in PBS + enzymes.

Tukey's multiple comparison test showed that the initial masses are similar ( $\alpha=0.05$ ).

Regression analysis showed degradation rates are significantly higher for:

- Chitosan fused with glycolic acid vs. chitosan fused with acetic acid ( $p<0.05$ )
- 10% collagen fused with glycolic acid vs. chitosan fused with acetic acid ( $p<0.05$ )
- Chitosan fused with glycolic acid vs. 10% collagen fused with acetic acid ( $p<0.05$ )
- 10% collagen fused with glycolic acid vs. 10% collagen fused with acetic acid ( $p<0.05$ )

ANOVA analysis showed significant interaction or difference in the degradation profile in PBS based on acetic acid (Figure 15). It also showed increased degradation with time and it distinguished between different degradation groups;  $\chi$ tosan-CaP, acet\_ac,

10Coll- $\chi$ tosan-CaP, acet\_ac and 10Coll- $\chi$ tosan-CaP, glyc\_ac displayed the highest degradation rate: 2.0-2.4 % $\Delta$ m/day.

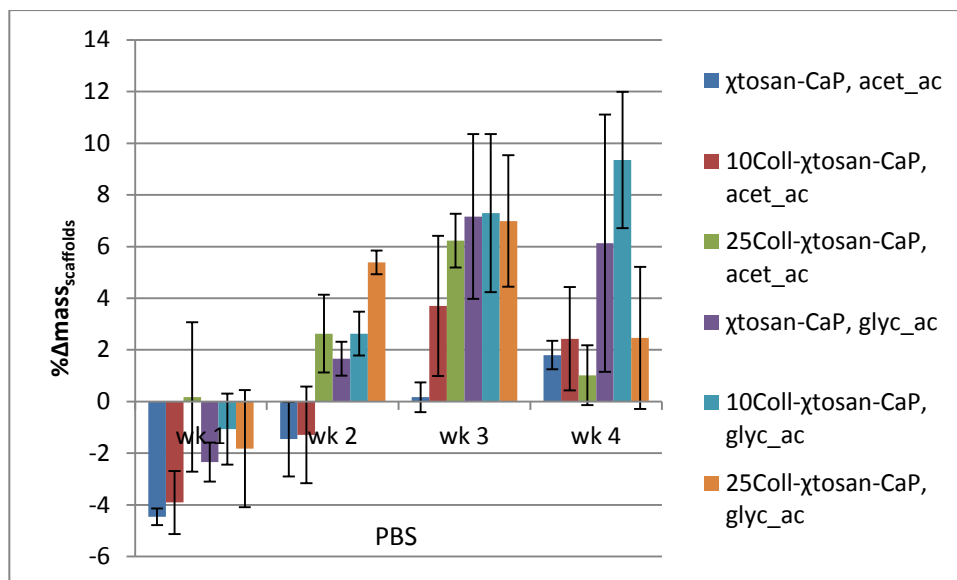


**Figure 15.** Degradation of scaffolds in PBS.

Tukey's multiple comparison test showed that the initial masses of 25% collagen beads fused with glycolic acid are significantly higher than chitosan beads fused with glycolic acid ( $p < 0.05$ ).

Regression analysis showed degradation rates are significantly higher for:

- Chitosan fused with acetic acid vs. 25% collagen fused with acetic acid ( $p < 0.05$ )
- 10% collagen fused with acetic acid vs. 25% collagen fused with acetic acid ( $p < 0.05$ )
- 10% collagen fused with glycolic acid vs. 25% collagen fused with acetic acid ( $p < 0.05$ )

### *Osteoblasts' attachment and proliferation on scaffolds*

For osteoblasts attached on scaffolds, the groups were significantly different ( $p < 0.05$ , one-way ANOVA) and Tukey's test showed a higher attachment for acetic acid-fusion vs. glycolic acid-fusion of the chitosan microparticles. Post hoc analysis showed there was attachment was higher for 10% collagen microparticles fused with glycolic acid than both 10% collagen and 25% collagen microparticles fused with acetic acid, and that attachment on chitosan microparticles fused with acetic acid was higher than 10% collagen microparticles fused with glycolic acid (Figure 16). Chitosan microparticles fused with either acid and 25% collagen-chitosan-calcium phosphate microspheres fused with glycolic acid displayed the highest cell attachment:  $2.7 \pm 1.2\%$ .

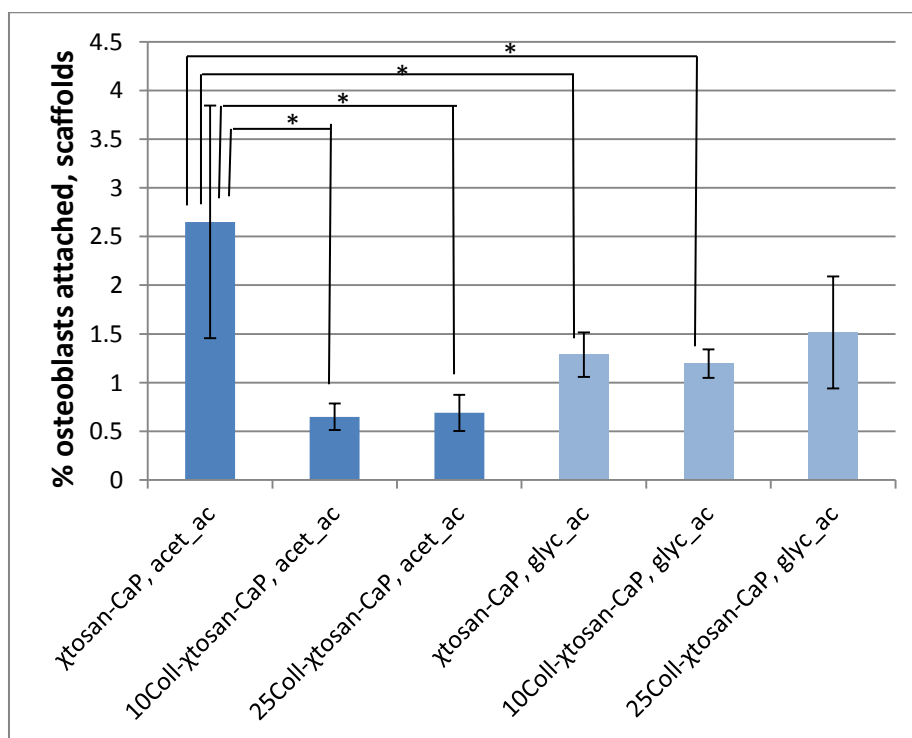


**Figure 16.** Osteoblasts' attachment on scaffolds ( $n=4$ , except chitosan-calcium phosphate microparticles fused with acetic acid, where  $n=3$ ). \* = difference between groups ( $p < 0.05$ )

Overall, cells proliferated on all treatment groups of scaffolds over the 7 day-cell culture period (Figure 17). At the end of a week, osteoblasts proliferated 4-7x on scaffolds (only twice on 10% collagen microparticles fused with glycolic acid). Regression analysis showed a difference on osteoblasts' growth based on group for 10% collagen-chitosan-calcium phosphate scaffolds. Tukey's multiple comparison test showed significantly higher number of osteoblasts/scaffold with time for all scaffolds except for 10% collagen microparticles fused with glycolic acid ( $p < 0.05$ ). There were no statistical differences between day 1 and day 3 for all scaffold groups except the above-mentioned 10% collagen microparticles fused with glycolic acid. Moreover, there was no significant difference between day 3 and 7 for chitosan microparticles fused with glycolic acid.



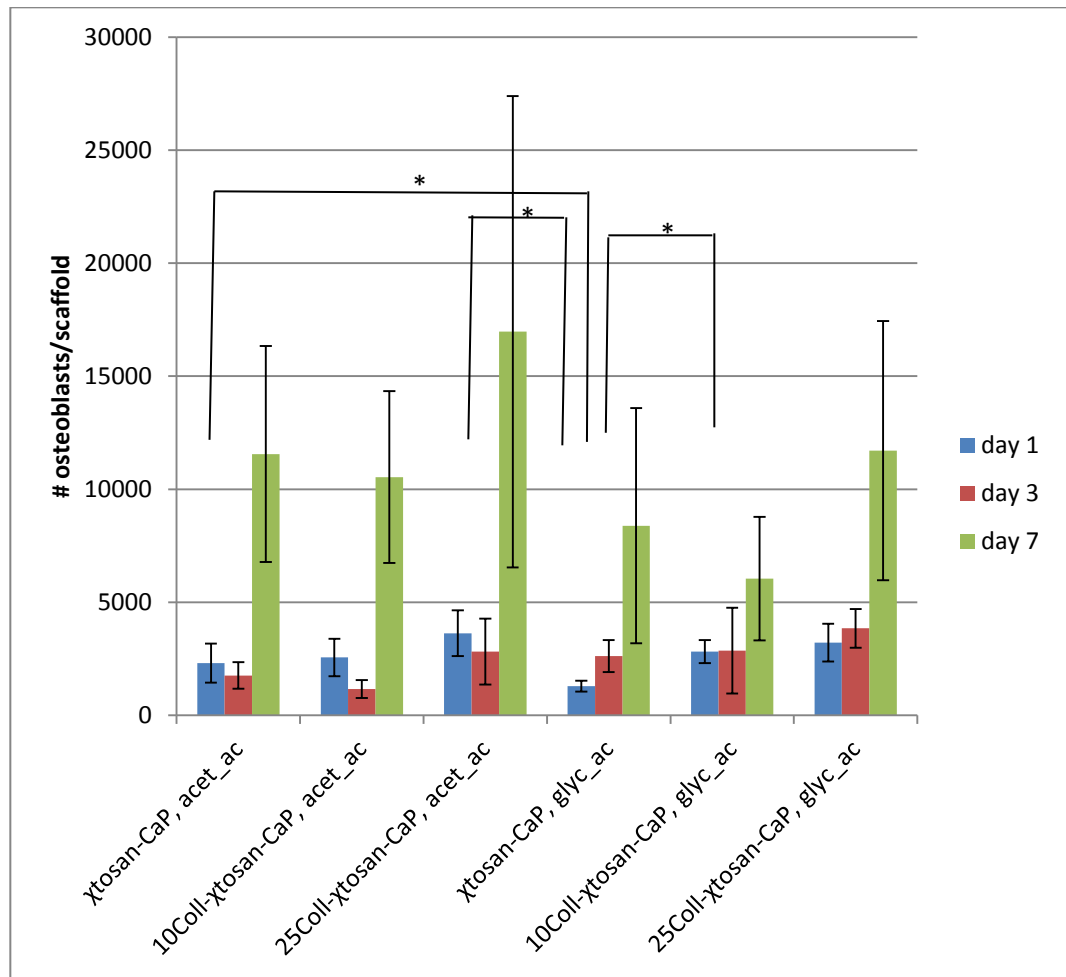


**Figure 17.** Osteoblasts' growth on scaffolds. Regression analysis showed the number of osteoblasts increased with time ( $p < 0.05$ ) and the cell proliferation rate is higher for: chitosan fused with acetic acid than 10% collagen fused with glycolic acid; 10% collagen fused with acetic acid than 10% collagen fused with glycolic acid; 25% collagen fused with acetic acid than 10% collagen fused with glycolic acid. \*=difference between groups ( $p < 0.05$ ),  $n=4$ .

## CHAPTER 5: DISCUSSION

A bone graft should possess adequate porosity, degradability, biocompatibility and initial mechanical strength to provide a framework for cells to attach and proliferate while maintaining bone volume/shape.<sup>76</sup> The predecessors of the present scaffolds showed promising results. When compared to plain chitosan scaffolds, the predecessor composite chitosan-hydroxapatite scaffolds exhibited rougher surface and greater surface area for cell attachment, about 3x higher Young's modulus and increased pre-osteoblast proliferation.<sup>107</sup> The chitosan-crystalline calcium phosphate scaffolds were tougher and more flexible than what has been reported for pure calcium phosphate scaffolds.<sup>107</sup> Chitosan-hydroxyapatite scaffolds developed by Chesnutt et al.,<sup>107</sup> Reves<sup>42</sup> and Nguyen<sup>164</sup> suffered from low degradation and mechanical strength. The mechanical strength of the scaffolds was higher than that of hydrated chitosan/collagen hydrogels (18.9 kPa)<sup>147</sup> and that of Infuse® Bone Graft, which is essentially a collagen sponge, with properties up to 1 kPa.<sup>165</sup>

Additionally, Reves et al. noticed decreased cytocompatibility with the presence of hydroxyapatite (unpublished results).<sup>42</sup> To overcome these limits and improve on the degradation and cytocompatibility of microsphere-based scaffold design, this research incorporated collagen, a biodegradable native component of bone that shows excellent attachment and interaction with cells,<sup>146,147,151,153-157,166</sup> into the chitosan-calcium phosphate microparticles. Further, for increased mechanical strength, we hypothesized that fusion with glycolic acid would melt chitosan-collagen-calcium phosphate beads more than acetic acid, providing higher Young's modulus than acetic acid fusion.

## Part 1. Microparticles

The hydroxyproline assay showed that approximately 25.5-30.3% collagen was incorporated into beads based on initial collagen amount added to composite solution mix.

It has been observed that human bone marrow cells attach to and proliferate better on rougher hydroxyapatite surfaces as compared smoother surfaces.<sup>167</sup> The microparticles displayed roughness, which may have aided cell attachment. All composite beads exhibited an ellipsoidal shape with a sphericity index (i.e. major axis: minor axis) of  $1.3 \pm 0.2$ . We predicted that the surface tension would gather the chitosan-calcium phosphate solution drops into spheres. The microparticles looked spherical when hydrated, but that was not the case in the dry state. Due to the fact that the microparticles were left in precipitating base solution for a short time to prevent the degradation of collagen, there was reduced time for induction of chitosan and calcium phosphate crystallinity. The XRD spectra did reveal decreases in crystallinity for chitosan and CaP in composites, especially as the amount of collagen increased in the formulation. It may be that the microparticles flattened out under their own weight during drying.

An aim of this work was to make composite chitosan-CaP materials with either 10% or 25% collagen. Compositional analysis based on the hydroxyproline assay for collagen and combustion for ash/mineral content indicated that the 10Coll- $\chi$ tosan-CaP particles had actual compositions of  $2.6 \pm 0.2\%$  collagen,  $6.8 \pm 0.8\%$  CaP and  $90.6 \pm 0.8\%$   $\chi$ tosan and that the 25Coll- $\chi$ tosan-CaP particles had actual compositions of  $7.6 \pm 0.8\%$  collagen,  $9.1 \pm 1.2\%$  CaP and  $83.3 \pm 2.0\%$   $\chi$ tosan.

For both chitosan-collagen composites, 26-30% of the initial collagen was incorporated into the microparticles. The lower incorporation of collagen in the microparticles may be due to the following reasons: 1) degradation of collagen in the base

solution during the 10-20 min. interval the microparticles were in the highly alkaline pH (~13) and 2) the presence of salts in the lyophilized collagen used to make the beads, showed by the hydroxyproline assay (10.6%), which was not accounted for when calculating the mass of lyophilized collagen needed to make 10 or 25% collagen microparticles.

In determining the mineral content for the composite microparticles due to the addition of the  $\text{Ca}^{2+}$  and  $\text{PO}_4^{3-}$  salts, it was noted that the chitosan material itself exhibited some residual ash content ( $<0.2\%$ ), which was likely due to residual calcium carbonate from the processing of the materials from original shrimp shells.<sup>168</sup> This amount of ash though was very small ( $\sim 100\times$  less) relative to the overall ash content measured for composites made with solutions containing calcium and phosphate salts and was not considered to add appreciably to the overall mineral component of the composites. All composite microparticles were loaded with the same amount of salts. The decreased calcium phosphate of the 10% collagen composites shown by the ash content may really only be an artifact of the number of washes that were performed to get the pH 7.4-7.8, which could have washed some of the salt away. Hence, all groups were loaded with a similar ratio of Ca:P.

The microparticles' composition does not reflect the relative percentages of components of native bone, except for collagen. Collagen is 19.8-20.1% of bone<sup>47</sup> and 10% of adult bone mass is collagen,<sup>169</sup> which explains why we chose 10-25% collagen. Since the mineral part of bone is underrepresented (6.8-9.1%), an area of improvement is to use a degradable Mg alloy or porous hydroxyapatite to replace the mineral part of bone (up to 69%<sup>47</sup>).

XRD indicated the presence of crystalline chitosan and crystalline forms of CaP

(e.g. a peak for HA at  $2\theta=32^\circ$  with other peaks masked in the background:  $2\theta=26^\circ$  and  $2\theta=40^\circ$ , and a peak at  $2\theta=34.4^\circ$  for TCP). This indicated that even though the beads were in precipitating solution for a short time, there was some induction of crystalline forms (the chitosan and HA peaks are similar to those observed by Reves<sup>66</sup>). The relatively lower intensity of the CaP crystalline peaks as compared to those seen by Chesnutt<sup>40</sup> is reflective of the lower concentration of crystalline CaP forms which is attributed to the short time in base solution. The XRD spectra were noisy due to the presence of chitosan. It was observed that with addition of 10 mass% collagen to the composite, crystalline peaks for chitosan ( $2\theta=12^\circ$ , hydrous peak and  $2\theta=20^\circ$ , anhydrous peak) and HA/TCP decreased and disappeared in the 25% collagen composite microparticles. Consequently, the collagen-containing microparticles are more amorphous than chitosan itself, despite chitosan being a crystalline polymer.<sup>170</sup> This suggests that the addition of collagen interfered with or inhibited the formation of chitosan and CaP crystalline structures. This effect has been seen by others, e.g. Chen et al.<sup>171</sup>

*In vitro* degradation was due to simple hydrolysis and leaching of calcium phosphate salts/minerals. The degradation was 2.5 times greater in solutions with enzymes as compared to the control solution without enzymes. This was expected since the lysozyme and collagenase are the main degradation mechanisms for chitosan and collagen, respectively. However, it appeared that there was no statistically significant difference in degradation rates between different microparticles in either the control or the enzyme degradation solutions. This was contrary to our proposed hypothesis that collagen would increase degradation. Nevertheless, it was important that the degradation of the microparticles increased to 20% after 6 weeks. At two weeks, the mass loss of chitosan beads was 12.5%, 6.25 times higher than that observed by Chesnutt (who saw only 2%

mass loss over 2 weeks in PBS with 5 times higher lysozyme concentration)<sup>107</sup> and Reves, who did not see mass loss over a month.<sup>66</sup> The mass loss of beads at two weeks was similar (although slightly smaller) to that of chitosan beads without calcium phosphate prepared by Mecwan (~15%).<sup>89</sup> The higher degradation rate may be attributed in part to the reduced crystallinity of 61% DDA chitosan compared to the 92.3% DDA chitosan employed by Reves and Chesnutt. The low degree of deacetylation chitosan degrades faster than high DDA chitosan due to looser chain packing of the polymer, making the polymer chains more susceptible to enzymatic degradation by lysozyme.<sup>66</sup> It is noted that the chitosan-calcium phosphate microspheres prepared by Chesnutt et al. exhibited a high chitosan crystallinity index of ~80%.<sup>107</sup> The degradation of the composite microspheres in this study after one month,  $15.1 \pm 8.5\%$ , was intermediate when compared to those reported for several types of chitosan/ $\beta$ -TCP/PMMA microspheres prepared via a emulsion method by Lin L-C et al. which exhibited between 4 and 31% mass loss, with the higher mass loss associated with lower PMMA.<sup>172</sup> However, Lin et al.'s microspheres-cement constructs exhibited a low porosity and no cytocompatibility is assessed. In another study by Yan et al., after cross-linking with 0.5% genipin, the degradation degree of 1:1 collagen:chitosan scaffolds was below 1% in 100  $\mu\text{g/mL}$  collagenase after 12 h,<sup>173</sup> which would project to complete degradation in two months. However, the concentration of the collagenase solution was twice than that used in the present study and no lysozyme was used. The limitation of their study was the storage modulus of the collagen-chitosan scaffolds, which is almost 24000x lower than that of bone, 11 GPa.<sup>174</sup>

*In vitro* cell viability studies on composite microparticles were conducted to observe cytocompatibility. In this study, fibroblast attachment to the microparticles averaging  $40.6 \pm 8.0\%$  was similar to  $42.21 \pm 9.15\%$  HEPM cell attachment to Reves'

microsphere-based scaffolds<sup>66</sup>, but was lower than the 60% attachment observed by Chesnutt,<sup>107</sup> which is considered good cell attachment. The osteoblast attachment to the microparticles,  $25.8 \pm 8.3\%$  was lower than the fibroblast and HEPM cell attachment. There was no difference in the attachment or growth of fibroblasts and osteoblasts between the different composite microparticles. This was contrary to the proposed hypothesis that the addition of collagen would improve both cell attachment and growth. It is noted that attachment and proliferation of fibroblasts was greater than that of osteoblasts, but this is likely due to the difference in initial cell seeding densities, since fibroblasts were seeded at a higher concentration than osteoblasts. LIVE/DEAD assay confirmed the presence of cells, although it wasn't able to show proliferation for all groups. All cells proliferated in time based on the CellTiter-Glo® Luminescent Cell Viability Assay. The highest cell increase after a week was seen in fibroblasts on beads, followed by osteoblasts on beads. The fibroblast proliferation from day 1 to day 7 was 6 fold and the osteoblast proliferation was ~4 fold, compared to 1.6, 1.5 and 1.9 fold proliferation for MC3T3-E1 on chitosan, collagen/chitosan, TGF- $\beta$ 1-loaded collagen/chitosan microgranules, respectively.<sup>175</sup> The one-week cell proliferation in this study is higher than the two-week proliferation of MG63 osteoblast-like cells cultured on collagen–nanohydroxyapatite beads: 1.33x.<sup>97</sup> The fibroblasts and osteoblasts showed adequate proliferation when compared to other cells on substrates with maximum two out of three components of the present microparticles.<sup>97,175</sup> We can conclude that the composite microparticles show improved cytocompatibility.

## **Part 2. Scaffolds**

To make 3D scaffolds, microparticles were fused together by adding dilute acetic or glycolic acid to make the outer surfaces sticky, and then the microparticles were loosely

packed together and allowed to dry. The porosity and pore sizes of the scaffolds were determined based on the Archimedes' principle and by analyzing images of scaffolds, respectively. The porosity of the scaffolds was found to range from  $19.4 \pm 2.6$  to  $23.4 \pm 6.3\%$  and there were no differences based on either the composition of the particles or the type of fusing acid used. This porosity is lower than that reported for other microparticle-based scaffolds:  $33.7 \pm 5.2$ – $35.8 \pm 2.1\%$ .<sup>40,42</sup> The lower porosity is largely attributed to the ellipsoidal shape the microparticles. It has been suggested that a minimum of 30% porosity is needed to provide sufficient space for bone/tissue ingrowth.<sup>80</sup> Improvement in the shape and/or fusing of the particles will be needed to achieve this minimum porosity threshold.

Nevertheless, pore sizes for all scaffolds were found to range from 100-400  $\mu\text{m}$  which are similar to pore sizes reported for other microparticle-based scaffolds (100-800  $\mu\text{m}$  in diameter<sup>66,107</sup>) and above the minimum 50  $\mu\text{m}$  size reported as needed for osteogenesis.<sup>66</sup> Thus, while the porosity of the scaffolds should be increased, the overall pore size is adequate for bone tissue engineering applications.

With regard to color hue perception, the darkening of the scaffolds may be an effect of  $\gamma$ -sterilization.

Ideally, bone scaffolds should be able to bear compressive loads and have enough porosity to allow bone ingrowth and still provide mechanical stability. High levels of porosity cannot be reached without compromising mechanical stability of the chitosan scaffolds. It was suggested that the porosity of bone scaffolds be at least 30%.<sup>80</sup> Knowing that cancellous bone consists of 30% bone and 70% void volume, the scaffolds should have about 30% porosity to allow for native bone ingrowth, while the scaffolds degrade in time.<sup>176</sup> If needed, the porosity can be increased by making the microparticles spherical.



Spherical beads can be obtained by lowering the dripping rate on the syringe pumps or by reducing the volume of acid added to fuse the beads. Less acid for fusion would result in less bead fusion and larger pores. The porosity of the collagen-chitosan-calcium phosphate scaffolds was not affected by the acids used to fuse the beads in this study and was slightly lower than that of chitosan/PLAGA sintered microsphere scaffolds (~35%)<sup>177</sup> and lower than that of other rapid prototyped, lyophilized or other porous formed chitosan-based scaffolds.<sup>90,92,95,96,155</sup> Higher porosity facilitates bone ingrowth better, but that comes with a cost: decreased stiffness.

Young's modulus was computed from the lower linear region of the stress-strain curve because that pertains to the compression of the scaffold with pores (a bone graft structure that will be seen by bone *in vivo*). The two values for strain were chosen to be below the yield strain for bone.<sup>152</sup> Even though bone is linearly elastic up to strain of 0.7% and yields plastically at strains of about 3%,<sup>152</sup> the strain values were chosen to be  $\epsilon=5\%$  and 10% because they fall in the first linear region of the stress-strain curve for the scaffolds. Only Young's modulus at 5% strain is presented. Glycolic acid-fused scaffolds exhibited lower Young's modulus except for 10% collagen. The packing of the microparticles is one of the factors influencing stiffness. Glycolic acid, which is stronger than acetic acid and whose concentration was twice that of acetic acid in this study, may have dissolved chitosan and collagen too much, resulting in a weaker structure. The values of Young's modulus of the present scaffolds are about 10 times lower than the inferior limit of the range of compressive elastic modulus reported for cancellous bone: 10-2000 MPa.<sup>43</sup> This implies that these scaffolds will need further improvement to be load-bearing. Even though the moduli of the scaffolds from this study are 9 times lower than those obtained by Chesnutt et al.,<sup>40</sup>  $9.29\pm0.8$  MPa for rehydrated chitosan-calcium phosphate

scaffolds, the 20x greater degradation rate of the present scaffolds compensates for the lower Young's modulus. In addition, after a month, new bone should infiltrate the scaffold and start taking a part of the load that was originally only on the scaffold.<sup>55,57</sup> Young's modulus, E, of the present scaffolds is lower than some bone regeneration biomaterials containing CaP, PLAGA or PCL<sup>29,32,90,121,172</sup> and higher than that of hydrated chitosan/collagen hydrogels (18.9 kPa)<sup>147</sup> (Table 5). Some of the Young's modulus values will be over-estimated in case of the dry samples (non-physiologically relevant).

**Table 5.** Young's modulus of various bone scaffolds.

Bone scaffold physical state and composition	Young's modulus (MPa)	Reference
Hydrated chitosan-calcium phosphate scaffolds	9.29±0.8	Chesnutt et al. <sup>40</sup>
Hydrated CaP/polyurethane composites	2500-3600	Yoshii et al. <sup>29</sup>
Dry chitosan/β-TCP microspheres in PMMA cement	400-1200	Lin et al. <sup>172</sup>
Dry rapid prototyping-PCL scaffolds	12.5 ± 2.3 in tension	Ahn et al. <sup>90</sup>
Dry porous sintered microsphere scaffolds based on cellulose derivatives	227±59— 292±40	Kumbar et al. <sup>121</sup>
Dry electrohydrodynamic -PCL scaffolds	6.3 ± 1.8 in tension	Ahn et al. <sup>90</sup>
Dry chitosan/HA nanocomposites in 50–50 ratio	17560	Verma et al. <sup>32</sup>
Dry polygalacturonic acid/HA nanocomposites in 50–50 ratio	29810	Verma et al. <sup>32</sup>
Dry chitosan/HA/polygalacturonic acid nanocomposites	23620	Verma et al. <sup>32</sup>
Hydrated chitosan/collagen hydrogels	0.0189	Wang et al. <sup>147</sup>

*In vitro* degradation studies were conducted on scaffolds to investigate the effect of collagen on the degradation profile. At most 9.4±2.6% degradation of scaffolds was observed in solutions without enzymes, whereas in solutions with enzymes, degradation

was 2-2.5x greater ( $25.8 \pm 3.4\%$ ), indicating that enzymes would affect degradation.

Similar to the microparticles, it does not appear that composition had any affect, but it does appear that the type of fusing acid did, with the glycolic acid-fused constructs having greater mass loss than the acetic acid-fused scaffolds. The degradation is higher than that of lysine-triisocyanate-based polyurethane-CaP (PUR) composites: PUR/HA-12% after 6 weeks and PUR/TCP-5% after 6 weeks,<sup>29</sup> porous sintered microsphere scaffolds based on cellulose derivatives-10–15% after 24 weeks.<sup>121</sup> The degradation of scaffolds in the control solution may be due to the following processes: dissolution of salts and simple polymer hydrolysis. The two processes plus enzymatic hydrolysis of the polymers occur in the lysozyme and collagenase solution, which almost tripled the mass loss. Jiang et al. reported that chitosan-PLGA sintered microsphere-based scaffolds had  $\sim 0.5\text{wt}\%$  loss, three times lower than the  $1.5\text{wt}\%$  loss seen for PLGA sintered scaffolds after 12 weeks of degradation.<sup>177</sup> This shows the interaction between the polymers: the increase in chitosan content decreases the degradation rate of the chitosan-collagen-based scaffolds. On the contrary, the results of our study do not support any interaction between chitosan and collagen polymers that can influence degradation.

*In vitro* cell viability studies on scaffolds were conducted to observe if there were any cytotoxic effects with the increased calcium content and type of acid used for fusion of scaffolds. In terms of cell attachment, osteoblasts grew more on chitosan microparticles fused with acetic acid and 25% collagen microparticles fused with glycolic acid than the other 4 groups ( $p < 0.05$ ). The cell attachment was lower than that of HEP-2 cells on chitosan-HA-calcium phosphate scaffolds ( $> 60\%$  attachment after 2 h<sup>40</sup> and  $42.21 \pm 9.15\%$ <sup>66</sup>), but this may be explained by the 10x higher initial cell seeding concentration in the last two studies. The initial % of cells attached can be explained by

the initial cell seeding concentration. The seeding concentration was 43.1 times lower than for NIH-3T3 fibroblasts on beads. Additionally, the initial % of cells attached can be explained by the fact that the pores of the scaffolds may have been filled with medium before the pipetting of the cells, leaving cells to attach only to the surface of the scaffolds. Moreover, two factors can explain the low cell attachment: the pull of gravity of cells toward the bottom of the well where each scaffold lay and the propensity of cells toward tissue culture plastic compared to the scaffold material. Shaking scaffolds of medium before pipetting the cells may have increased the cell attachment, because cells would have gone through the scaffold pores and spent more time, which meant more cells could attach before being pulled by gravity toward the tissue culture plastic-bottom of the well.

LIVE/DEAD assay confirmed the presence of cells, although it wasn't able to show proliferation for all groups. In spite of osteoblasts growing on scaffolds, their low initial seeding concentration ( $9.1 \times 10^3$  cells/mL) and the fact that the scaffolds weren't shaken to leave the pores free of medium before seeding with cells gave misleading LIVE/DEAD images with low cell numbers (not presented). The cells didn't completely cover the scaffolds. All cells proliferated in time, as shown by CellTiter-Glo®, although 10% collagen beads fused with acetic acid showed a slight decrease in number on day 3, but increased in number on day 7. The cells proliferated approximately 7x in a one-week period. Looking at proliferation of osteoblasts or osteoblast-like cells on other bone regeneration biomaterials, the proliferation of osteoblasts in the present study is better than the average (higher than proliferation in 80% of the studies below), as it is higher than scaffolds that contain CaP in the form of apatite or TCP, collagen, gelatin, chitosan<sup>29,40,92-94,96,156</sup> and smaller than the proliferation of scaffolds composed of chitosan, CaP in the form of HA or PCL<sup>90,155</sup> (Table 6).

**Table 6.** Proliferation of osteoblasts or osteoblast-like cells on bone scaffolds.

Scaffold	Time	Prolifera- tion (times or fold)	Reference
PLLA scaffolds coated with apatite	8 days	1.25	Chen Y. et al. <sup>92</sup>
apatite-coated PLGA /HA scaffolds	day 7—day14	1.3	Kim S.S. et al. <sup>93</sup>
nanocomposite gelatin/10 and 30%HA	7 days	1.6	Kim H.W. et al. <sup>96</sup>
PLLA scaffolds coated with apatite/collagen	8 days	1.75	Chen Y. et al. <sup>92</sup>
polyurethane/HA	day 2— day 5	2	Yoshii et al. <sup>29</sup>
CMs (chitosan microspheres)/nHAC/PLLA scaffolds	day 2— day 8	2.2	Niu et al. <sup>156</sup>
nHAC(nanohydroxyapatite/collagen)/PLLA	day 2— day 8	2.5	Niu et al. <sup>156</sup>
SBF-treated HA-added microporous PCL scaffolds	day2—day30	2.6	Ciapetti et al. <sup>94</sup>
chitosan-calcium phosphate composite scaffolds	7 days	3	Chesnutt et al. <sup>40</sup>
polyurethane/TCP	day 2— day 5	4	Yoshii et al. <sup>29</sup>
chitosan scaffolds	day 1— day 6	7	Pallela et al. <sup>155</sup>
chitosan-HA scaffolds	day 1— day 6	~11.5	Pallela et al. <sup>155</sup>
chitosan-HA-marine sponge collagen scaffolds	day 1— day 6	~13.5	Pallela et al. <sup>155</sup>
control rapid prototyping-PCL scaffolds	3 days	20	Ahn et al. <sup>90</sup>

Collagen addition did not impact bead degradation and cell attachment and proliferation, so  $\chi$ tosan-CaP, 10Coll- $\chi$ tosan-CaP and 25Coll- $\chi$ tosan-CaP are viable microparticles for use as building blocks in bone grafts, ligaments or tissue fillers.

In order to determine which scaffold combination provides the best bone graft, cell proliferation was considered as the primary factor in ranking scaffolds, Young's modulus

was the second factor and the degradation in PBS+enzymes was the third factor. Cell attachment and porosity were considered as less important factors and are presented for informative purposes, since cell proliferation is more important than attachment and cell viability should explained by the porosity. Ranking of the scaffolds is presented in table 7.

**Table 7.** Ranking of the scaffolds based on top three factors. +++means best or belongs to group 1 (as mentioned earlier) and + denotes the lowest outcome or belongs to group 3.

<i>Factors</i>	$\chi$ tosan-CaP-acet_ac	10Coll- $\chi$ tosan-CaP, acet_ac	25Coll- $\chi$ tosan-CaP, acet_ac	$\chi$ tosan-CaP, glyc_ac	10Coll- $\chi$ tosan-CaP, glyc_ac	25Coll- $\chi$ tosan-CaP, glyc_ac
<b>Cell Proliferation</b>	+++	+++	+++	++	+	++
<b>Young's modulus</b>	++	+	++	+	++	+
<b>Degradation</b>	+	+	+	++	++	+
<b>Cell attachment</b>	++	+	+	++	++	++
<b>Porosity</b>	++	++	++	+	++	++
<b>Ranking</b>	①	②	①	②	②	③

In summary, chitosan-calcium phosphate and 25% collagen-chitosan-calcium phosphate beads fused with acetic acid seem the most suitable bone graft. They are followed by:  $\chi$ tosan-CaP, glyc\_ac; 10Coll- $\chi$ tosan-CaP, acet\_ac, 10Coll- $\chi$ tosan-CaP, glyc\_ac and lastly, by 10Coll- $\chi$ tosan-CaP, glyc\_ac. Thus, glycolic acid-fused beads

performed worse as a potential bone graft, but all formulations show promise in bone tissue engineering.

If any of the formulations for scaffolds have to be chosen for further research, based on Young's modulus, the best scaffolds would be the ones fused with acetic acid and 10% collagen fused with glycolic acid. Based on degradation, the scaffolds fused with glycolic acid degrade almost 2x as fast than the ones fused with acetic acid. Since cells proliferate on all scaffolds and the number of cells that landed on the scaffold may differ, the scaffolds may be considered similar in proliferation. Following this rationale, since proliferation seems similar, the best scaffold in terms of degradation and stiffness would be 10% collagen-calcium phosphate-chitosan microparticles fused with glycolic acid. Lastly, it would be of interest to increase Young's modulus to make the scaffolds load-bearing.

Furthermore, with the current mechanical properties and degradation profile, the microparticles can serve as tissue fillers for craniofacial defects and should be tested *in vivo*.

## CHAPTER 6: CONCLUSIONS

In this preliminary study, the design criteria were to improve the degradation of previous chitosan-CaP microsphere-based scaffolds, perhaps improving cytocompatibility and mechanical properties. To meet these design criteria, three composite microparticle formulations with chitosan, calcium phosphate and variable percentages of collagen were made by precipitation. These composite microspheres were evaluated *in vitro* for their potential as bone tissue fillers. The microparticles were fused with either acetic or glycolic acid and evaluated *in vitro* as potential bone scaffolds.

It was found that the microspheres with the target 10.0% and 25.0% collagen incorporated only about 30% of the theoretical collagen. XRD analysis indicated that chitosan and the crystalline form of calcium phosphate, HA, is present, as well as TCP.

All bead types degraded approximately 20% within 6 weeks, which predicts degradation within 8 months, below the 13 month-remodeling phase and maturation of bone.<sup>46</sup> More NIH/3T3 fibroblasts than Saos-2 osteoblasts attached to the beads during the 7-week culture period with no difference between microparticle types, which showed good attachment, cytocompatibility and proliferation. Consequently, the data do not support the hypothesis because the addition of collagen did not enhance degradation and cytocompatibility of the microspheres. The proliferation was higher than in other studies.<sup>97,175</sup> Hence, all bead formulations (with and without collagen) may be used as tissue fillers in craniofacial defects, osteoporosis or at the interface between bone and ligament or bone and tendon, or potentially as ligament replacement (in a different shape, of course).

The scaffolds were made from the three types of microparticles and fused with two acids to evaluate differences in porosity, mechanical properties, cell attachment and



proliferation. We demonstrated that, in spite of the overall decreased scaffold porosity (~19-28%), the remaining pores were of adequate size for cell penetration. The at least quadruple growth of osteoblasts on scaffolds stands as evidence for the biocompatible properties of the composites. Glycolic acid-fused scaffolds exhibited lower Young's modulus except for 10% collagen than acetic acid-fused scaffolds ( $E \sim 1$  MPa) at 5% strain. Young's moduli for all scaffolds were about 10 times lower than the inferior limit of the range of compressive elastic modulus reported for cancellous bone: 10-2000 MPa,<sup>43</sup>. All scaffolds, regardless of composition, displayed ~20% degradation in one month, which prognosticated a 6-month dissolution. Moreover, all osteoblasts attached and proliferated approximately 7x in a one-week period, which was higher than the proliferation seen in several other studies.<sup>29,40,92-94,96,146,147,156,157</sup>

The addition of collagen to the microsphere-based scaffolds did not affect degradation, cytocompatibility or Young's modulus, which means that the hypothesis was not supported. Collagen may not have had an effect due to the low collagen incorporation (at most 7.6% collagen when compared to the mass of collagen and chitosan). In conclusion, the collagen-chitosan-calcium phosphate scaffolds are promising candidates for bone grafts that resorb and show good cytocompatibility.

## CHAPTER 7: FUTURE WORK

The results of this study showed about 30% incorporation of collagen in the microspheres. One recommendation would be to look for ways of attaching collagen to chitosan to favor higher retention. Another recommendation would be to use an alternative base solution that will not degrade collagen.

The microparticles' composition does not reflect the relative percentages of components of native bone. Only collagen follows closely bone composition. Collagen is 19.8-20.1% of bone<sup>47</sup> and 10% of adult bone mass is collagen,<sup>169</sup> while we chose 10-25% collagen. Another recommendation is to use a porous hydroxyapatite instead of calcium phosphate and to increase its mass at the loss of chitosan to replace the mineral part of bone (69% by mass)<sup>47</sup> and provide higher Young's modulus to make the scaffolds load-bearing.

Knowing that cancellous bone consists of 30% bone and 70% void volume, the scaffolds should have about 30% porosity to allow for native bone ingrowth, while the scaffolds degrade in time.<sup>176</sup> The porosity of the collagen-chitosan-calcium phosphate scaffolds can be increased by making the microparticles spherical. Spherical beads can be obtained by lowering the dripping rate on the syringe pumps or by reducing the volume of acid added to fuse the beads.

One approach to obtain higher cell attachment on scaffolds (if other cells, such as mesenchymal stem cells are to be tested) is to seed scaffolds with a higher cell concentration (in the range of  $10^5$  cells/mL). Shaking scaffolds of medium before pipetting the cells may increase the cell attachment, because cells would spend more time through the scaffold pores, which means more cells can attach before being pulled by gravity toward the tissue culture plastic-bottom of the well where the scaffolds are kept.

Additionally, the scaffolds can serve as anterior cruciate ligament, ACL, replacement. For this purpose, the solution would have to be dried in strands that mimic the anatomy of ligaments and tested in tension.

Moreover, different techniques (for example,  $\text{HNO}_3$ ) can be explored for fusing these composite collagen-chitosan-calcium phosphate microspheres into 3D bone scaffolds. It would be of interest to conduct a long-term degradation study on these composite bone scaffold constructs fused by different techniques to evaluate their mechanical integrity over the degradation time period. Likewise, of interest would be the evaluation of the pattern of long-term cell growth on the composite collagen-chitosan-calcium phosphate scaffolds in terms of bone cell morphology, gene expression and mineralization markers, such as alkaline phosphatase, calcium content, collagen type I and II, osteopontin, osteocalcin and bone sialoprotein.

The long-term ambition of this work is the implementation of at least one of these types of microparticles and scaffolds as a medical device for use in the clinical setting. Prior to that, the scaffolds should be evaluated for bone-forming properties for at least four months in a Sprague-Dawley rat model. The microspheres can be inserted to fill a calvarial defect, while the scaffolds can be inserted in a critical-sized defect in a rat femur. Histology may be used to assess the ability of the biomaterials to aid in bone plerosis and larger animals may be used prior to human assessment in clinical trials.

## REFERENCES

1. Bishop GB, Einhorn TA. Current and future clinical applications of bone morphogenetic proteins in orthopaedic trauma surgery. *International orthopaedics* 2007;31(6):721-7.
2. Khan SN, Cammisa FP, Jr., Sandhu HS, Diwan AD, Girardi FP, Lane JM. The biology of bone grafting. *The Journal of the American Academy of Orthopaedic Surgeons* 2005;13(1):77-86.
3. Brydone AS, Meek D, Maclaine S. Bone grafting, orthopaedic biomaterials, and the clinical need for bone engineering. *Proceedings of the Institution of Mechanical Engineers. Part H, Journal of engineering in medicine* 2010;224(12):1329-43.
4. Khan Y, Yaszemski MJ, Mikos AG, Laurencin CT. Tissue engineering of bone: material and matrix considerations. *The Journal of bone and joint surgery. American volume* 2008;90 Suppl 1:36-42.
5. Nandi SK, Roy S, Mukherjee P, Kundu B, De DK, Basu D. Orthopaedic applications of bone graft & graft substitutes: a review. *The Indian journal of medical research* 2010;132:15-30.
6. <http://robertgougaloff.wordpress.com/2008/09/03/a-little-bit-on-bone-grafting/>. A little bit on bone grafting.... Robertgougaloff.(2008). Accessed on December, 24th 2011
7. Lynch SEH, C.E.; BioMimetic Therapeutics, Inc. (Franklin, TN), assignee. Compositions and methods for arthrodetic procedures USA. 2012.
8. Burg KJ, Porter S, Kellam JF. Biomaterial developments for bone tissue engineering. *Biomaterials* 2000;21(23):2347-59.
9. [https://www.oxhp.com/secure/policy/bone\\_healing\\_fusion\\_1010.html](https://www.oxhp.com/secure/policy/bone_healing_fusion_1010.html). Bone or Soft Tissue Healing and Fusion Enhancement Products Oxford U.(2011). Accessed on January,19th 2012
10. Armentano I, Dottori M, Fortunati E, Mattioli S, Kenny JM. Biodegradable polymer matrix nanocomposites for tissue engineering: A review. *Polymer Degradation and Stability* 2010;95(11):2126-2146.
11. Lebourg M, Sabater Serra R, Más Estellés J, Hernández Sánchez F, Gómez Ribelles J, Suay Antón J. Biodegradable polycaprolactone scaffold with controlled porosity obtained by modified particle-leaching technique. *Journal of Materials Science: Materials in Medicine* 2008;19(5):2047-2053.
12. Athanasiou KA, Niederauer GG, Agrawal CM. Sterilization, toxicity, biocompatibility and clinical applications of polylactic acid/polyglycolic acid copolymers. *Biomaterials* 1996;17(2):93-102.
13. Wu L, Ding J. In vitro degradation of three-dimensional porous poly(D,L-lactide-co-glycolide) scaffolds for tissue engineering. *Biomaterials* 2004;25(27):5821-30.
14. Chen D, Zhao M, Mundy GR. Bone Morphogenetic Proteins. *Growth Factors* 2004;22(4):233-241.
15. <http://emedicine.medscape.com/article/1230616-overview#aw2aab6b3>. Bone Graft Substitute Materials Laurencin CT, Magge, A., Khan, Y.(2011). Accessed on December, 29th 2011
16. McKay WF, Peckham SM, Badura JM. A comprehensive clinical review of recombinant human bone morphogenetic protein-2 (INFUSE Bone Graft). *International*

- orthopaedics 2007;31(6):729-34.
17. <http://www.medtronic.com/for-healthcare-professionals/products-therapies/spinal-orthopedics/therapies/spinal-fusion/index.htm>. Spinal Fusion. 2010). Accessed on January, 20th 2012
18. <http://www.fda.gov/MedicalDevices/Safety/AlertsandNotices/PublicHealthNotifications/ucm062000.htm>. FDA Public Health Notification: Life-threatening Complications Associated with Recombinant Human Bone Morphogenetic Protein in Cervical Spine Fusion. Schultz DG.(2008). Accessed on March, 3rd 2012
19. <http://www.accessdata.fda.gov/scripts/cdrh/cfdocs/cfRL/rl.cfm>. Establishment Registration & Device Listing (search product code NEK). 2012). Accessed on January, 20th 2012
20. [http://www.rndsystems.com/product\\_results.aspx?k=BMP-7](http://www.rndsystems.com/product_results.aspx?k=BMP-7). Product search results. 2012). Accessed on 2012 March, 21st
21. Schmidmeier GS, P.; Wildemann, B.; Haas, N.P. Use of bone morphogenetic proteins for treatment of non-unions and future perspectives. *Injury* 2007;38(S4):S35-S31.
22. Cahill KS, Chi JH, Day A, Claus EB. Prevalence, Complications, and Hospital Charges Associated With Use of Bone-Morphogenetic Proteins in Spinal Fusion Procedures. *JAMA: The Journal of the American Medical Association* 2009;302(1):58-66.
23. Wong DA, Kumar A, Jatana S, Ghiselli G, Wong K. Neurologic impairment from ectopic bone in the lumbar canal: a potential complication of off-label PLIF/TLIF use of bone morphogenetic protein-2 (BMP-2). *The spine journal : official journal of the North American Spine Society* 2008;8(6):1011-8.
24. <http://clinicaltrials.gov/ct2/show/NCT00942045>. Osteocel® Plus in Anterior Cervical Discectomy and Fusion (ACDF). 2012). Accessed on March, 3rd 2012
25. Knutsen G, Drogset JO, Engebretsen L, Grontvedt T, Isaksen V, Ludvigsen TC, Roberts S, Solheim E, Strand T, Johansen O. A randomized trial comparing autologous chondrocyte implantation with microfracture. Findings at five years. *The Journal of bone and joint surgery. American volume* 2007;89(10):2105-12.
26. Holzwarth JM, Ma PX. Biomimetic nanofibrous scaffolds for bone tissue engineering. *Biomaterials* 2011;32(36):9622-9.
27. Ding L, Davidchack RL, Pan J. A molecular dynamics study of Young's modulus change of semi-crystalline polymers during degradation by chain scissions. *Journal of the Mechanical Behavior of Biomedical Materials* 2012;5(1):224-230.
28. Dong Y, Ruan Y, Wang H, Zhao Y, Bi D. Studies on glass transition temperature of chitosan with four techniques. *Journal of Applied Polymer Science* 2004;93(4):1553-1558.
29. Yoshii T, Dumas JE, Okawa A, Spengler DM, Guelcher SA. Synthesis, characterization of calcium phosphates/polyurethane composites for weight-bearing implants. *Journal of Biomedical Materials Research Part B: Applied Biomaterials* 2012;100B(1):32-40.
30. Li Z, Yubao L, Aiping Y, Xuelin P, Xuejiang W, Xiang Z. Preparation and &lt;i>in vitro&lt;/i> investigation of chitosan/nano-hydroxyapatite composite used as bone substitute materials. *Journal of Materials Science: Materials in Medicine* 2005;16(3):213-219.
31. Zhang Y, Zhang M. Three-dimensional macroporous calcium phosphate bioceramics with nested chitosan sponges for load-bearing bone implants. *Journal of biomedical materials research* 2002;61(1):1-8.
32. Verma DK, K.S.; Katti, D.R.; Mohanty, B. Mechanical response and multilevel structure of biomimetic hydroxyapatite/polygalacturonic/chitosan nanocomposites.

- Materials Science and Engineering, C 2008;28:399-405.
33. Bumgardner JDW, R.; Gerard, P.D.; Bergin, P.; Chestnutt, B.; Marini, M.; Ramsey, V.; Elder, S.H.; Gilbert, J.A. Chitosan: potential use as a bioactive coating for orthopaedic and craniofacial/dental implants. *Journal of Biomaterials Science, Polymer Edition* 2003;14(5):423-238.
  34. Di Martino A, Sittering M, Risbud MV. Chitosan: a versatile biopolymer for orthopaedic tissue-engineering. *Biomaterials* 2005;26(30):5983-90.
  35. Khor E, Lim LY. Implantable applications of chitin and chitosan. *Biomaterials* 2003;24(13):2339-49.
  36. Kim IY, Seo SJ, Moon HS, Yoo MK, Park IY, Kim BC, Cho CS. Chitosan and its derivatives for tissue engineering applications. *Biotechnology advances* 2008;26(1):1-21.
  37. Kumar MNVR. A review of chitin and chitosan applications. *Reactive & Functional Polymers* 2000;46(1):1-27.
  38. Shi C, Zhu Y, Ran X, Wang M, Su Y, Cheng T. Therapeutic potential of chitosan and its derivatives in regenerative medicine. *The Journal of surgical research* 2006;133(2):185-92.
  39. Sinha VR, Singla AK, Wadhawan S, Kaushik R, Kumria R, Bansal K, Dhawan S. Chitosan microspheres as a potential carrier for drugs. *International Journal of Pharmaceutics* 2004;274(1-2):1-33.
  40. earch. Part A 2009;88(2):491-502.
  41. Chesnutt BM, Yuan Y, Buddington K, Haggard WO, Bumgardner JD. Composite chitosan/nano-hydroxyapatite scaffolds induce osteocalcin production by osteoblasts in vitro and support bone formation in vivo. *Tissue engineering. Part A* 2009;15(9):2571-9.
  42. Reves BT, Bumgardner JD, Cole JA, Yang Y, Haggard WO. Lyophilization to improve drug delivery for chitosan-calcium phosphate bone scaffold construct: a preliminary investigation. *Journal of biomedical materials research. Part B, Applied biomaterials* 2009;90(1):1-10.
  43. Keavney TMH, W.C. Mechanical properties of cortical and cancellous bone; 1992. 285 p.
  44. Lee SH, Shin H. Matrices and scaffolds for delivery of bioactive molecules in bone and cartilage tissue engineering. *Advanced drug delivery reviews* 2007;59(4-5):339-59.
  45. Logeart-Avramoglou D, Anagnostou F, Bizios R, Petite H. Engineering bone: challenges and obstacles. *Journal of cellular and molecular medicine* 2005;9(1):72-84.
  46. Roberts WE. Bone tissue interface. *Journal of dental education* 1988;52(12):804-9.
  47. Rhoades RAT, G.A. *Medical Physiology*. Boston; 1995.
  48. Ding MD, M.; Danielsen, C.C.; Kabel, J.; Hvid, I.; Linde, F. Age variations in the properties of human tibial trabecular bone. *Journal of Bone and Joint Surgery (British Volume)* 1997;79-B:995-1002.
  49. Michael H. Ross WP. *Histology: a text and atlas*. Baltimore, MD: Lippincott Williams & Wilkins; 2006. 906 p.
  50. Michael H. Ross WP, Todd A. *Atlas of descriptive histology*. Sunderland, MA: Sinauer Associates, INC.; 2009. 367 p.
  51. Kaplan RJ. *Physical Medicine and Rehabilitation Review: Pearls of Wisdom*. McGraw Hill; 2005.
  52. <http://web.mit.edu/newsoffice/2007/bone-0906.html>. MIT probes secret of bone's strength. Brehm D.(2007). Accessed on January, 28th 2012

53. Buckwalter JAE, T.A.; Simon, S.R. Orthopaedic Basic Science: Biology and Biomechanics of the Musculoskeletal System: American Academy fo Orthopaedic Surgeons; 2000.
54. Qin Z, Gautieri A, Nair AK, Inbar H, Buehler MJ. Thickness of Hydroxyapatite Nanocrystal Controls Mechanical Properties of the Collagen–Hydroxyapatite Interface. *Langmuir* 2011.
55. Kalfas IH. Principles of bone healing. *Neurosurgical focus* 2001;10(4):E1.
56. Agna JW, Knowles HC, Jr., Alverson G. The mineral content of normal human bone. *The Journal of clinical investigation* 1958;37(10):1357-61.
57. Carano RA, Filvaroff EH. Angiogenesis and bone repair. *Drug discovery today* 2003;8(21):980-9.
58. Johnell O, Kanis JA. An estimate of the worldwide prevalence and disability associated with osteoporotic fractures. *Osteoporosis international : a journal established as result of cooperation between the European Foundation for Osteoporosis and the National Osteoporosis Foundation of the USA* 2006;17(12):1726-33.
59. Belmont PJ, Jr., Thomas D, Goodman GP, Schoenfeld AJ, Zacchilli M, Burks R, Owens BD. Combat musculoskeletal wounds in a US Army Brigade Combat Team during operation Iraqi Freedom. *The Journal of trauma* 2011;71(1):E1-7.
60. McIntyre T, Hughes CD, Pauyo T, Sullivan SR, Rogers SO, Jr., Raymonville M, Meara JG. Emergency surgical care delivery in post-earthquake Haiti: Partners in Health and Zanmi Lasante experience. *World journal of surgery* 2011;35(4):745-50.
61. Hill DA, Delaney LM, Duflou J. A population-based study of outcome after injury to car occupants and to pedestrians. *The Journal of trauma* 1996;40(3):351-5.
62. Ries LAGS, M.A.; Gurney, J.G.; Linet, M.; Tamra, T.; Young, J.L.; Bunin, G.R. Cancer Incidence and Survival among Children and Adolescents: United States SEER Program 1975-1995, National Cancer Institute, SEER Program. NIH Pub. No. 99-4649. Bethesda, MD; 1999.
63. Hughes MSA, J.O. The Use of Implantable Bone Stimulators in Nonunion Treatment. *Orthopedics* 2010;151-157.
64. Marino JT, Ziran BH. Use of Solid and Cancellous Autologous Bone Graft for Fractures and Nonunions. *The Orthopedic clinics of North America* 2010;41(1):15-26.
65. <http://www.orthoped.org/bone-fracture-healing.html>. Bone Fracture Healing. 2010). Accessed on December, 28th 2011
66. Reves BT. Preliminary investigation of lyophilization to improve drug delivery of chitosan-calcium phosphate bone scaffold construct. Memphis: University of Memphis; 2008. 128 p.
67. Lines LD. The management of ballistic trauma: an infection control perspective. *British journal of nursing* 2005;14(4):196-9.
68. Petersen K, Riddle MS, Danko JR, Blazes DL, Hayden R, Tasker SA, Dunne JR. Trauma-related infections in battlefield casualties from Iraq. *Annals of surgery* 2007;245(5):803-11.
69. Thibodeau G. A. PKT. *Anatomy and Physiology*: Mosby 2003.
70. Bernstein J. *Musculoskeletal Medicine*: American Academy of Orthopaedic Surgeons; 2003.
71. Suzuki A, Terai H, Toyoda H, Namikawa T, Yokota Y, Tsunoda T, Takaoka K. A biodegradable delivery system for antibiotics and recombinant human bone morphogenetic protein-2: A potential treatment for infected bone defects. *Journal of orthopaedic research : official publication of the Orthopaedic Research Society*

- 2006;24(3):327-32.
72. Stephan SJ, Tholpady SS, Gross B, Petrie-Aronin CE, Botchway EA, Nair LS, Ogle RC, Park SS. Injectable tissue-engineered bone repair of a rat calvarial defect. *The Laryngoscope* 2010;120(5):895-901.
73. Horner EA, Kirkham J, Wood D, Curran S, Smith M, Thomson B, Yang XB. Long bone defect models for tissue engineering applications: criteria for choice. *Tissue engineering. Part B, Reviews* 2010;16(2):263-71.
74. Kanakaris NK, Giannoudis PV. The health economics of the treatment of long-bone non-unions. *Injury* 2007;38 Suppl 2:S77-84.
75. Dahabreh Z, Dimitriou R, Giannoudis PV. Health economics: A cost analysis of treatment of persistent fracture non-unions using bone morphogenetic protein-7. *Injury* 2007;38(3):371-377.
76. Mao JS, Zhao LG, Yin YJ, Yao KD. Structure and properties of bilayer chitosan-gelatin scaffolds. *Biomaterials* 2003;24(6):1067-74.
77. Whang K, Thomas, C.H., Healey, K.E., Nuber, G. A novel method to fabricate bioabsorbable scaffolds. *Polymers* 1995;36:837-42.
78. Wongwitwichot P, Kaewsrirachan J, Chua KH, Ruszymah BH. Comparison of TCP and TCP/HA Hybrid Scaffolds for Osteoconductive Activity. *The open biomedical engineering journal* 2010;4:279-85.
79. Hutmacher DW. Scaffolds in tissue engineering bone and cartilage. *Biomaterials* 2000;21(24):2529-43.
80. Borden M, Attawia M, Khan Y, Laurencin CT. Tissue engineered microsphere-based matrices for bone repair: design and evaluation. *Biomaterials* 2002;23(2):551-9.
81. Boyan BD, Hummert TW, Dean DD, Schwartz Z. Role of material surfaces in regulating bone and cartilage cell response. *Biomaterials* 1996;17(2):137-46.
82. Fisher JP, Lalani Z, Bossano CM, Brey EM, Demian N, Johnston CM, Dean D, Jansen JA, Wong ME, Mikos AG. Effect of biomaterial properties on bone healing in a rabbit tooth extraction socket model. *Journal of biomedical materials research. Part A* 2004;68(3):428-38.
83. Ohgushi H, Caplan AI. Stem cell technology and bioceramics: from cell to gene engineering. *Journal of biomedical materials research* 1999;48(6):913-27.
84. Khan SN, Tomin E, Lane JM. Clinical applications of bone graft substitutes. *The Orthopedic clinics of North America* 2000;31(3):389-98.
85. Lee GH, Khoury JG, Bell JE, Buckwalter JA. Adverse reactions to OsteoSet bone graft substitute, the incidence in a consecutive series. *The Iowa orthopaedic journal* 2002;22:35-8.
86. Beuerlein MJS, McKee MD. Calcium Sulfates: What Is the Evidence? *Journal of Orthopaedic Trauma* 2010;24:S46-S51 10.1097/BOT.0b013e3181cec48e.
87. Porter JR, Ruckh TT, Popat KC. Bone tissue engineering: a review in bone biomimetics and drug delivery strategies. *Biotechnology progress* 2009;25(6):1539-60.
88. Boeree NR, Dove J, Cooper JJ, Knowles J, Hastings GW. Development of a degradable composite for orthopaedic use: mechanical evaluation of an hydroxyapatite-polyhydroxybutyrate composite material. *Biomaterials* 1993;14(10):793-796.
89. Mecwan MM. Design and Evaluation of a Novel Composite Chitosan-Poly(Lactide-co-Glycolide) Microsphere Based System for Bone Tissue Engineering Applications. Memphis: University of Memphis; 2011.
90. Ahn SH, Lee HJ, Kim GH. Polycaprolactone Scaffolds Fabricated with an Advanced Electrohydrodynamic Direct-Printing Method for Bone Tissue Regeneration.



- Biomacromolecules 2011;12(12):4256-4263.
91. [https://www.unitedhealthcareonline.com/ccmcontent/ProviderII/UHC/en-US/Assets/ProviderStaticFiles/ProviderStaticFilesPdf/Tools%20and%20Resources/Policies%20and%20Protocols/Medical%20Policies/Medical%20Policies/Bone\\_Healing\\_and\\_Fusion\\_Enhancement\\_Products.pdf](https://www.unitedhealthcareonline.com/ccmcontent/ProviderII/UHC/en-US/Assets/ProviderStaticFiles/ProviderStaticFilesPdf/Tools%20and%20Resources/Policies%20and%20Protocols/Medical%20Policies/Medical%20Policies/Bone_Healing_and_Fusion_Enhancement_Products.pdf). Bone or soft tissue healing and fusion enhancement products. 2011). Accessed on January, 30th 2012
  92. Chen Y, Mak AFT, Wang M, Li J, Wong MS. PLLA scaffolds with biomimetic apatite coating and biomimetic apatite/collagen composite coating to enhance osteoblast-like cells attachment and activity. *Surface and Coatings Technology* 2006;201(3–4):575-580.
  93. Kim SS, Park MS, Gwak SJ, Choi CY, Kim BS. Accelerated bonelike apatite growth on porous polymer/ceramic composite scaffolds in vitro. *Tissue engineering* 2006;12(10):2997-3006.
  94. Ciapetti G, Ambrosio L, Savarino L, Granchi D, Cenni E, Baldini N, Pagani S, Guizzardi S, Causa F, Giunti A. Osteoblast growth and function in porous poly epsilon-caprolactone matrices for bone repair: a preliminary study. *Biomaterials* 2003;24(21):3815-24.
  95. Lickorish D, Ramshaw JA, Werkmeister JA, Glattauer V, Howlett CR. Collagen-hydroxyapatite composite prepared by biomimetic process. *Journal of biomedical materials research. Part A* 2004;68(1):19-27.
  96. Kim HW, Kim HE, Salih V. Stimulation of osteoblast responses to biomimetic nanocomposites of gelatin-hydroxyapatite for tissue engineering scaffolds. *Biomaterials* 2005;26(25):5221-30.
  97. Tsai S-W, Hsu F-Y, Chen P-L. Beads of collagen–nanohydroxyapatite composites prepared by a biomimetic process and the effects of their surface texture on cellular behavior in MG63 osteoblast-like cells. *Acta biomaterialia* 2008;4(5):1332-1341.
  98. Li LH, Kommareddy KP, Pilz C, Zhou CR, Fratzl P, Manjubala I. In vitro bioactivity of bioresorbable porous polymeric scaffolds incorporating hydroxyapatite microspheres. *Acta biomaterialia* 2010;6(7):2525-31.
  99. Kim IS, Park JW, Kwon IC, Baik BS, Cho BC. Role of BMP, betaig-h3, and chitosan in early bony consolidation in distraction osteogenesis in a dog model. *Plastic and reconstructive surgery* 2002;109(6):1966-77.
  100. Madhally SV, Matthew HW. Porous chitosan scaffolds for tissue engineering. *Biomaterials* 1999;20(12):1133-42.
  101. Muzzarelli RAA. Osteogenesis promoted by calcium phosphate dicarboxyboxymethyl chitosan. *Carbohydrate Polymers* 1998;36:267-76.
  102. Ge Z, Baguenard S, Lim LY, Wee A, Khor E. Hydroxyapatite–chitin materials as potential tissue engineered bone substitutes. *Biomaterials* 2004;25(6):1049-1058.
  103. Muzzarelli RAM-B, M.; Tietz, C.; Biagini, R.; Ferioli, G.; Brunelli, M.A.; Fini, M.; Giardino, R.; Ilari, P.; Biagini, G. Stimulatory effect on bone formation exerted by a modified chitosan. *Biomaterials* 1994;15(13):1075-81.
  104. Lee YM, Park YJ, Lee SJ, Ku Y, Han SB, Klokkevold PR, Chung CP. The bone regenerative effect of platelet-derived growth factor-BB delivered with a chitosan/tricalcium phosphate sponge carrier. *Journal of periodontology* 2000;71(3):418-24.
  105. Park D-J, Choi B-H, Zhu S-J, Huh J-Y, Kim B-Y, Lee S-H. Injectable bone using chitosan-alginate gel/mesenchymal stem cells/BMP-2 composites. *Journal of Cranio-Maxillofacial Surgery* 2005;33(1):50-54.

106. Haberstroh K, Ritter K, Kuschnierz J, Bormann K-H, Kaps C, Carvalho C, Mülhaupt R, Sittinger M, Gellrich N-C. Bone repair by cell-seeded 3D-bioplotting composite scaffolds made of collagen treated tricalciumphosphate or tricalciumphosphate-chitosan-collagen hydrogel or PLGA in ovine critical-sized calvarial defects. *Journal of Biomedical Materials Research Part B: Applied Biomaterials* 2010;93B(2):520-530.
107. Chesnutt BC. Composite chitosan/calcium phosphate biomaterials for bone tissue engineering. Memphis: University of Memphis; 2008. 157 p.
108. Wang J, de Boer J, de Groot K. Proliferation and differentiation of MC3T3-E1 cells on calcium phosphate/chitosan coatings. *Journal of dental research* 2008;87(7):650-4.
109. Chua PH, Neoh KG, Kang ET, Wang W. Surface functionalization of titanium with hyaluronic acid/chitosan polyelectrolyte multilayers and RGD for promoting osteoblast functions and inhibiting bacterial adhesion. *Biomaterials* 2008;29(10):1412-21.
110. Yuan Y, Chesnutt BM, Wright L, Haggard WO, Bumgardner JD. Mechanical property, degradation rate, and bone cell growth of chitosan coated titanium influenced by degree of deacetylation of chitosan. *Journal of biomedical materials research. Part B, Applied biomaterials* 2008;86(1):245-52.
111. Greene AH, Bumgardner JD, Yang Y, Moseley J, Haggard WO. Chitosan-coated stainless steel screws for fixation in contaminated fractures. *Clinical orthopaedics and related research* 2008;466(7):1699-704.
112. Zhang Y, Zhang M. Synthesis and characterization of macroporous chitosan/calcium phosphate composite scaffolds for tissue engineering. *Journal of biomedical materials research* 2001;55(3):304-12.
113. Zhang Y, Zhang M. Calcium phosphate/chitosan composite scaffolds for controlled in vitro antibiotic drug release. *Journal of biomedical materials research* 2002;62(3):378-86.
114. Kong L, Gao Y, Cao W, Gong Y, Zhao N, Zhang X. Preparation and characterization of nano-hydroxyapatite/chitosan composite scaffolds. *Journal of biomedical materials research. Part A* 2005;75(2):275-82.
115. Yin Y, Ye F, Cui J, Zhang F, Li X, Yao K. Preparation and characterization of macroporous chitosan-gelatin/beta-tricalcium phosphate composite scaffolds for bone tissue engineering. *Journal of biomedical materials research. Part A* 2003;67(3):844-55.
116. Arpornmaeklong P, Pripatnanont P, Suwatwirote N. Properties of chitosan-collagen sponges and osteogenic differentiation of rat-bone-marrow stromal cells. *International Journal of Oral and Maxillofacial Surgery* 2008;37(4):357-366.
117. Zhang Y, Venugopal JR, El-Turki A, Ramakrishna S, Su B, Lim CT. Electrospun biomimetic nanocomposite nanofibers of hydroxyapatite/chitosan for bone tissue engineering. *Biomaterials* 2008;29(32):4314-22.
118. Xianmiao C, Yubao L, Yi Z, Li Z, Jidong L, Huanan W. Properties and in vitro biological evaluation of nano-hydroxyapatite/chitosan membranes for bone guided regeneration. *Materials Science and Engineering: C* 2009;29(1):29-35.
119. Manjubala I, Scheler S, Bossert J, Jandt KD. Mineralisation of chitosan scaffolds with nano-apatite formation by double diffusion technique. *Acta biomaterialia* 2006;2(1):75-84.
120. Li X, Feng Q, Liu X, Dong W, Cui F. Collagen-based implants reinforced by chitin fibres in a goat shank bone defect model. *Biomaterials* 2006;27(9):1917-23.
121. Kumbar SG, Toti US, Deng M, James R, Laurencin CT, Aravamudhan A, Harmon M, Ramos DM. Novel mechanically competent polysaccharide scaffolds for bone tissue engineering. *Biomedical materials* 2011;6(6):065005.

122. Borden M, El-Amin SF, Attawia M, Laurencin CT. Structural and human cellular assessment of a novel microsphere-based tissue engineered scaffold for bone repair. *Biomaterials* 2003;24(4):597-609.
123. Seol Y-J, Lee J-Y, Park Y-J, Lee Y-M, Ku Y, Rhyu I-C, Lee S-J, Han S-B, Chung C-P. Chitosan sponges as tissue engineering scaffolds for bone formation. *Biotechnology Letters* 2004;26(13):1037-1041.
124. Jameela SR, Misra A, Jayakrishnan A. Cross-linked chitosan microspheres as carriers for prolonged delivery of macromolecular drugs. *Journal of Biomaterials Science, Polymer Edition* 1995;6(7):621-632.
125. Li JD, Y.M.; Liang, H.B. Influence of molecular parameters on the degradation of chitosan by a commercial enzyme. *Polymer Degradation and Stability* 2007;92(3):515-524.
126. Zhang H, Neau SH. In vitro degradation of chitosan by a commercial enzyme preparation: effect of molecular weight and degree of deacetylation. *Biomaterials* 2001;22(12):1653-8.
127. Thein-Han WW, Kitiyanant Y. Chitosan scaffolds for in vitro buffalo embryonic stem-like cell culture: an approach to tissue engineering. *Journal of biomedical materials research. Part B, Applied biomaterials* 2007;80(1):92-101.
128. Wenling C, Duohui J, Jiamou L, Yandao G, Nanming Z, Xiufang Z. Effects of the degree of deacetylation on the physicochemical properties and Schwann cell affinity of chitosan films. *Journal of biomaterials applications* 2005;20(2):157-77.
129. Amaral IF, Sampaio P, Barbosa MA. Three-dimensional culture of human osteoblastic cells in chitosan sponges: the effect of the degree of acetylation. *Journal of biomedical materials research. Part A* 2006;76(2):335-46.
130. Cohen S, Alonso MJ, Langer R. Novel approaches to controlled-release antigen delivery. *International journal of technology assessment in health care* 1994;10(1):121-30.
131. Jalil R, Nixon JR. Biodegradable poly(lactic acid) and poly(lactide-co-glycolide) microcapsules: problems associated with preparative techniques and release properties. *Journal of microencapsulation* 1990;7(3):297-325.
132. Kitchell JPW, D.L. Poly(Lactic Glycolic Acid) Biodegradable Drug Polymer Matrix Systems. *Methods in enzymology* 1985;112:436-438.
133. L.S. Nair CTL. Biodegradable polymers as biomaterials. . *Progress in Polymer Science* 2007;32(8-9):762-798.
134. Yilgor P TK, Reis RL, Hasirci N, Hasirci V. . Incorporation of a sequential BMP-2/BMP-7 delivery system into chitosan-based scaffolds for bone tissue engineering. *Biomaterials* 2009;30(21):3551-9.
135. Friedlander GEM, H.J.; Goldberg, V.M. Bone Graft and Bone Graft Substitutes: American Academy of Orthopaedic Surgeons; 2006.
136. Hench LLB, S. Biomaterials Science: An Introduction to Materials in Medicine: Elsevier Academic Press; 2004.
137. Muzzarelli C, Muzzarelli RA. Natural and artificial chitosan-inorganic composites. *Journal of inorganic biochemistry* 2002;92(2):89-94.
138. Zhang Y, Ni M, Zhang M, Ratner B. Calcium phosphate-chitosan composite scaffolds for bone tissue engineering. *Tissue engineering* 2003;9(2):337-45.
139. Rusu VMN, C.H.; Wilke, M.; Tiersch, B.; Fratzl, P.; Peter, M.G. Size-controlled hydroxyapatite nanoparticles as self-organized organic-inorganic composite materials. *Biomaterials* 2005;26(26):5414-26.

140. <http://www.uweb.engr.washington.edu/research/tutorials/naturalpolymers.html>. Biomaterials Tutorial Natural Polymers Cuy J.(2004). Accessed on December, 29th 2011
141. Alberts BB, D.; Lewis, J.; Raff, M.; Roberts, K.; Watson, J.D. Molecular biology of the cell. New York: Garland Publishing; 1994. 978-80 p.
142. Weiner S, Wagner HD. THE MATERIAL BONE: Structure-Mechanical Function Relations. Annual Review of Materials Science 1998;28(1):271-298.
143. Han BH, L.L.H.; Cheung, D.; Cordoba, F.; Nimni, M. Polypeptide growth factors with a collagen binding domain: Their potential for tissue repair and organ regeneration. Austin: RG Landes; 1999.
144. Vaissiere GC, B.; Herbage, D.; Damour, O. Comparative analysis of different collagen-based biomaterials as scaffolds for long-term culture of human fibroblasts. Medical & Biological Engineering & Computing 2000;38:205-10.
145. Tan W, Krishnaraj R, Desai TA. Evaluation of nanostructured composite collagen--chitosan matrices for tissue engineering. Tissue engineering 2001;7(2):203-10.
146. Wang L, Stegemann JP. Glyoxal crosslinking of cell-seeded chitosan/collagen hydrogels for bone regeneration. Acta biomaterialia 2011;7(6):2410-7.
147. Wang L, Stegemann JP. Thermogelling chitosan and collagen composite hydrogels initiated with beta-glycerophosphate for bone tissue engineering. Biomaterials 2010;31(14):3976-85.
148. Nitzsche H, Lochmann A, Metz H, Hauser A, Syrowatka F, Hempel E, Muller T, Thurn-Albrecht T, Mader K. Fabrication and characterization of a biomimetic composite scaffold for bone defect repair. Journal of biomedical materials research. Part A 2010;94(1):298-307.
149. Xu Z, Neoh KG, Lin CC, Kishen A. Biomimetic deposition of calcium phosphate minerals on the surface of partially demineralized dentine modified with phosphorylated chitosan. Journal of biomedical materials research. Part B, Applied biomaterials 2011;98(1):150-9.
150. Zhao L, Tang M, Weir MD, Detamore MS, Xu HH. Osteogenic media and rhBMP-2-induced differentiation of umbilical cord mesenchymal stem cells encapsulated in alginate microbeads and integrated in an injectable calcium phosphate-chitosan fibrous scaffold. Tissue engineering. Part A 2011;17(7-8):969-79.
151. Lian Q, Li DC, He JK, Wang Z. Mechanical properties and in-vivo performance of calcium phosphate cement-chitosan fibre composite. Proceedings of the Institution of Mechanical Engineers. Part H, Journal of engineering in medicine 2008;222(3):347-53.
152. Gibson LJA, M.F. Cellular Solids Structure & Properties. Fairview Park: Pergamon Press, Inc., Maxwell House; 1987.
153. Li DX, Fan HS, Zhu XD, Tan YF, Xiao WQ, Lu J, Xiao YM, Chen JY, Zhang XD. Controllable release of salmon-calcitonin in injectable calcium phosphate cement modified by chitosan oligosaccharide and collagen polypeptide. Journal of materials science. Materials in medicine 2007;18(11):2225-31.
154. Ravindran SG, Q.; Kotecha, M.; Magin, R.L.; Karol, S.; Bedran-Russo, A.; George, A. Biomimetic Extracellular Matrix-Incorporated Scaffold Induces Osteogenic Gene Expression in Human Marrow Stromal Cells. Tissue engineering. Part A 2011.
155. Pallela RV, J.; Janapala, V.R.; Kim, S.K. Biophysicochemical evaluation of chitosan-hydroxyapatite-marine sponge collagen composite for bone tissue engineering. Journal of biomedical materials research. Part A 2011(100A):486-95.
156. Niu XF, Y.; Liu, X.; Li, X.; Li, P.; Wang, J.; Sha, Z.; Feng, Q. Repair of bone defect in

- femoral condyle using microencapsulated chitosan, nanohydroxyapatite/collagen and poly(L-lactide)-based microsphere-scaffold delivery system. *Artificial Organs* 2011;35(7).
157. Zhang LT, P.; Zhang, W.; Xu, M.; Wang, Y. Effect of chitosan as a dispersant on collagen-hydroxyapatite composite matrices. *Tissue engineering. Part C, Methods* 2010;16(1):71-9.
  158. Wang Y, Zhang L, Hu M, Liu H, Wen W, Xiao H, Niu Y. Synthesis and characterization of collagen-chitosan-hydroxyapatite artificial bone matrix. *Journal of biomedical materials research. Part A* 2008;86(1):244-52.
  159. Hamilton V, Yuan Y, Rigney DA, Puckett AD, Ong JL, Yang Y, Elder SH, Bumgardner JD. Characterization of chitosan films and effects on fibroblast cell attachment and proliferation. *Journal of materials science. Materials in medicine* 2006;17(12):1373-81.
  160. McCanless JD. Annual Meeting of the Orthopaedic Research Society. Abstract 35, poster #1437. New Orleans, LA; 2010.
  161. <http://www.kolagena.co.nz/research-from-glavin.php>. Polish fish collagen preparation Biologically active natural collagen. KOLAGENA.(2011). Accessed on October, 6th 2011
  162. Victor S, Kumar T. BCP ceramic microspheres as drug delivery carriers: synthesis, characterisation and doxycycline release. *Journal of Materials Science: Materials in Medicine* 2008;19(1):283-290.
  163. [http://www.stattools.net/Comp2Regs\\_Pgm.php](http://www.stattools.net/Comp2Regs_Pgm.php). program Ctrl.(Accessed on February, 3rd 2012
  164. Nguyen DT. Design and evaluation of chitosan-calcium phosphate scaffolds constructed from air dried and lyophilized microspheres. Memphis: University of Memphis; 2010.
  165. Borene ML, Barocas VH, Hubel A. Mechanical and cellular changes during compaction of a collagen-sponge-based corneal stromal equivalent. *Annals of biomedical engineering* 2004;32(2):274-83.
  166. Luo T, Zhang W, Shi B, Cheng X, Zhang Y. Enhanced bone regeneration around dental implant with bone morphogenetic protein 2 gene and vascular endothelial growth factor protein delivery. *Clinical oral implants research* 2011.
  167. Deligianni DD, Katsala ND, Koutsoukos PG, Missirlis YF. Effect of surface roughness of hydroxyapatite on human bone marrow cell adhesion, proliferation, differentiation and detachment strength. *Biomaterials* 2001;22(1):87-96.
  168. Wainwright SAB, W.D.; Currey, J.D. and Gosline, J.M. *Mechanical Design in Organisms*. Princeton: Princeton University Press; 1976.
  169. <http://depts.washington.edu/bonebio/ASBMRed/structure.html>. Bone Structure and Function. Jane Lian JGaSO.(2004). Accessed on January, 16th 2012
  170. Apter JT. Correlation of visco-elastic properties with microscopic structure of large arteries. IV. Thermal responses of collagen, elastin, smooth muscle, and intact arteries. *Circulation research* 1967;21(6):901-18.
  171. Chen Z, Mo X, He C, Wang H. Intermolecular interactions in electrospun collagen–chitosan complex nanofibers. *Carbohydrate Polymers* 2008;72(3):410-418.
  172. Lin L-C, Chang S-J, Kuo SM. Evaluation of chitosan/ $\beta$ -tricalcium phosphate microspheres as a constituent to PMMA cement. *Journal of Materials Science: Materials in Medicine* 2005;16(6):567-574.
  173. Yan LP, Wang YJ, Ren L, Wu G, Caridade SG, Fan JB, Wang LY, Ji PH, Oliveira JM,

- Oliveira JT and others. Genipin-cross-linked collagen/chitosan biomimetic scaffolds for articular cartilage tissue engineering applications. *Journal of biomedical materials research. Part A* 2010;95(2):465-75.
174. Schuster M, Turecek C, Varga F, Lichtenegger H, Stampfl J, Liska R. 3D-shaping of biodegradable photopolymers for hard tissue replacement. *Applied Surface Science* 2007;254(4):1131-1134.
  175. Lee JY, Kim KH, Shin SY, Rhyu IC, Lee YM, Park YJ, Chung CP, Lee SJ. Enhanced bone formation by transforming growth factor-beta1-releasing collagen/chitosan microgranules. *Journal of biomedical materials research. Part A* 2006;76(3):530-9.
  176. Chiroff RT, White EW, Weber KN, Roy DM. Tissue ingrowth of Replamineform implants. *Journal of biomedical materials research* 1975;9(4):29-45.
  177. Jiang T, Nukavarapu SP, Deng M, Jabbarzadeh E, Kofron MD, Doty SB, Abdel-Fattah WI, Laurencin CT. Chitosan-poly(lactide-co-glycolide) microsphere-based scaffolds for bone tissue engineering: in vitro degradation and in vivo bone regeneration studies. *Acta biomaterialia* 2010;6(9):3457-70.

## APPENDIX A: DEGRADATION, CELL ATTACHMENT & GROWTH ON MICROPARTICLES

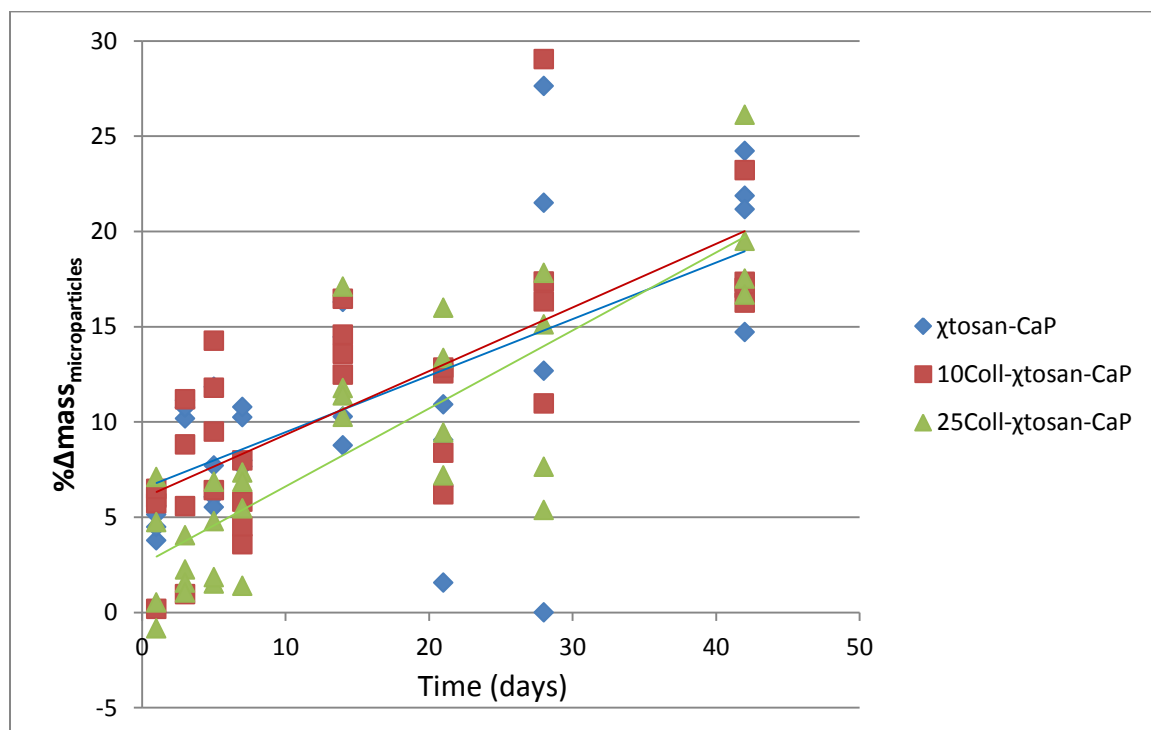


**Figure 1.** Degradation of microparticles in PBS + enzymes. Tukey's test and one-way ANOVA showed that all initial masses are statistically different ( $p < 0.05$ ). Regression analysis showed that the degradation rates are similar ( $\alpha = 0.05$ ).  $n = 4$

**Table 1.** Regression lines of the degradation of microparticles in PBS + enzymes. There is no statistically significant difference in slope or degradation rate between groups.

Groups	$R^2$	Regression lines
χtosan-CaP	0.3820	$Y = 0.2965x + 6.4989$
10Coll-χtosan-CaP	0.5217	$Y = 0.3336x + 5.9993$
25Coll-χtosan-CaP	0.6888	$Y = 0.4094x + 2.5201$

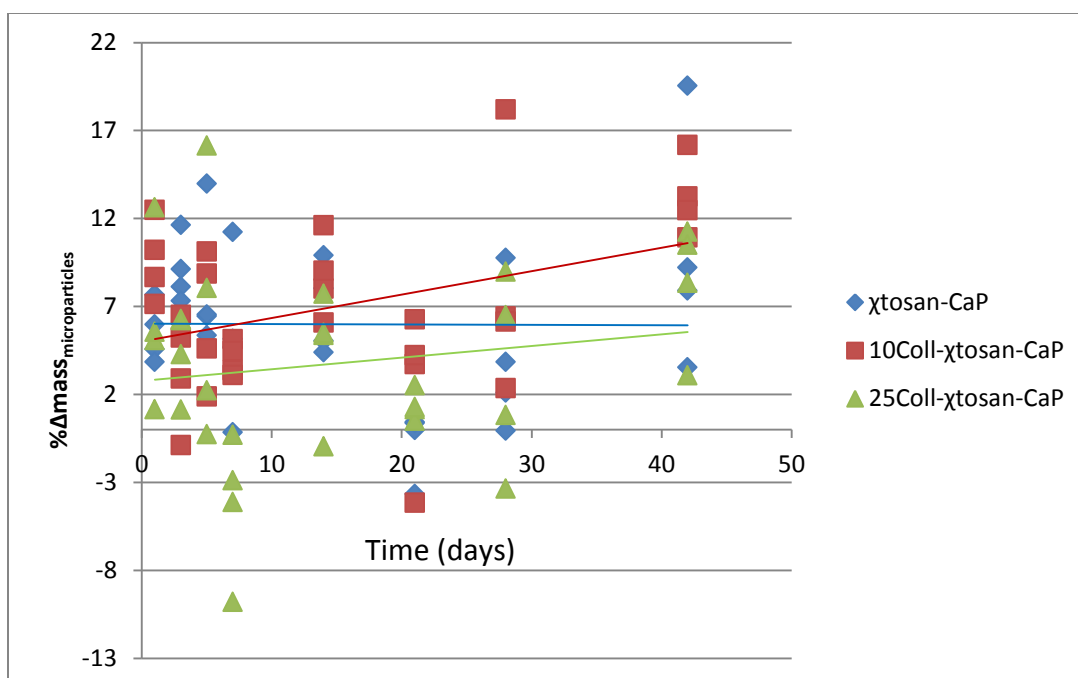


**Figure 2.** Degradation of microparticles in PBS (control). One-way ANOVA and Tukey's test showed that all initial masses are statistically different ( $p < 0.05$ ). The beads showed a loss of mass over time. Regression analysis<sup>163</sup> showed there were no differences in the degradation rate ( $p < 0.05$ ).  $n=4$

**Table 2.** Regression lines of the degradation of microparticles in PBS. There is no statistically significant difference in slope or degradation rate between groups.

Groups	$R^2$	Regression lines
$\chi$ tosan-CaP	5E-5	$Y = -0.0024x + 6.0286$
10Coll- $\chi$ tosan-CaP	0.1446	$Y = 0.1332x + 5.0050$
25Coll- $\chi$ tosan-CaP	0.0285	$Y = 0.0664x + 2.7645$

**Table 3.** Cell attachment on microparticles.

Cell attachment (%)			
Microparticles	$\chi$ tosan-CaP	10Coll- $\chi$ tosan-CaP	25Coll- $\chi$ tosan-CaP
<i>fibroblasts</i>	<b>40.6±8.0</b>	<b>38.5±6.8</b>	<b>43.2±8.7</b>
<i>osteoblasts</i>	<b>27.3±13.1</b>	<b>22.5±6.0</b>	<b>27.6±4.8</b>



The results of the proliferation study are summarized in table 4.

**Table 4.** Cell proliferation on microparticles on the last day of proliferation

# cells/microparticle			
<b>Microparticles</b>	$\chi$ tosan-CaP	10Coll- $\chi$ tosan-CaP	25Coll- $\chi$ tosan-CaP
<i>fibroblasts</i>	<b>5744±1343</b>	<b>6324±792</b>	<b>5536±1077</b>
<i>osteoblasts</i>	<b>4965±1459</b>	<b>4910±359</b>	<b>5579±1173</b>

**Table 5.** Regression lines of fibroblasts' proliferation on microparticles. There is no statistically significant difference in slope or proliferation rate between groups.

Groups	R <sup>2</sup>	Regression lines
$\chi$ tosan-CaP	0.8691	Y=787.34x+170.04
10Coll- $\chi$ tosan-CaP	0.9717	Y=846.47x+443.64
25Coll- $\chi$ tosan-CaP	0.8844	Y=681.86 x+840.84

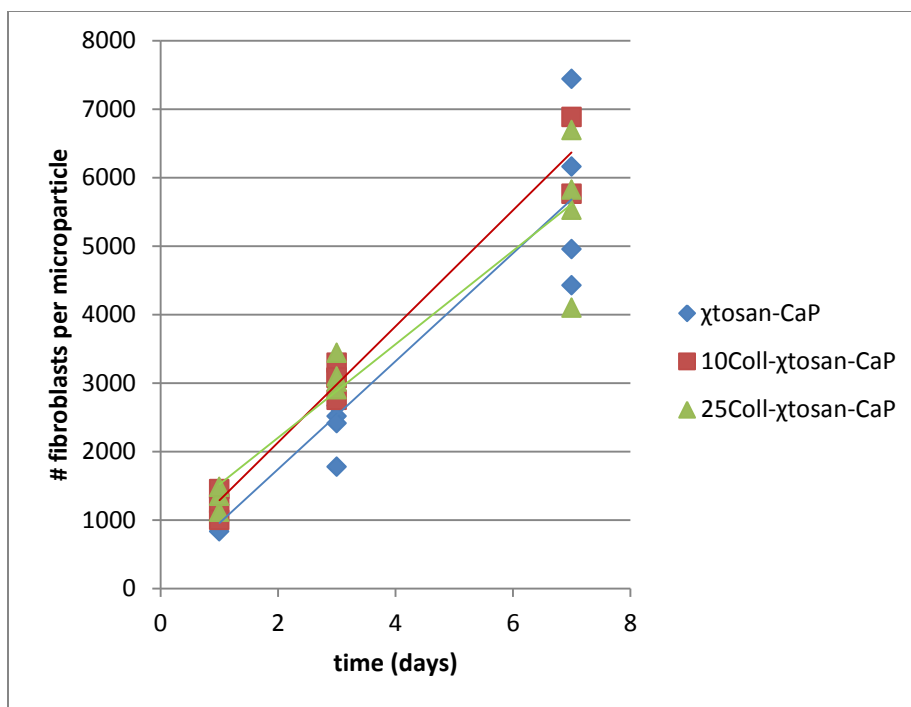


**Figure 3.** Regression for fibroblasts' proliferation of microparticles. There is no statistically significant difference in the proliferation rate ( $\alpha=0.05$ ).

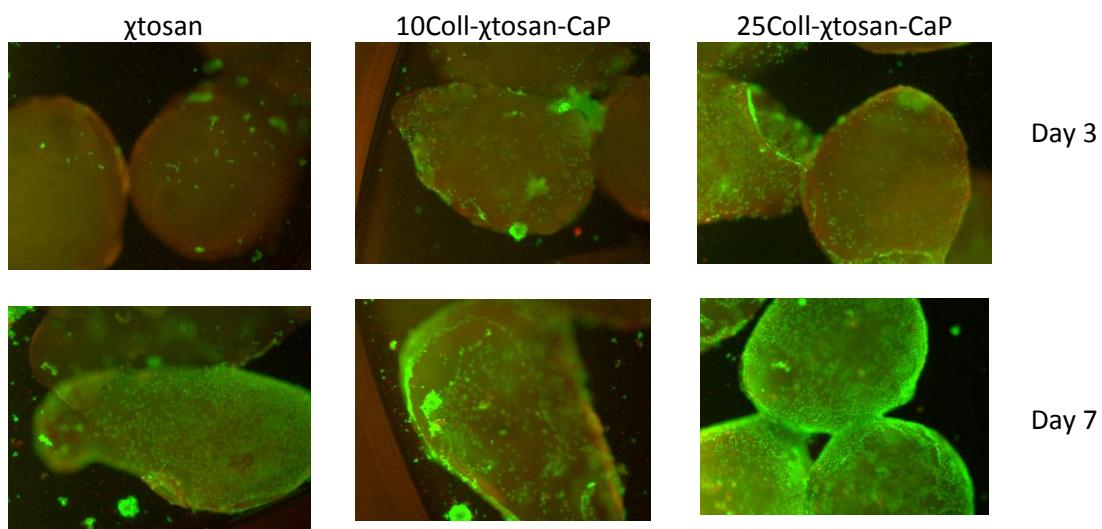


**Figure 4.** Fibroblasts' viability on microparticles.

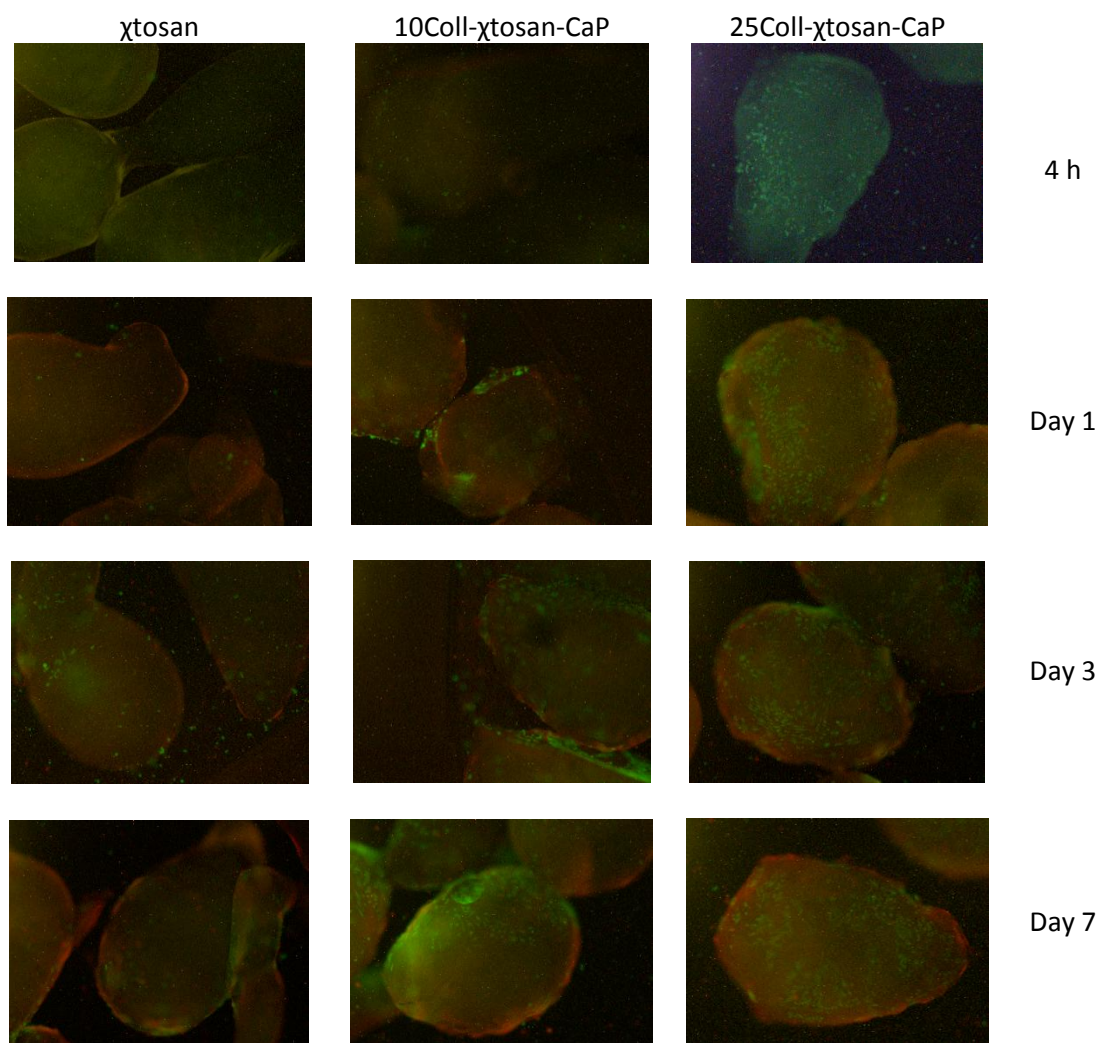


**Figure 5.** Osteoblasts' viability on microparticles.

## APPENDIX B: YOUNG'S MODULUS, DEGRADATION AND VIABILITY OF OSTEOBLASTS ON SCAFFOLDS

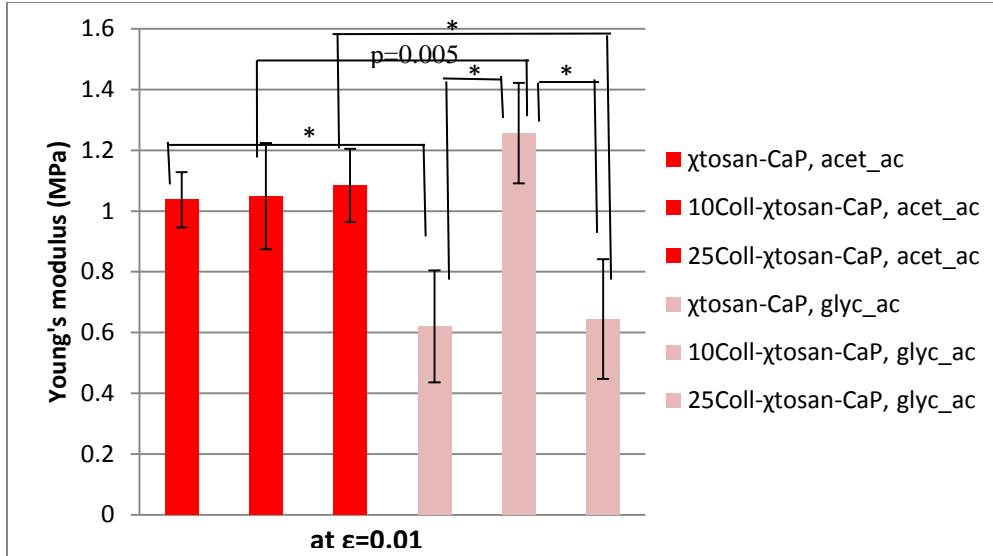


**Figure 6.** Young's modulus in compression of composite scaffolds for  $\epsilon=0.1$  (n=10).

Acet\_ac: acetic acid; glyc\_ac: glycolic acid. Two-way ANOVA showed that all three types of microparticles fused acetic acid differ from those fused with glycolic acid. Error bars are standard deviations. \*=difference between groups ( $p<0.001$ ).

**Table 6.** Regression lines of the degradation of scaffolds in PBS +enzymes.

Groups	$R^2$	Regression lines	Statistical significance in slope
1=χtosan-CaP, acet_ac	0.9302	$Y=4.0960x-4.9639$	1 vs. 2 ( $p<0.05$ )
2=χtosan-CaP, glyc_ac	0.8822	$Y=6.5865x-1.9860$	1 vs. 4 ( $p<0.05$ )
3=10Coll-χtosan-CaP, acet_ac	0.6220	$Y=3.4877x-2.2552$	2 vs. 3 ( $p<0.05$ )
4=10Coll-χtosan-CaP, glyc_ac	0.8648	$Y=6.4632x-0.9183$	3 vs. 4 ( $p<0.05$ )
5=25Coll-χtosan-CaP, acet_ac	0.6453	$Y=4.4350x+2.9949$	
6=25Coll-χtosan-CaP, glyc_ac	0.6478	$Y=4.7718x+6.0838$	

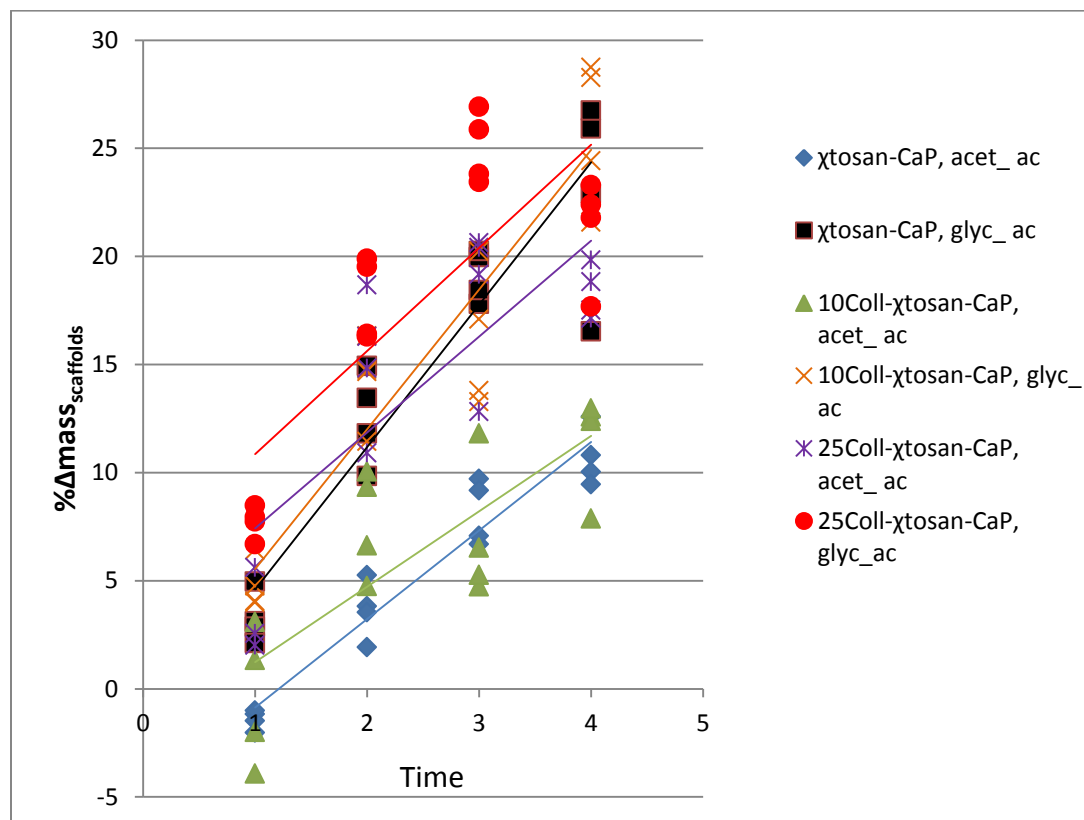


**Figure 7.** Degradation of scaffolds fused with acetic vs. glycolic acid in PBS + enzymes.

N=4

**Table 7.** Regression lines of the degradation of scaffolds in PBS.

Groups	R <sup>2</sup>	Regression lines	Statistical significance in slope
1=χtosan-CaP, acet_ac	0.8857	Y=2.0398x-6.0857	1 vs. 5 (p<0.05)
2=χtosan-CaP, glyc_ac	0.6407	Y=2.1123x-3.5685	3 vs. 5 (p<0.05)
3=10Coll-χtosan-CaP, acet_ac	0.5933	Y=2.3998x-5.7657	4 vs. 5 (p<0.05)
4=10Coll-χtosan-CaP, glyc_ac	0.6851	Y=2.4057x-2.7063	
5=25Coll-χtosan-CaP, acet_ac	0.0599	Y=0.6124x+0.9824	
6=25Coll-χtosan-CaP, glyc_ac	0.1757	Y=1.4450x-0.3592	

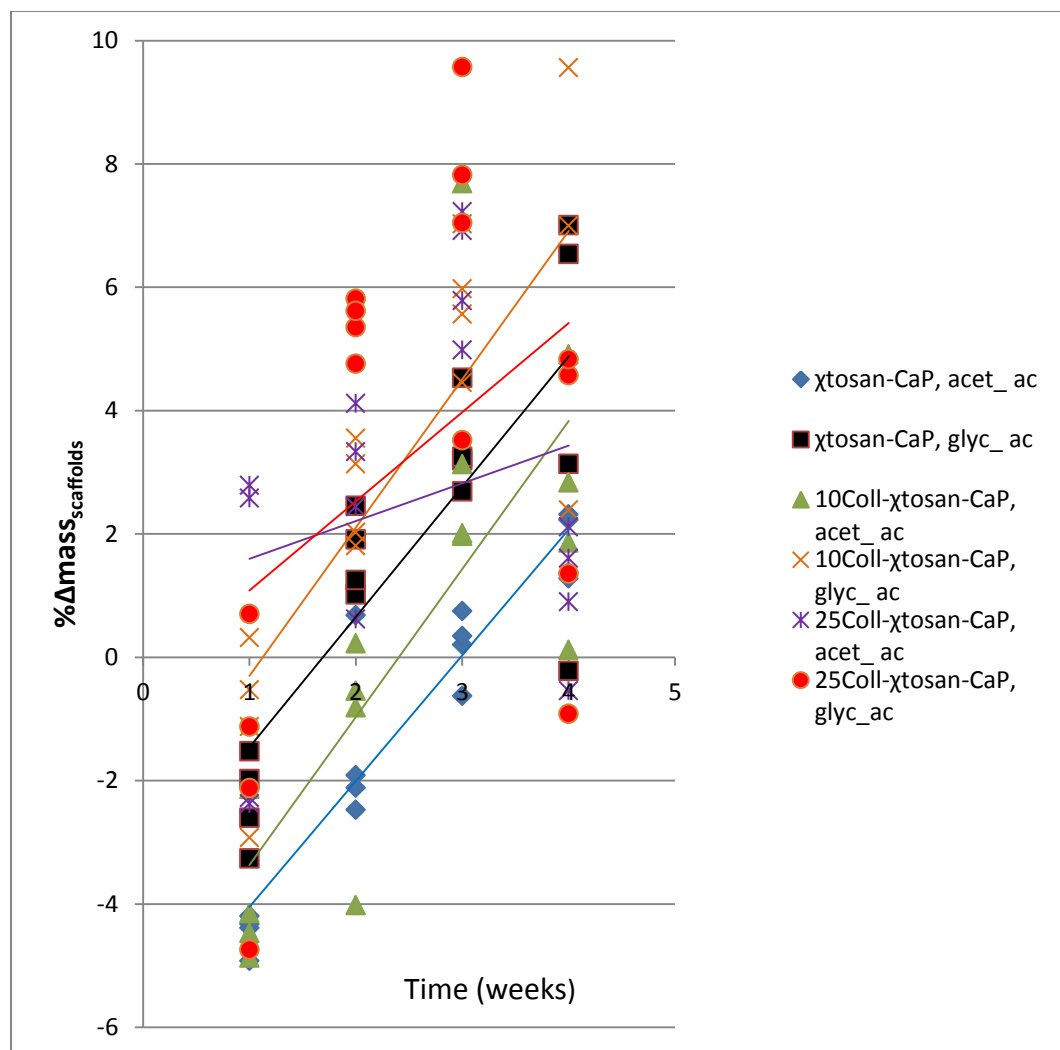


**Figure 8.** Degradation of scaffolds fused with acetic vs. glycolic acid in PBS. N=4

**Table 8.** Regression lines of the osteoblasts' proliferation on scaffolds.

Groups	R <sup>2</sup>	Regression lines	Statistical significance in slope
1=χtosan-CaP, acet_ac	0.6633	Y=1670.2x-913.08	1 vs. 4 (p<0.05)
2=χtosan-CaP, glyc_ac	0.5644	Y=1219 x-370.6	3 vs. 4 (p<0.05)
3=10Coll-χtosan-CaP, acet_ac	0.6481	Y=1474.7 x-654.68	4 vs. 5 (p<0.05)
4=10Coll-χtosan-CaP, glyc_ac	0.4018	Y=574.48 x+1802.4	
5=25Coll-χtosan-CaP, acet_ac	0.5162	Y=2410.5 x-1033.4	
6=25Coll-χtosan-CaP, glyc_ac	0.5910	Y=1493.8 x+779.79	

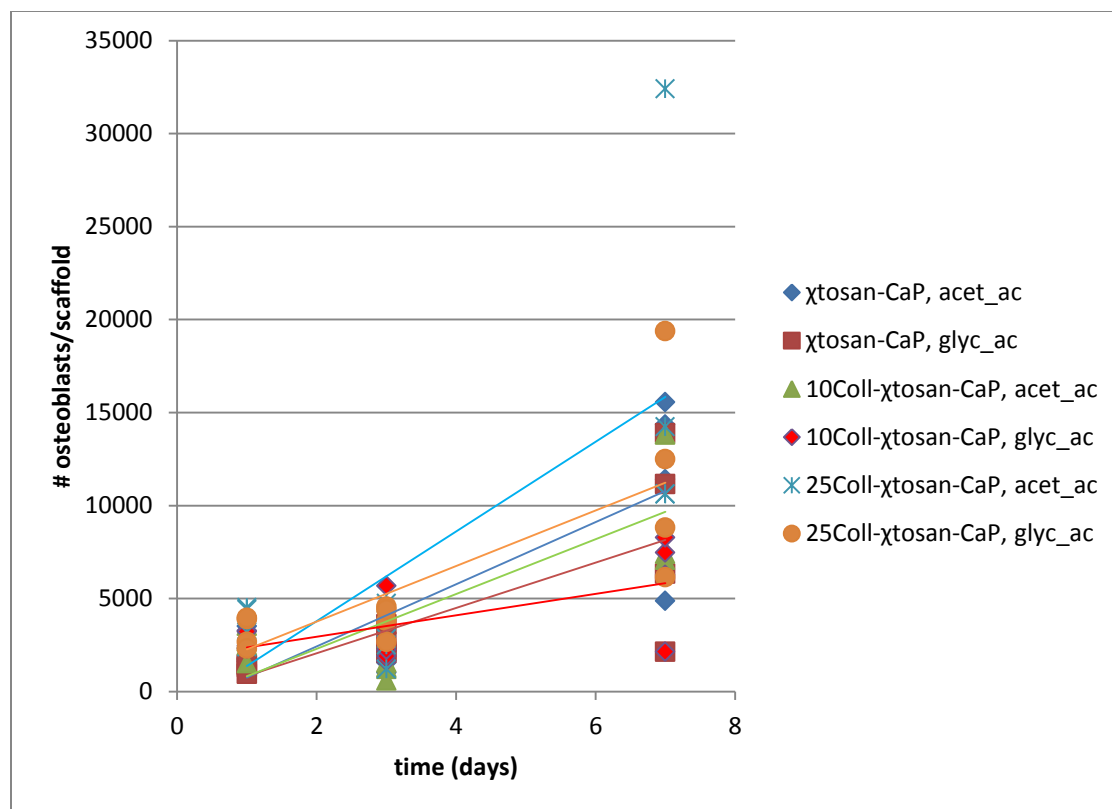


**Figure 9.** Regression analysis of osteoblasts' proliferation on scaffolds.

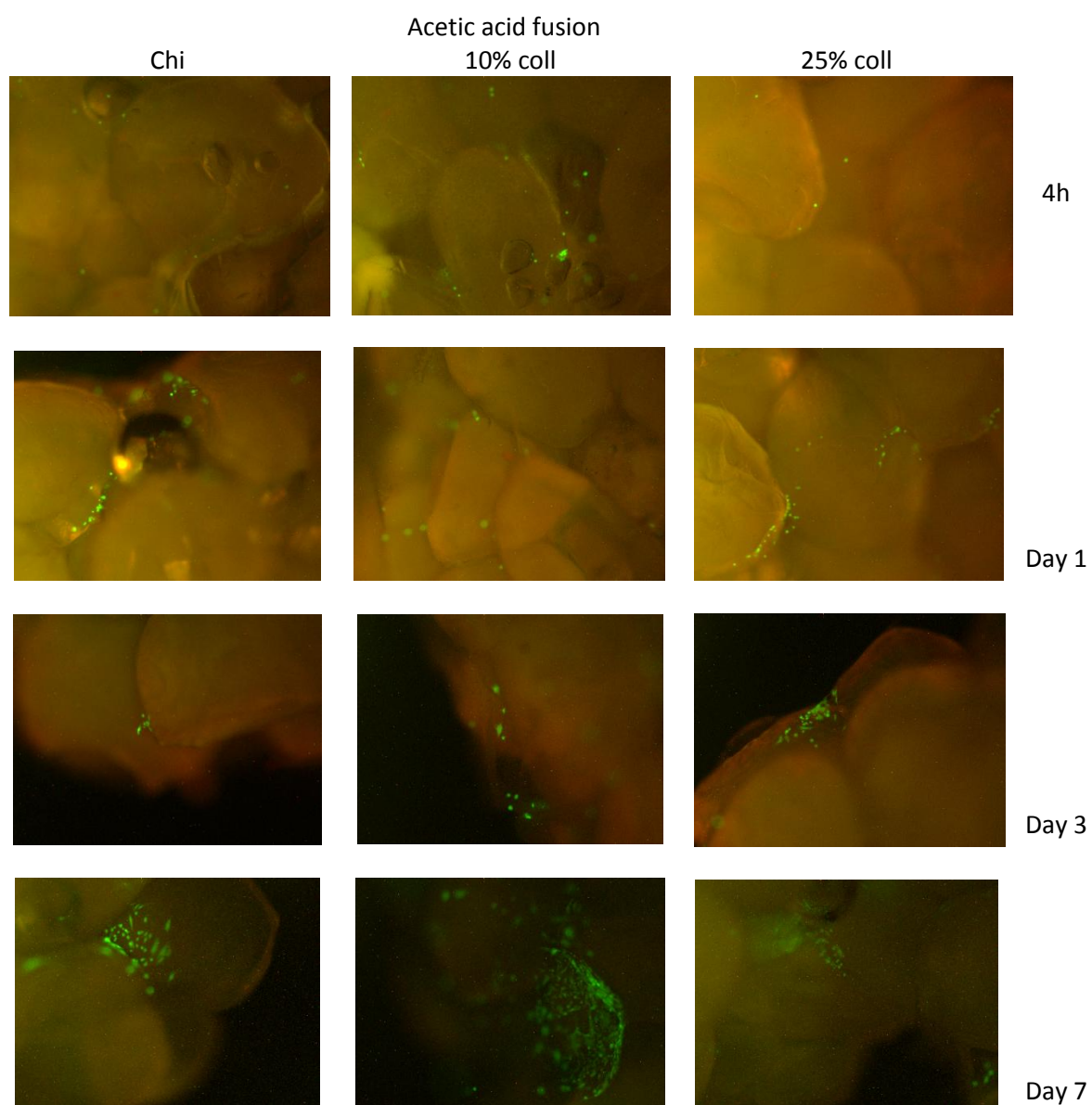


**Figure 10.** Osteoblasts' viability on scaffolds fused with acetic acid.



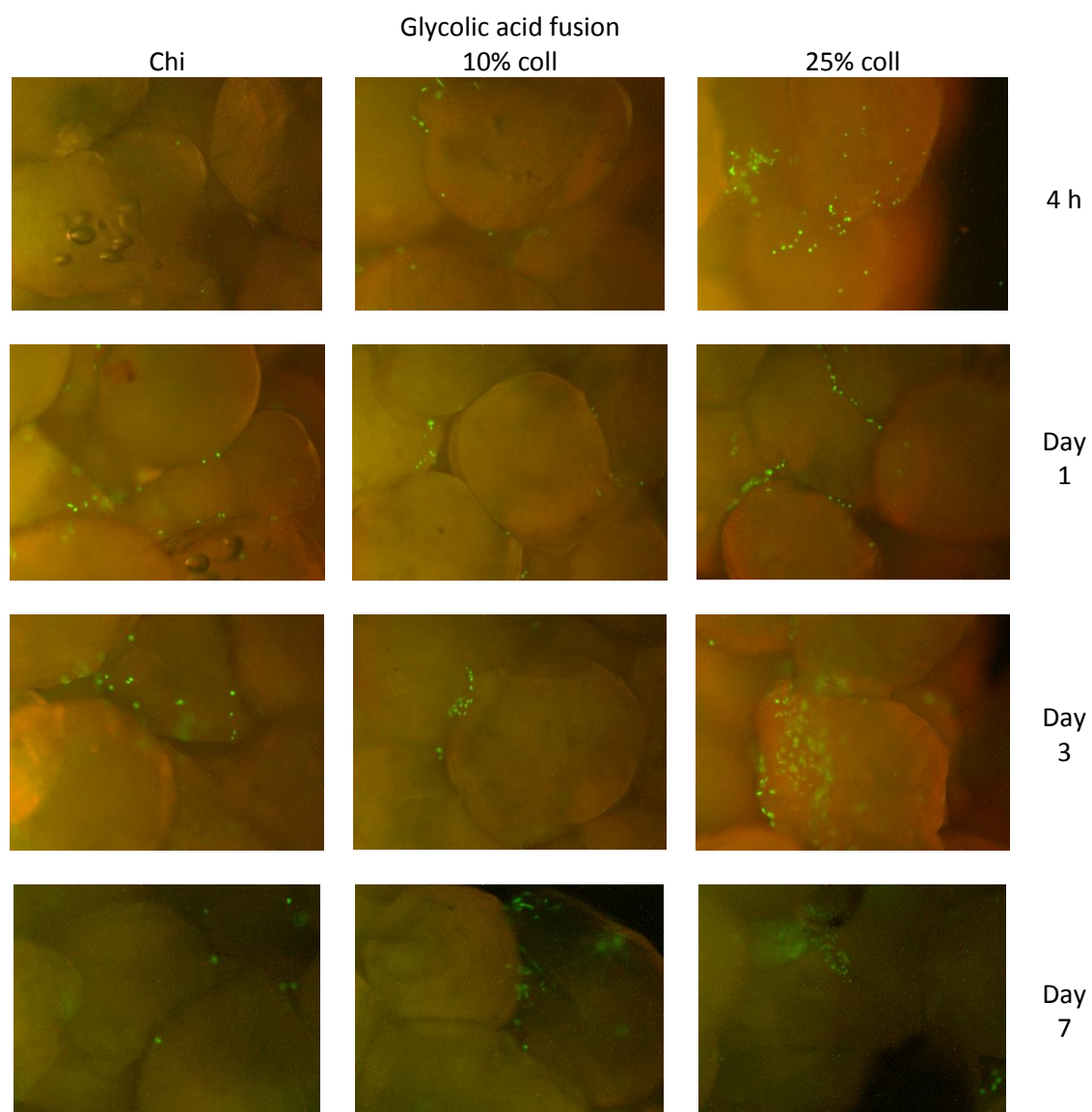


**Figure 11.** Osteoblasts' viability on scaffolds fused with glycolic acid.